EARTHQUAKE ENGINEERING TO EXTREME EVENTS

ISSN 1520-295X

Assessment of Base-Isolated Nuclear Structures for Design and Beyond-Design Basis Earthquake Shaking

by
Yin-Nan Huang, Andrew S. Whittaker,
Robert P. Kennedy and Ronald L. Mayes

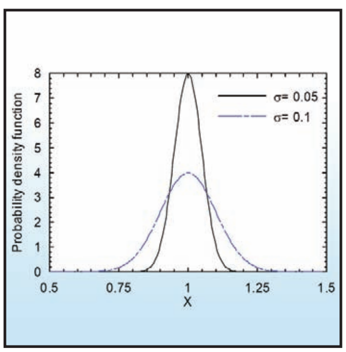

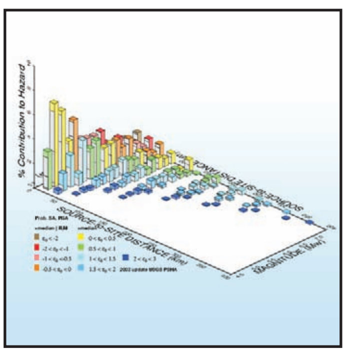

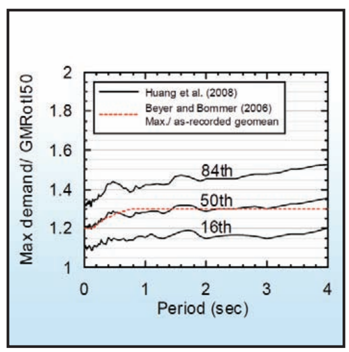

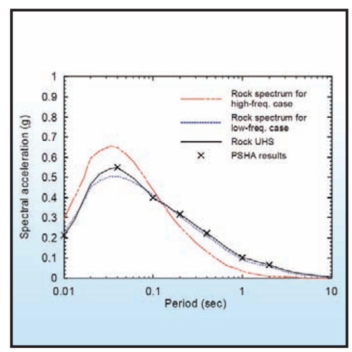

Technical Report MCEER-09-0008

August 20, 2009

This research was conducted at the University at Buffalo, State University of New York and was supported primarily by the Earthquake Engineering Research Centers Program of the National Science Foundation under award number EEC 9701471.

NOTICE

Assessment of Base-Isolated Nuclear Structures for Design and Beyond-Design Basis Earthquake Shaking

by

Yin-Nan Huang,[1] Andrew S. Whittaker,[2] Robert P. Kennedy[3] and Ronald L. Mayes[4]

Publication Date: August 20, 2009
Submittal Date: June 26, 2009

Technical Report MCEER-09-0008

Task Number 10.4.2

NSF Master Contract Number EEC 9701471

1 Post-doctoral Research Associate, Department of Civil, Structural and Environmental Engineering, University at Buffalo, State University of New York
2 Professor, Department of Civil, Structural and Environmental Engineering, University at Buffalo, State University of New York
3 RPK Structural Mechanics Consulting
4 Staff Consultant, Simpson Gumpertz & Heger, Inc.

MCEER
University at Buffalo, State University of New York
Red Jacket Quadrangle, Buffalo, NY 14261
Phone: (716) 645-3391; Fax (716) 645-3399
E-mail: *mceer@buffalo.edu*; WWW Site: *http://mceer.buffalo.edu*

Preface

The Multidisciplinary Center for Earthquake Engineering Research (MCEER) is a national center of excellence in advanced technology applications that is dedicated to the reduction of earthquake losses nationwide. Headquartered at the University at Buffalo, State University of New York, the Center was originally established by the National Science Foundation in 1986, as the National Center for Earthquake Engineering Research (NCEER).

Comprising a consortium of researchers from numerous disciplines and institutions throughout the United States, the Center's mission is to reduce earthquake losses through research and the application of advanced technologies that improve engineering, pre-earthquake planning and post-earthquake recovery strategies. Toward this end, the Center coordinates a nationwide program of multidisciplinary team research, education and outreach activities.

MCEER's research is conducted under the sponsorship of two major federal agencies: the National Science Foundation (NSF) and the Federal Highway Administration (FHWA), and the State of New York. Significant support is derived from the Federal Emergency Management Agency (FEMA), other state governments, academic institutions, foreign governments and private industry.

MCEER's NSF-sponsored research objectives are twofold: to increase resilience by developing seismic evaluation and rehabilitation strategies for the post-disaster facilities and systems (hospitals, electrical and water lifelines, and bridges and highways) that society expects to be operational following an earthquake; and to further enhance resilience by developing improved emergency management capabilities to ensure an effective response and recovery following the earthquake (see the figure below).

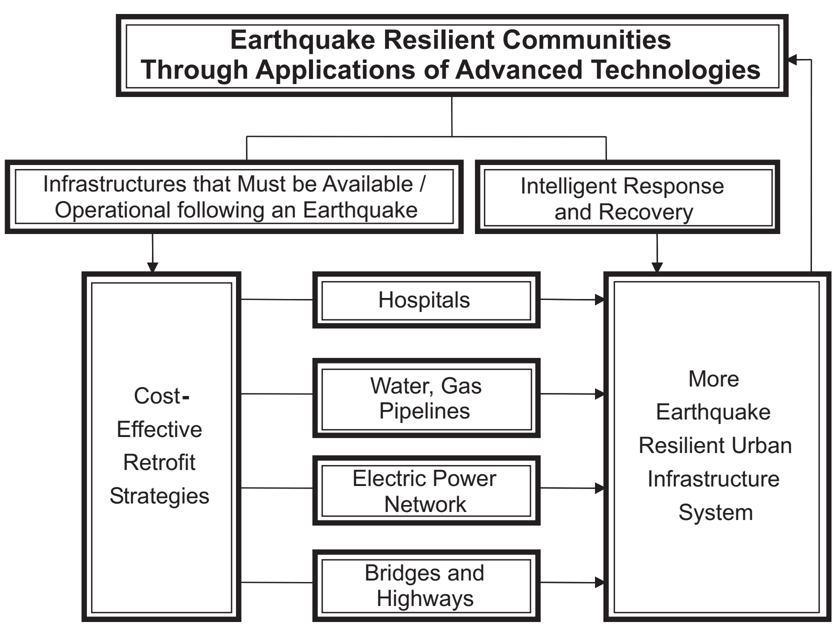

A cross-program activity focuses on the establishment of an effective experimental and analytical network to facilitate the exchange of information between researchers located in various institutions across the country. These are complemented by, and integrated with, other MCEER activities in education, outreach, technology transfer, and industry partnerships.

This report presents the technical basis for proposed changes to the 2010 edition of ASCE Standard 4, Seismic Analysis of Safety-related Nuclear Structures. Three performance statements aiming at achieving the objectives of ASCE 43-05, Seismic Design Criteria for Structures, Systems and Components in Nuclear Facilities, are assessed in the study: 1) individual isolators shall suffer no damage for design level earthquake shaking, 2) the probability of the isolated nuclear structure impacting surrounding structure (moat) for 100% (150%) design level earthquake shaking is 1% (10%) or less, and 3) individual isolators sustain gravity and earthquake-induced axial loads at 90^th percentile lateral displacements consistent with 150% design level earthquake shaking. Nonlinear response-history analysis is performed in support of performance statements 2 and 3, accounting for the variability in both earthquake ground motions and seismic isolator properties. Lead rubber, low damping rubber and Frictional Pendulum base isolators are considered. Representative rock and soft soil sites in the Eastern, Central and Western United States are addressed. Eleven sets of ground motions are recommended for response-history analysis of base isolated nuclear structures. The median displacement response of a best-estimate model subjected to spectrum compatible design level ground motions should be increased by a factor of 3 to achieve the performance objectives of ASCE 43-05.

ABSTRACT

Two ASCE standards are relevant to the analysis and design of new nuclear power plants (NPPs): ASCE 4-98, *Seismic Analysis of Safety-related Nuclear Structures and Commentary* (ASCE 2000) and ASCE 43-05, *Seismic Design Criteria for Structures, Systems and Components in Nuclear Facilities* (ASCE 2005). Section 1.3 of ASCE 43-05 presents dual performance objectives for nuclear structures: 1) 1% probability of unacceptable performance for 100% design basis earthquake (DBE) shaking, and 2) 10% probability of unacceptable performance for 150% DBE shaking. ASCE Standard 4-98, which includes provisions for the analysis and design of seismic isolation systems, is being updated at the time of this writing, and the studies reported herein are undertaken by the authors to provide the technical basis for proposed changes to the 2010 edition of the standard.

Three performance statements for achieving the above two performance objectives of ASCE 43-05 are used for this study, namely, 1) individual isolators shall suffer no damage in design earthquake shaking, 2) the probability of the isolated nuclear structure impacting surrounding structure (moat) for 100% (150%) design earthquake shaking is 1% (10%) or less, and 3) individual isolators sustain gravity and earthquake-induced axial loads at 90th percentile lateral displacements consistent with 150% design earthquake shaking. Nonlinear response-history analysis was performed in support of performance statements 2 and 3, accounting for the variability in both earthquake ground motion and isolator material properties. Lead-rubber, low-damping rubber and Friction Pendulum™ seismic isolators are considered.

For representative rock and soft soil sites in the Central and Eastern United States and Western United States, estimates are made of 1) the ratio of the 99%-ile displacement (force) computed using a distribution of DBE spectral demands and distributions of isolator mechanical properties to the median isolator displacement (force) computed using best-estimate properties and spectrum-compatible DBE ground motions; 2) the ratio of the 90%-ile displacement (force) computed using a distribution of 150% DBE spectral demands and distributions of isolator mechanical properties to the median isolator displacement (force) computed using best-estimate properties and spectrum-compatible DBE ground motions; and 3) the number of sets of three-component ground motions to be used for response-history analysis to develop a reliable estimate of the median displacement (force).

Eleven sets of ground motions are recommended for response-history analysis of base-isolated nuclear structures. The median response of a best-estimate model subjected to spectrum-compatible DBE ground motions should be increased by a factor of 3 to achieve the performance objectives of ASCE 43-05.

ACKNOWLEDGMENTS

The research presented in this report was supported in part by a grant from New York State and a grant from the Lawrence Berkeley National Laboratory (LBL) at the University of California, Berkeley under contract to the United States Nuclear Regulatory Commission (USNRC). This support is gratefully acknowledged.

The authors thank Professor Michael Constantinou of the University at Buffalo and Mr. George Abatt of M&D Professional Services for reviewing and commenting on a draft of this report.

Any opinions, findings and conclusions or recommendations expressed in this publication are those of the authors and do not necessarily reflect the views of LBL, USNRC, MCEER or New York State.

TABLE OF CONTENTS

SECTION TITLE PAGE

TABLE OF CONTENTS (CONT'D)

SECTION TITLE **PAGE**

LIST OF FIGURES

FIGURE **TITLE** **PAGE**

LIST OF FIGURES (CONT'D)

FIGURE **TITLE** **PAGE**

LIST OF TABLES

TABLE TITLE PAGE

LIST OF TABLES (CONT'D)

LIST OF ACRONYMS

AASHTO	=	American Society of State Highway and Transportation Officials
ASCE	=	American Society of Civil Engineers
CDF	=	Cumulative Distribution Function
CEUS	=	Central and Eastern United States
DBE	=	Design Basis Earthquake
ENA	=	Eastern North America
ESP	=	Early Site Permit
FP	=	Friction Pendulum
LDR	=	Low Damping Rubber
LR	=	Lead Rubber
MAFE	=	Mean Annual Frequency of Exceedance
NEHRP	=	National Earthquake Hazards Reduction Program
NGA	=	Next Generation Attenuation
NPP	=	Nuclear Power Plant
NSSS	=	Nuclear Steam Supply System
OSID	=	Onset of Significant Inelastic Deformation
PSHA	=	Probabilistic Seismic Hazard Analysis
PTFE	=	Polytetrafluoroethylene
SDC	=	Seismic Design Category
SDB	=	Seismic Design Basis
SSC	=	Structures, Systems and Components
SSE	=	Safe Shutdown Earthquake
UHS	=	Uniform Hazard Spectrum
URS	=	Uniform Risk Spectrum
USGS	=	United States Geological Survey
USNRC	=	United States Nuclear Regulatory Commission
WUS	=	Western United States

SECTION 1
SEISMIC ISOLATION OF NUCLEAR POWER PLANTS

1.1 Introduction

Seismic isolation devices have been used to protect buildings, bridges, and mission-critical infrastructure from the damaging effects of earthquake shaking. Nuclear structures and systems, (e.g., power plants and ballistic missile submarines) and other critical infrastructure (e.g., offshore platforms and LNG tanks) have been isolated using elastomeric and sliding isolation systems. In the United States, seismic isolation systems have been implemented in more than 80 buildings and 150 bridges since 1984 (Mayes 1998, 2006).

There are no applications of seismic isolation to nuclear structures in the United States at the time of this writing although some vendors of Nuclear Steam Supply Systems and power utilities are considering seismic isolation for new build plants. Design of new nuclear power plants (NPPs) will follow regulations, codes and standards set forth by the U.S. Nuclear Regulatory Commission (USNRC), the American Society of Civil Engineers (ASCE), the American Society of Mechanical Engineers, the American Concrete Institute (ACI), and the American Institute for Steel Construction (AISC), among others. Of these regulators and standards organizations, only the USNRC and ASCE will likely write rules related to the analysis and design of seismic isolation systems for new NPPs.

Two ASCE standards are relevant to the analysis and design of new NPPs: ASCE 4-98, *Seismic Analysis of Safety-related Nuclear Structures and Commentary* (ASCE 2000) and ASCE 43-05, *Seismic Design Criteria for Structures, Systems and Components in Nuclear Facilities* (ASCE 2005). ASCE Standard 4-98, which includes provisions for the analysis and design of seismic isolation systems, is being updated at the time of this writing, and the studies reported herein are undertaken by the authors to provide the technical basis for proposed changes to the 2010 edition of the standard.

Seismic isolation systems worthy of consideration for application in North America include two types of elastomeric bearings and one type of sliding bearing. Lead-Rubber (LR) and Low-Damping Rubber (LDR) bearings are examples of elastomeric bearings. The sliding bearing that is suitable for application to nuclear structures is the Friction Pendulum™ (FP) bearing. These elastomeric and sliding seismic isolation bearings are stiff in the vertical direction and flexible in any horizontal direction. The horizontal flexibility of the isolation system increases the fundamental period of the supported structure and reduces the inertial forces in the supported structure, enabling the secondary systems to be designed for much smaller forces and displacements than in a conventional (non-isolated) structure. Naeim and Kelly (1999) and Constantinou et al. (2007) provide much information of seismic isolation and isolators. Huang et al. (2008b, 2009) identifies the benefits of seismic isolation for nuclear structures using risk-based approaches that are consistent with US nuclear practice.

1.2 Performance objectives of ASCE 43-05 and USNRC Regulatory Guide 1.208

ASCE Standard 43-05 (ASCE 2005) provides criteria for the seismic analysis and design of safety-related Structures, Systems and Components (SSCs) of a broad class of nuclear facilities, including nuclear power plants. This standard combines a Seismic Design Category (SDC)[1] and a Limit State[2] to form a Seismic Design Basis (SDB). ASCE 43-05 presents design and analysis requirements for SDBs defined by 1) SDC 3, 4 and 5 associated with a quantitative target performance goals of 1×10^{-4}, 4×10^{-5} and 1×10^{-5}, respectively, and 2) Limit States A through D. The target performance goals given above are expressed as mean annual frequency of exceedance of the specified Limit State of the SSCs and can be used to set the spectral intensity of the design earthquake. New build containment vessels for nuclear power plants would be assigned to SDC 5 and Limit State D.

Section 2 of ASCE 43-05 presents a performance-based procedure for computing Design Basis Earthquake (DBE) spectral demands. The procedure is most different from the hazard-based procedure described in USNRC *Regulatory Guide 1.165* (USNRC 1997) for a Safe Shutdown Earthquake because

---

[1] ASCE 43 defines Seismic Design Category (SDC) on the basis of the "…severity of adverse radiological and toxicological effects of the hazards that may result from the failure of SSCs [structure, system, component] on workers, the public and the environment. SSCs may be assigned to SDCs that range from 1 to 5." A vessel containing a commercial nuclear reactor would be assigned to SDC 5.

[2] ASCE 43 defines a Limit State as the limiting acceptable condition of the SSC and the state can be characterized in terms of maximum allowable displacement, strain, ductility or stress. Four limit states are defined: A (short of collapse but stable), B (moderate permanent deformation), C (limited permanent deformation) and D (essentially elastic).

the ordinates of the design spectrum are computed on the basis of an annual frequency of unacceptable performance and not annual frequency of exceedance of earthquake hazard. Section 1.3 of ASCE 43-05 presents two performance objectives for nuclear structures, namely, 1) 1% probability of unacceptable performance for 100% DBE shaking, and 2) 10% probability of unacceptable performance for 150% DBE shaking. Kennedy (2007) performed a series of parametric studies using a wide range of hazard-curve slope and dispersions in system-level fragility curves and concluded that the annual frequency of unacceptable performance did not exceed 120% of the target value if analysis and design for SDC 5 and Limit State D followed the procedures of Sections 1.3 and Section 2 of ASCE 43-05.

In 2007, the USNRC issued *Regulatory Guide 1.208* (USNRC 2007) that permitted the use of the performance-based approach described in ASCE 43-05 to develop spectral demands for the design of SSCs in NPPs. Regulatory Guide 1.208 specifies a target mean annual frequency of exceedance of unacceptable performance of less than 1×10^{-5} for the onset of significant inelastic deformation (OSID), which corresponds to SDB-5D (i.e., SDC-5 and Limit State D) in ASCE 43-05. In Regulatory Guide 1.208, OSID is generally associated with “essentially elastic behavior” of SSCs and occurs well before seismically induced core damage. Analysis and design per Regulatory Guide 1.208 should result in an annual frequency of exceedance of core damage of much less than 1×10^{-5}.

1.3 Unacceptable performance of base-isolated NPPs

In base-isolated nuclear structures, the accelerations and deformations in SSCs are relatively small; the SSCs are expected to remain elastic for both DBE shaking and beyond design basis shaking. As such, unacceptable performance of an isolated nuclear structure will more likely involve either the failure of isolation bearings or impact of the isolated superstructure and surrounding building or geotechnical structures.

For the purpose of this study, we propose three performance statements for achieving the two performance objectives set forth in Section 1.3 of ASCE 43-05, namely, 1) individual isolators shall suffer no damage in DBE shaking, 2) the probability of the isolated nuclear structure impacting surrounding structure (moat) for 100% (150%) DBE shaking is 1% (10%) or less, and 3) individual isolators shall sustain gravity and earthquake-induced axial loads at 90th percentile lateral displacements consistent with 150% DBE shaking. Performance statement 1 can be realized by production testing of each isolator supplied to a project for median DBE displacements and co-existing gravity and earthquake-induced axial forces. Analysis can be used in support of performance statement 2 provided that the isolators are modeled correctly and the ground motion representations are reasonable. Performance statement 3 can be realized by prototype testing of a limited number of isolators for displacements and co-existing axial forces consistent with 150% DBE shaking, noting that an isolation system is composed of 10's to 100's of isolators and that failure of the isolation system would have to involve the simultaneous failure of a significant percentage of the isolators in the system.

1.4 Considerations for the performance assessment of isolated nuclear structures

The state-of-practice in selecting and scaling ground motions for design of conventional and isolated buildings and nuclear infrastructure involves selecting pairs of earthquake ground motions on the basis of earthquake magnitude, site-to-source distance and local soil conditions and scaling these motions to a design spectrum so that the resultant motions are spectrum-compatible. Although straightforward, such scaling cannot capture the distribution of spectral demand around the geometric mean demand, which is typically the product of a seismic hazard assessment. Alternate scaling procedures are used in this study to assess the performance of isolated nuclear structures.

The mechanical properties of typical seismic isolators such as LDR, LR and FP bearings will tend to vary from the values assumed for design both a) at the time of fabrication due to variability in basic material properties, and b) over the lifespan of the nuclear structure due to aging, contamination, ambient temperature, etc. The mechanical properties of LDR bearings are a function of the raw materials used, the choice of rubber compound and the thermal and pressure profiles used to cure the bearings. For LR bearings, the mechanical properties of the lead plug are a function of the confinement provided to the plug and the mechanical properties of the elastomer (rubber) per the LDR bearing. For FP bearings, only the coefficient of sliding friction varies because the second-slope stiffness of the bearing is a function of the radius of the sliding surface, which is constructed to very tight tolerances. Importantly, the variability of the mechanical properties of an assembly of isolators (the isolation system) will be smaller than the variability of individual isolators. The state-of-practice of seismic isolation system analysis and design is to develop lower and upper bound properties for the isolation system using property modification factors (e.g., Constantinou et al. 1999, 2007; AASHTO 1999, FEMA 2004), to use the best-estimate, lower-bound and upper-bound mechanical properties for analysis, and then envelope the resultant displacements and transmitted forces for design and assessment. The basic force-displacement relationship used to analyze LR and FP bearing isolation systems is shown in Figure 1-1. This model is fully defined by a

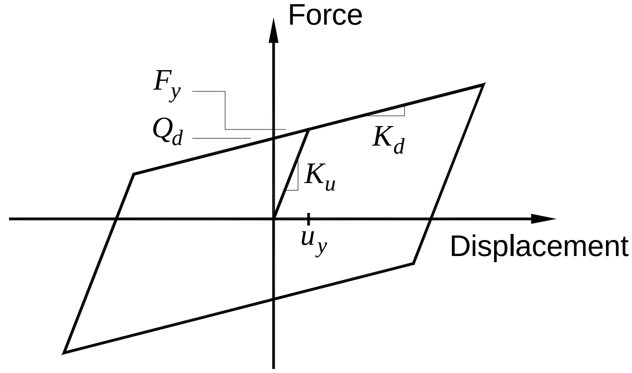

Figure 1-1. Assumed mechanical properties of the LR and FP bearings in a horizontal direction

characteristic strength, Q_d, and a second-slope (post-yield) stiffness, K_d. The second-slope stiffness is related to the isolated period through the supported weight, *W*. Low-damping rubber bearings are modeled typically as linearly elastic elements with displacement-independent damping.

1.5 Objectives of the study

The goals of the study presented in this report are three-fold, namely, for a) rock and soil sites in the Central and Eastern United States (CEUS) and for a rock site in the Western United States (WUS), and b) LR and FP bearings characterized by the hysteretic loop of Figure 1-1 and LDR bearings (CEUS rock site only), to

1. Determine the ratio of the 99%-ile estimate of the displacement (force) computed using a distribution of DBE spectral demands and distributions of isolator mechanical properties to the median isolator displacement (force) computed using best-estimate properties and spectrum-compatible DBE shaking

2. Determine the ratio of the 90%-ile estimate of the displacement (force) computed using a distribution of 150% DBE spectral demands and distributions of isolator mechanical properties to the median isolator displacement (force) computed using best-estimate properties and spectrum-compatible DBE shaking

3. Determine the number of sets of three-component ground motions to be used for response-history analysis to develop a reliable estimate of the median displacement (force).

In this study, we use sets of ground motions scaled to an appropriate distribution of spectral demand as well as motions compatible with a geomean spectrum, and an alternate presentation of isolator mechanical properties to that captured by lower- and upper-bound properties, to address these goals. Computations are performed for three sites (North Anna, Vogtle and Diablo Canyon), three types of isolators (LR and FP bearings for all three sites and LDR bearings for North Anna only), and realistic mechanical properties for these isolators.

The mechanical properties of LR and FP bearings will change with repeated cycling to large displacements at the isolated frequency as energy is dissipated by the lead core and by sliding friction, respectively. The heating of the lead core in the LR bearing and of the sliding surface (FP bearing) will reduce the energy dissipated by the isolation system at a given displacement and loading frequency. Studies are under way at the University at Buffalo (e.g., Kalpakidis 2008) to fully characterize the impact of these changes on the displacement response of an isolation system. The thermo-mechanical response of seismic isolation bearings is not addressed here.

1.6 Organization of the report

This introduction is followed by 6 sections. Section 2 introduces the base-isolation systems and numerical models analyzed in this study. Sections 3, 4 and 5 present the analyses for the sample CEUS rock, CEUS soil and WUS rock sites, respectively. Each of Sections 3, 4 and 5 includes information for DBE shaking, selection and scaling of ground motions, analysis procedure and results. Section 6 summarizes the results of Sections 3, 4 and 5 and provides recommendations on the analysis procedures for the seismic design of base-isolated nuclear structures, suitable for implementation in the next edition of ASCE Standard 4. Section 7 lists the references cited in this report.

SECTION 2
BASE ISOLATION SYSTEMS AND RESPONSE ANALYSIS

2.1 Base isolation hardware

Two types of elastomeric bearings and one sliding bearing are studied herein, namely, lead-rubber (LR), low-damping rubber (LDR) and Friction Pendulum™ (FP) bearings. All three are considered appropriate for the seismic isolation of nuclear and other mission-critical infrastructure. In this study, the isolators are assumed to be placed below a stiff concrete mat that supports an internal structure and a containment vessel. The isolated superstructure is assumed to be rigid, which is a good assumption because the translational periods of a containment vessel and an internal structure are typically less than 0.2 second.

Figure 2-1 presents a cut-away view of a LR bearing, composed of alternating layers of rubber (elastomer) and steel shims and the central lead core. The steel shims confine the deformation of the rubber in shear and increase the vertical stiffness of the isolator. (Insufficient vertical stiffness of isolators may result in rocking of the superstructure.) The lead core enables the isolator to dissipate substantial energy and its response to be modeled as bilinear. The restoring (re-centering) force is provided by the rubber. The characteristic strength Q_d of Figure 1-1 is governed by the dynamic yield strength of the lead core. The isolated period is determined by the shear stiffness of the elastomer, the bonded area and the total thickness of the rubber.

The construction of LDR bearings is similar to that of Figure 2-1 but without a central lead core. The force-displacement behavior of a LDR bearing is near linear and with an equivalent viscous damping ratio of between 2% to 4% of critical, depending on the bearing displacement (Kasalanti 2009).

Figure 2-2 presents components of two FP bearings: single concave (Figure 2-2a) and triple concave (Figure 2-2b). Figure 2-2a presents the articulated slider (which is coated with a low-friction composite material), a housing plate and a concave dish with a spherical inlay of stainless steel for a single concave bearing. The housing plate, shown in the right hand panel of Figure 2-2a, is inverted and installed on top of the articulated slider. The slider moves across the spherical surface during earthquake shaking. Earthquake-induced energy is dissipated by friction between the slider and the stainless steel inlay. The supported weight provides a restoring force. The isolated (sliding) period is determined by the radius of

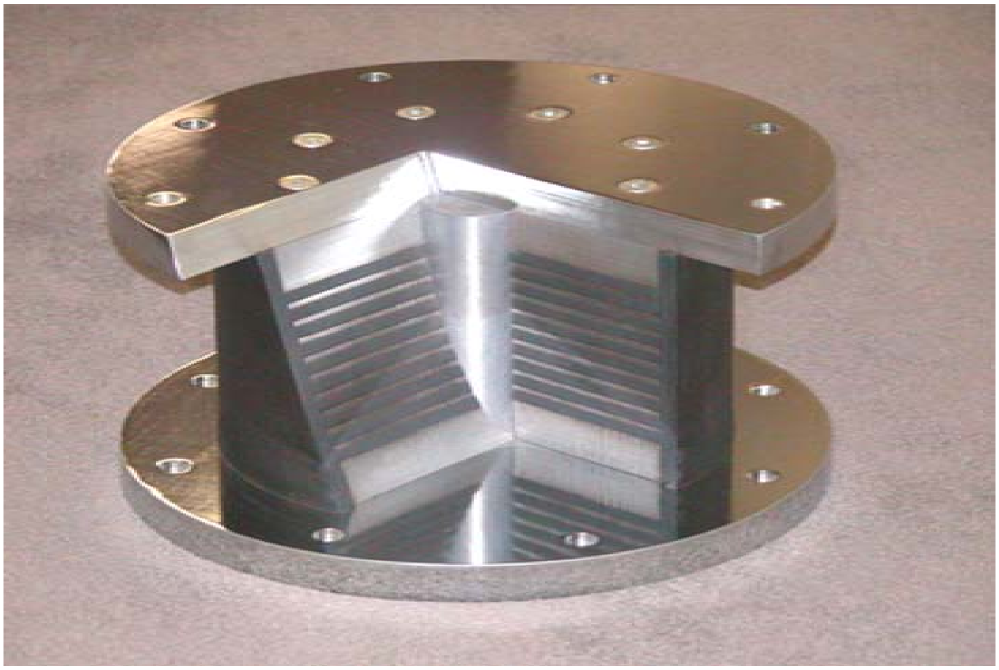

Figure 2-1. A cut-away view of a lead rubber bearing (courtesy of Dynamic Isolation Systems, Inc.)

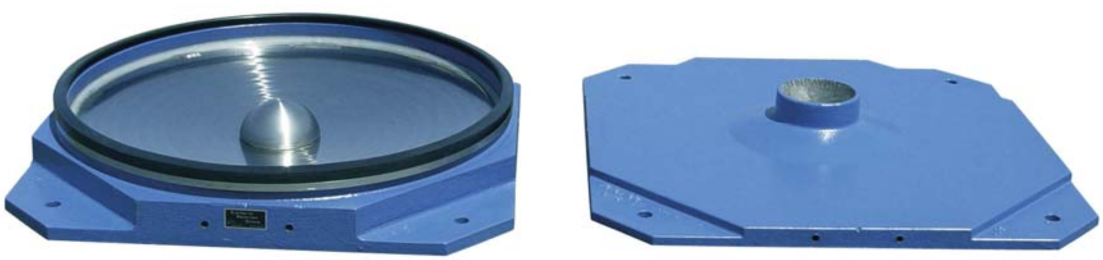

a. Single concave

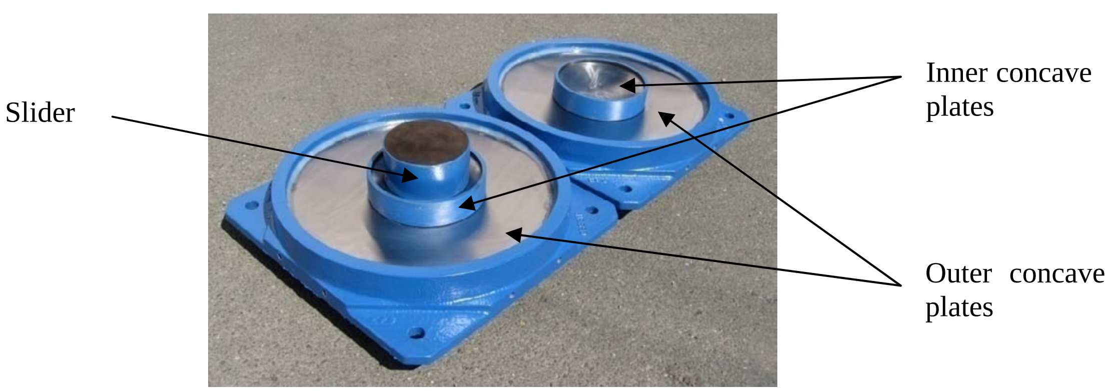

b. Triple concave

Figure 2-2. Friction Pendulum™ bearings (courtesy of Earthquake Protection Systems, Inc.)

the sliding surface. Figure 2-2b presents the slider and inner and outer concave plates for a triple concave bearing, where the isolated period is displacement dependent and determined by a combination of the radii of the sliding faces of the inner and outer plates (Fenz and Constantinou 2008a).

Constantinou et al. (2007) and Naeim and Kelly (1999) provide substantial information on the construction, analysis and design of elastomeric and sliding isolation systems for the interested reader.

2.2 Response-history analysis

SAP2000 Nonlinear (CSI 2007) was used to perform the response-history analysis of the models of base-isolated NPPs. Each model was composed of a rigid mass supported by a link element representing the isolation system. Each model had three degrees of freedom: two horizontal and one vertical. The models of the isolation systems are described in Section 2.3. The response-history analysis was performed using the Fast Nonlinear Analysis algorithm implemented in SAP2000 as Nonlinear Modal Time-History Analysis. Sample results were verified using an alternate algorithm in SAP2000 based on direct integration of the equations of motion.

For analysis of the (nonlinear) LR and FP isolation systems, 2% damping was assigned to each mode using values of effective isolation-system stiffness in the horizontal and vertical directions. In the horizontal directions, the effective stiffness was set equal to the post-yield stiffness of the isolation system. The effective stiffness in the vertical direction was set equal to the elastic stiffness for the LR isolation systems.

For analysis of the (linear) LDR isolation systems, 3% and 2% damping were assigned to the two horizontal modes and one vertical mode, respectively.

2.3 Models of isolation systems

The LR isolation systems were modeled using the “Rubber Isolator” link element in SAP2000. This element has coupled plasticity properties for the two horizontal displacements and linear stiffness properties for the vertical displacement. The plasticity model is similar to that of Figure 1-1 but the transition between the elastic stiffness and the post-yield stiffness is continuous. To study a wide range of isolation-system properties, 9 best-estimate models were prepared with characteristic strength Q_d equal to 3%, 6% and 9% of the supported weight W, and T_d (the period related to the post-yield stiffness of the isolator K_d through W) equal to 2, 3 and 4 seconds. Parameter T_v (the period related to the vertical stiffness of the isolation system K_v through W) was set to 0.05 second. Values of the key variables for the 9 best-estimate LR isolation-system models are presented in Table 2-1.

Friction Pendulum™ (FP) isolators were modeled using the "Friction Isolator" link element that has coupled plasticity properties for the two horizontal directions and a gap element in the vertical direction. The coefficient of friction for FP bearings depends on the sliding velocity and is computed in SAP2000 using the following equation (Constantinou et al. 1999, CSI 2007,)

$$\mu = \mu_{\max} - (\mu_{\max} - \mu_{\min}) \cdot e^{-aV} \tag{2.1}$$

where μ is the coefficient of sliding friction, varying between $\mu_{\max}$ and $\mu_{\min}$ (for high and very small velocities, respectively), a is a velocity-related parameter, and V is the sliding velocity. Figure 2-3 shows the velocity dependence of μ for a typical PTFE-type composite material in contact with polished stainless steel for a contact (normal) pressure of approximately 41 MPa. The curve of Figure 2-3 is generated using (2.1) and $\mu_{\max}$ = 6%, $\mu_{\min}$ = 3% and a = 55 sec/m (from the experimental data of Fenz and Constantinou 2008a). A value of a = 55 sec/m was adopted for this study. The hysteresis loop for the FP bearings will collapse to the bilinear loop of Figure 1-1 for Coulomb friction (i.e., $a = \infty$) with $Q_d = \mu_{\max} W$. Table 2-2 summaries the values of the key parameters for the 9 best-estimate FP isolation-system models analyzed in this study with $\mu_{\max}$ equal to 0.03, 0.06 and 0.09 and T_d equal to 2, 3 and 4 seconds. The yield displacement is set at 1 mm for all FP models but we note that the use of the triple concave FP bearing (e.g., Fenz and Constantinou 2008c) will increase the yield displacement to a value similar to that adopted for the LR models.

Low-damping rubber isolators were modeled in SAP2000 using the "Linear" link element where the elastic stiffness and damping can be assigned in each degree of freedom. Three best-estimate models were studied with T_h (the period related to the horizontal elastic stiffness of the isolator K_h through W) equal to 2, 3 and 4 seconds, and T_v equal to 0.05 second. Values of the key variables for the 3 best-estimate LDR isolation-system models are presented in Table 2-3.

2.4 Variations in material properties of isolators

Section 1.4 introduced the sources of variations in the mechanical properties of seismic isolators from the best-estimate values assumed for analysis and design. Variations in isolator properties are addressed in specifications and standards, including the AASHTO *Guide Specification for Seismic Isolation Design* (AASHTO 1999). The *Guide Specification* requires the analyst to estimate upper and lower bounds on the mechanical properties of the isolation system for the lifetime of the isolated bridge. Analysis is then performed for the best-estimate, lower-bound and upper-bound mechanical properties. An alternate approach was adopted here to enable efficient analysis and statistical interpretation of results.

To study the impact of these variations on the response of base-isolated NPPs, 2 sets of 30 mathematical models were developed for each best-estimate model of Table 2-1 through Table 2-3 by modifying the values of key parameters of the best-estimate model. For LR models, Q_d, K_d and K_v were assumed to vary; for FP models, only $\mu_{\max}$ was assumed to vary; and for LDR models, K_h and K_v were assumed to vary. One set of 30 models represents an isolation *system* with excellent control on the properties of individual isolators: the probability for the values of the key parameters of the isolation system described above to be within ±10% of the best-estimate values is 95% (Bin F1): upper- and lower-bound properties are +10% and -10% of the best-estimate properties, respectively, with 95% probability. The second set represents an isolation *system* with good control on the properties of individual isolators: the probability for the values of the key parameters of the isolation system to be within ±20% of the best-estimate values is 95% (Bin F2)[1]. We assume the distributions for the values of the key parameters to be normal. The criteria described herein require the coefficient of variation (i.e., the ratio of the standard deviation to the mean) of the normal distributions to be 0.05 for excellent control and 0.1 for good control. Figure 2-4 illustrates these distributions in parameters Q_d and K_d for LR isolation systems; for FP isolation systems, only Q_d varies and K_d is constant.

To develop the 2 sets of 30 mathematical models, 2 bins of 30 scale factors were generated first and presented in Table 2-4, where the factors for Bin F1 (F2) were obtained from a normal distribution with a mean of 1 and a standard deviation of 0.05 (0.1). Figure 2-5 presents the two normal distributions. For

[1] The ±10% and ±20% of best-estimate values apply to the mechanical properties of the isolation *system*. Given that an isolation system consists of a large number of isolators, larger percentage variations in the mechanical properties in individual isolators could be tolerated.

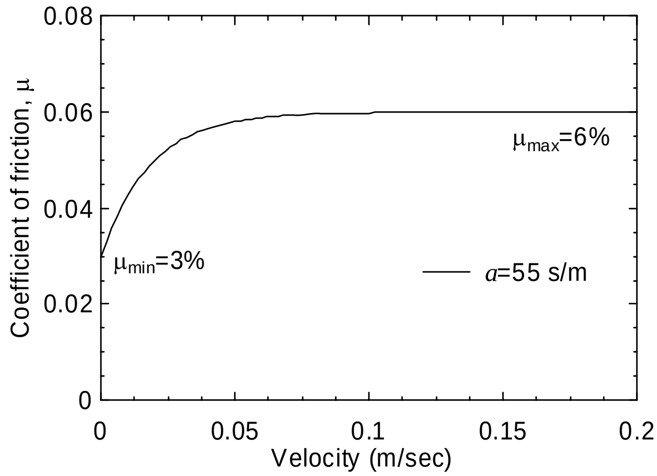

Figure 2-3. Influence of *a* on the velocity dependence of the coefficient of sliding friction

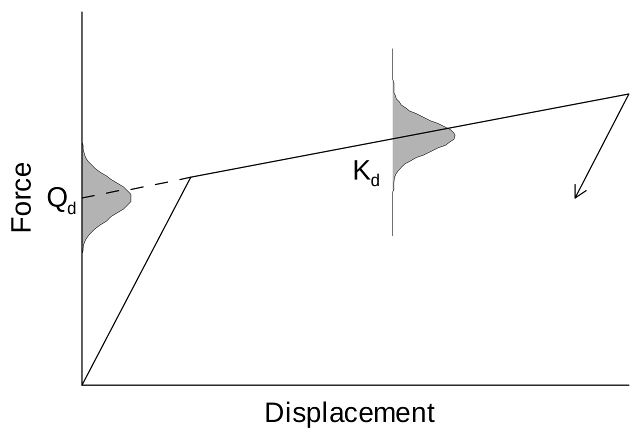

Figure 2-4. Variations in the mechanical properties of seismic isolation systems

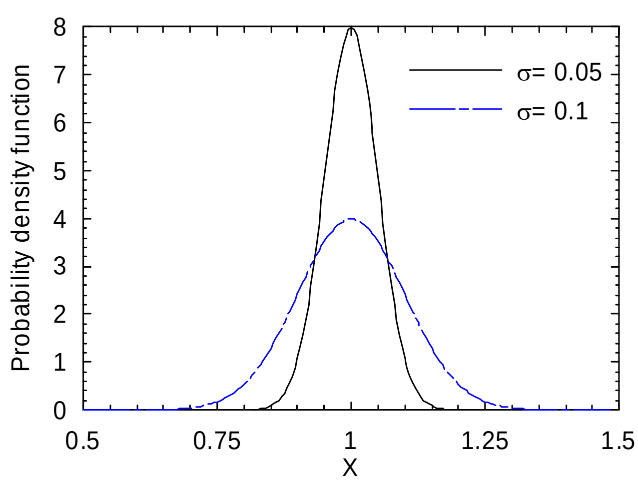

Figure 2-5. Normal distributions with a mean of 1 and standard deviations of 0.05 and 0.1

Table 2-1. Key parameters for the LR isolation systems[1]

Model no.	Model name	Q_d/W	T_d (sec)	T_v (sec)	u_y (mm)
LR-1	LR_T2Q3	0.03	2	0.05	25
LR-2	LR_T2Q6	0.06	2	0.05	25
LR-3	LR_T2Q9	0.09	2	0.05	25
LR-4	LR_T3Q3	0.03	3	0.05	25
LR-5	LR_T3Q6	0.06	3	0.05	25
LR-6	LR_T3Q9	0.09	3	0.05	25
LR-7	LR_T4Q3	0.03	4	0.05	25
LR-8	LR_T4Q6	0.06	4	0.05	25
LR-9	LR_T4Q9	0.09	4	0.05	25

1. See Figure 1-1 for definitions of Q_d, K_d and u_y; T_d is related to K_d through the supported weight, W, and T_v is related to the vertical stiffness of bearings through W.

Table 2-2. Key parameters for the FP isolation systems[1,2]

Model no.	Model name	$\mu_{\max}$	$\mu_{\min}$	a (s/m)	u_y (mm)
FP-1	FP_T2Q3	0.03	0.015	55	1
FP-2	FP _T2Q6	0.06	0.030	55	1
FP-3	FP _T2Q9	0.09	0.045	55	1
FP-4	FP _T3Q3	0.03	0.015	55	1
FP-5	FP _T3Q6	0.06	0.030	55	1
FP-6	FP _T3Q9	0.09	0.045	55	1
FP-7	FP _T4Q3	0.03	0.015	55	1
FP-8	FP _T4Q6	0.06	0.030	55	1
FP-9	FP _T4Q9	0.09	0.045	55	1

1. See Figure 2-3 for definitions of $\mu_{\max}$, $\mu_{\min}$ and a.
2. The yield displacement of 1 mm applies to the single concave FP bearing; the yield displacement of the triple concave FP bearing will approach that of the LR bearing.

Table 2-3. Key parameters for the LDR isolation systems

Model no.	Model name	T_h (sec)	T_v (sec)	Damping ratio
LDR-1	LDR_T2	2	0.05	0.03
LDR-2	LDR_T3	3	0.05	0.03
LDR-3	LDR_T4	4	0.05	0.03

Table 2-4. Scale factors for mechanical properties of bearings

i	F1	F2
1	0.894	0.787
2	0.918	0.836
3	0.931	0.862
4	0.940	0.881
5	0.948	0.896
6	0.955	0.910
7	0.961	0.922
8	0.966	0.933
9	0.971	0.943
10	0.976	0.952
11	0.981	0.962
12	0.985	0.970
13	0.990	0.979
14	0.994	0.987
15	0.998	0.996
16	1.002	1.004
17	1.006	1.013
18	1.011	1.021
19	1.015	1.030
20	1.019	1.039
21	1.024	1.048
22	1.029	1.057
23	1.034	1.067
24	1.039	1.078
25	1.045	1.090
26	1.052	1.104
27	1.060	1.119
28	1.069	1.138
29	1.082	1.165
30	1.106	1.213

each of these curves in Figure 2-5, the area under the curve was divided into 30 equal segments; the *midpoint* value[2] in each segment is reported in Table 2-4.

The generation of the 2 sets of 30 models for each LR isolation system is presented below to demonstrate the process. For each best-estimate model of Table 2-1, the values of Q_d, K_d and K_v were scaled by 2 sets of factors: [$F1_i^{Q_d}$, $F1_i^{K_d}$, $F1_i^{K_v}$] and [$F2_i^{Q_d}$, $F2_i^{K_d}$, $F2_i^{K_v}$], where $F1_i^{Q_d}$, $F1_i^{K_d}$ and $F1_i^{K_v}$ ($F2_i^{Q_d}$, $F2_i^{K_d}$ and $F2_i^{K_v}$) are the scale factors for Q_d, K_d and K_v, respectively, determined from bin F1 (F2) of Table 2-4 using the Latin Hypercube Sampling procedure (Nowak and Collins 2000) and i = 1 through 30. For each value of i, a new model was developed for each case of excellent and good control.

The implementation of the Latin Hypercube Sampling procedure that was used to select [$F1_i^{Q_d}$, $F1_i^{K_d}$, $F1_i^{K_v}$] to be applied to the parameters of the best-estimate model follows steps 1 through 4:

1. Develop a 30×3 matrix with entries in each column equal to those in the second column of Table 2-4.
2. Select the first combination of [$F1_i^{Q_d}$, $F1_i^{K_d}$, $F1_i^{K_v}$] by randomly selecting a value from each column.
3. Select the second combination by randomly choosing one of the 29 remaining values in each column.
4. Continue this process until all 30 combinations have been assembled.

The procedures described above were repeated for the FP and LDR isolation systems of Table 2-2 and Table 2-3, respectively. These models were used in the response-history analysis to study the impact of variations in the mechanical properties of isolation systems on the response of base-isolated NPPs.

---

[2] The *midpoint* value divides the area under the curve in each segment into halves.

SECTION 3
RESPONSE ANALYSIS FOR CEUS ROCK SITES

3.1 Design basis earthquake

The site of the North Anna nuclear power plant (NPP) in Louisa County, Virginia, is a representative rock site for NPPs in the Central and Eastern US (CEUS). The Design Basis Earthquake (DBE) for the study at the North Anna site is introduced in this subsection. Section 3.2 presents the development of DBE-matched ground motions used in the response-history analysis. Section 3.3 defines four sets of response-history analyses to investigate the impact of distribution in both spectral demands and bearing properties on the response of base-isolated nuclear structures. Analysis results are presented in Sections 3.4.1 through 3.4.3 for Lead Rubber (LR), Friction Pendulum (FP) and Low Damping Rubber (LDR) bearings, respectively.

The horizontal and vertical DBE spectra for the North Anna site are presented in Figure 3-1 using both normal and logarithmic scales. The horizontal spectrum of Figure 3-1 is a uniform-risk spectrum (URS) corresponding to a mean annual frequency of exceedance (MAFE) of 10^{-5} based on the data presented in an Early Site Permit (ESP) Application report for North Anna (Dominion Nuclear North Anna, LLC 2006). The horizontal DBE spectrum of Figure 3-1 was scaled using the V/H factors of Table 3-1 to form the vertical DBE spectrum.

The technical basis for the V/H factors of Table 3-1 is Bozorgnia and Campbell (2004). They studied the ratio of V/H using 443 accelerograms from 36 worldwide earthquakes with moment magnitude (M_w) between 4.7 and 7.7 and the distance to seismogenic rupture (r_{seis}) smaller than 60 km. They concluded that V/H is strongly dependent on natural period, distance and site condition and weakly dependent on magnitude and faulting mechanism. They developed a set of recommendations for V/H that are presented in Figure 3-2. The ratios of Figure 3-2a are for firm soil sites (NEHRP Site Class D) and those of Figure 3-2b are for firm rock, soft rock and very firm soil sites (primarily NEHRP Site Class C and B/C boundary).

Both panels of Figure 3-2 indicate V/H equal to 0.5 at periods greater than 0.3 second although Bozorgnia and Campbell note that V/H equal to 0.5 at periods greater than 1 second is conservative for soil sites (Figure 3-2a) but unconservative for rock sites (Figure 3-2b), where V/H is slightly greater than 0.5 at 1 second, approaching a value of 0.7 at about 4 seconds.

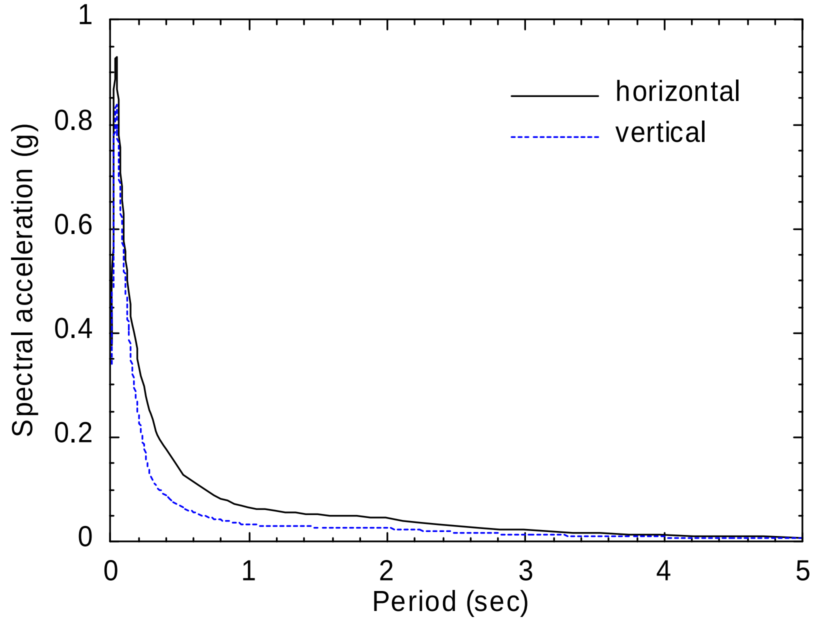

a. normal scale

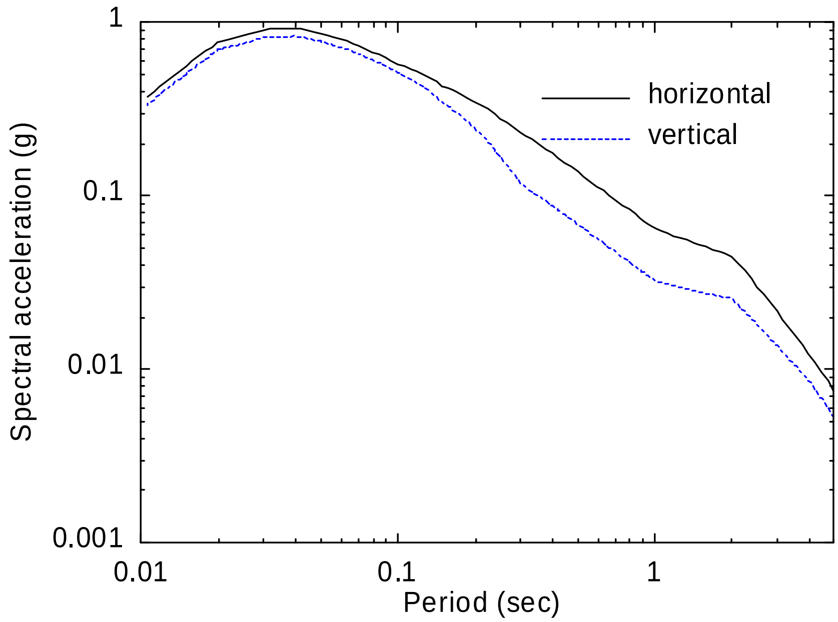

b. logarithmic scale

Figure 3-1. Horizontal and vertical DBE spectra for the North Anna NPP site and 5% damping in normal and logarithmic scales

Table 3-1. V/H for the North Anna NPP sites

Period (sec)	V/H
≤ 0.1	0.9
0.3	0.5
1	0.5
≥ 4	0.7

Table 3-2. Analysis sets for this study

Set	Ground motions	Number of models	Quality control on individual isolators	Number of realizations for force and displacement
G0	100% (150%) of the DBE spectrum-compatible ground motions of Figure 3-5	1	NA	30
M0	100% (150%) of the maximum-minimum spectra compatible ground motions of Figure 3-6	1	NA	30
M1	100% (150%) of the maximum-minimum spectra compatible ground motions of Figure 3-6	30	excellent	900
M2	100% (150%) of the maximum-minimum spectra compatible ground motions of Figure 3-6	30	good	900

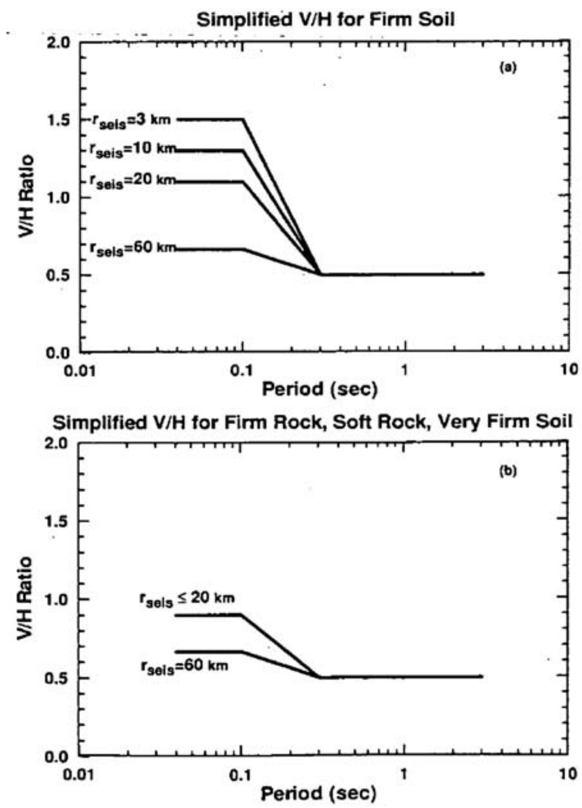

Figure 3-2. Simplified V/H response spectral ratios of Bozorgnia and Campbell (2004)

Since the V/H spectral ratios of Figure 3-2 are distance dependent, the seismic hazard curves and deaggregation results for the North Anna site were generated using USGS Java ground motion parameter calculator (USGS 2009b) and interactive deaggregation tool (USGS 2008) to determine the controlling distance. Figure 3-3 presents the deaggregation of the hazard at periods of 0.2 and 2 seconds and a MAFE of 2×10^{-4} for North Anna[1]. In Figure 3-3, the distance for the peak magnitude-distance (M_w-r) bin is 14.0 km at a period of 0.2 second and 540 km at a period of 2 seconds.

The V/H spectral ratios of Table 3-1 for the North Anna NPP site are based on the ratios of Figure 3-2b, modified as noted above at a period of 4 second, and the governing distances of Figure 3-3. Linear interpolation is used between the reported periods.

3.2 Selection and scaling of ground motions

3.2.1 DBE spectrum-compatible ground motions

Since the number of strong ground-motion records in CEUS is limited, synthetic ground motions were developed in 2 steps. Step 1 involved the use of the computer code "Strong Ground Motion Simulation" (SGMS, Halldorsson 2004) to generate CEUS-type seed ground motions, which were then spectrally matched to the DBE spectra of Figure 2 in step 2 using the computer code RSPMATCH (Abrahamson 1998).

The SGMS code is based on the Specific Barrier Model, which provides a complete and self-consistent description of the heterogeneous earthquake faulting process and can capture the high-frequency content in CEUS ground motions (Halldorsson and Papageorgiou 2005). RSPMATCH adjusts the spectral ordinates of the seed motions by adding wavelets to the acceleration time series in the time domain.

The SGMS code requires the user to provide information on the site condition and the magnitude and distance for the scenario event of interest to simulate ground motions. For the North Anna study, the assumed site condition is rock. Given that the ground motions were being prepared for analysis of base-

---

[1] The USGS interactive deaggregation tool now provides information for an annual frequency of exceedance smaller than 2×10^{-4}, which was the smallest frequency available at the time the study of this section was initiated. The deaggregation results for North Anna at a MAFE of 10^{-4} and periods of 0.2 and 2 seconds are not significantly different than those presented in Figure 3-3. The modal events at MAFE of 10^{-4} and 2×10^{-4} are nearly identical at periods of 0.2 and 2 seconds.

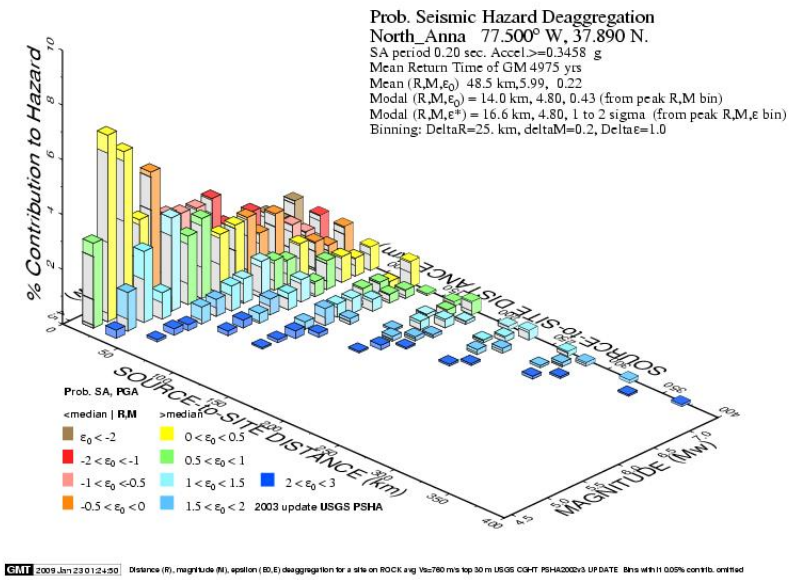

a. 0.2 second

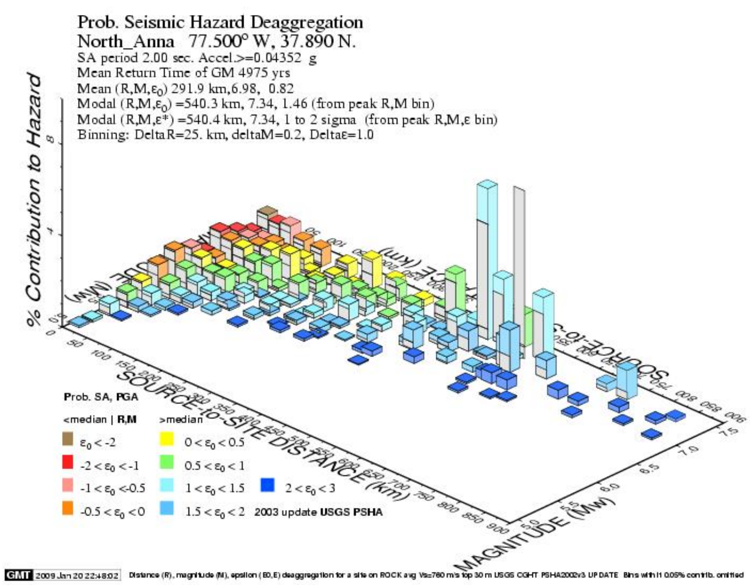

b. 2 seconds

Figure 3-3. Deaggregation of the seismic hazard at periods of 0.2 and 2 seconds at an annual frequency of exceedance of $2{\times}10^{-4}$ for the North Anna NPP site

isolated structures, we developed seed motions initially using the modal event in Figure 3-3b, namely, M_w = 7.3 and r = 540 km. The spectral shapes of the resultant ground motions are significantly different from the DBE spectrum of Figure 3-1. This significant difference in spectral shape made it extremely difficult to use the spectrum-matching routine because the solution would not converge. Instead, we used the modal and mean events in Figure 3-3a, namely, [M_w = 4.8 and r = 14 km] and [M_w = 6.0 and r = 48 km], to develop the seed ground motions.

Thirty sets of DBE spectrum-compatible ground motions were developed using the procedure described above. Each set of ground motions includes 2 horizontal components and a vertical component. Panels a, c and e of Figure 3-4 present a sample set of DBE spectrum-compatible ground motions and panels b, d and f present the target and achieved spectral accelerations for the time series of panels a, c and e, respectively. The spectral accelerations for each time series of panels a, c and e of Figure 3-4 closely match the target. Panels a, b and c of Figure 3-5 present the spectral accelerations for horizontal components 1 and 2 and the vertical component, respectively, of all 30 sets of DBE spectrum-compatible ground motions. Each spectrum of Figure 3-5 closely matches the target.

3.2.2 Maximum-minimum spectra compatible ground motions

A second set of 30 pairs ground motions, termed maximum-minimum spectra compatible ground motions, were developed by amplitude scaling the 30 sets of DBE spectrum-compatible ground motions of Figure 3-5 to represent the maximum spectral demand and the demand at the orientation perpendicular to the maximum direction, termed the *minimum* demand.

For each set of DBE spectrum-compatible motions, the 2 horizontal components were amplitude scaled by F_{H_i} and $1/F_{H_i}$, respectively, and the vertical component was amplitude scaled by F_{V_i}. The factor F_{H_i} (F_{V_i}) was determined using a lognormal distribution with θ of 1.3 (1.0) and β of 0.13 (0.18) using the Latin Hypercube Sampling procedure (Nowak and Collins 2000). Panels a, b and c of Figure 3-6 present the spectral accelerations for the horizontal components 1 and 2 and vertical component, respectively, of all 30 sets of DBE spectrum-compatible ground motions.

The distributions of F_{H_i} and F_{V_i} are based on the study of Huang et al. (2007, 2008), where the ratio of maximum to geometric-mean (hereafter termed geomean) spectral demands was studied using 147 pairs of near-fault records with M_w of 6.5 and greater and the closest site-to-source distance of 15 km and less. In their study, the maximum spectral demand at a given period was defined as the maximum of the

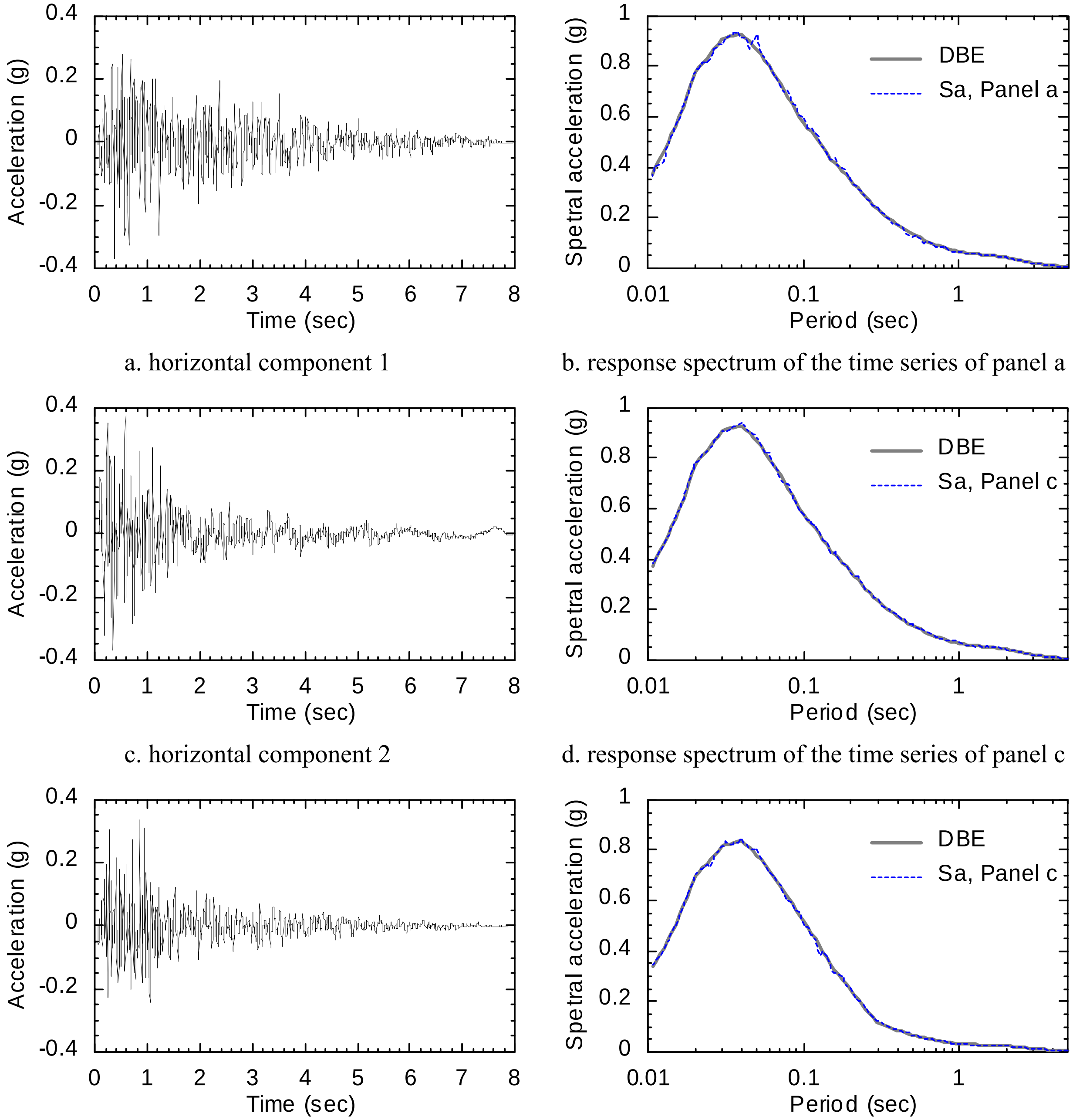

a. horizontal component 1 b. response spectrum of the time series of panel a

c. horizontal component 2 d. response spectrum of the time series of panel c

e. vertical component f. response spectrum of the time series of panel e

Figure 3-4. Sample spectrally matched acceleration time series and the corresponding 5% damped response spectra

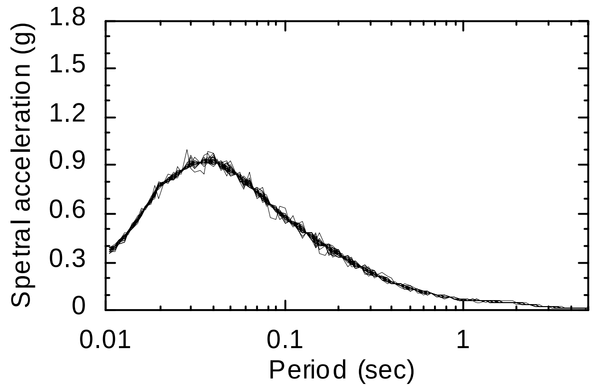

a. horizontal component 1

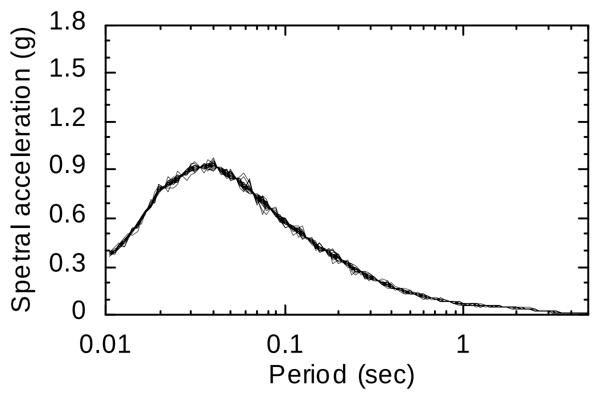

b. horizontal component 2

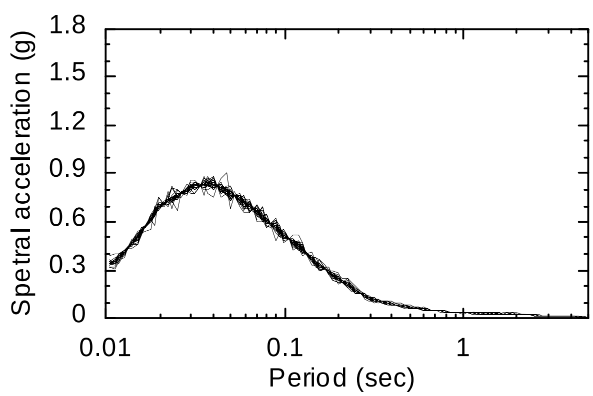

c. vertical component

Figure 3-5. Five-percent damped response spectra for the 30 sets of DBE spectrum-compatible ground motions for the North Anna site

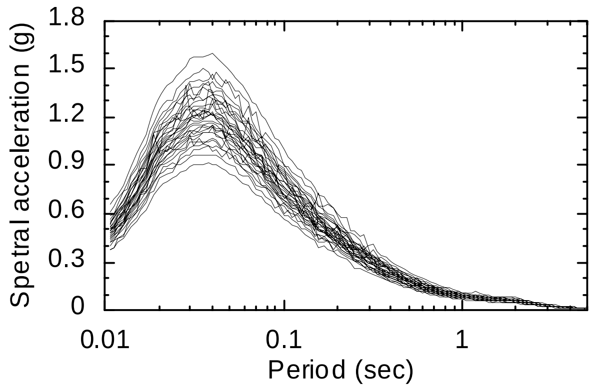

a. maximum component

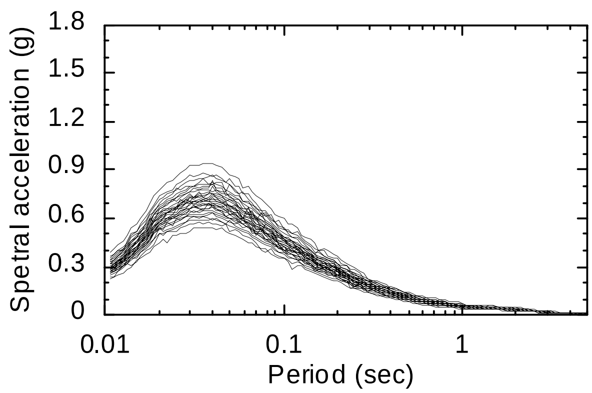

b. minimum component

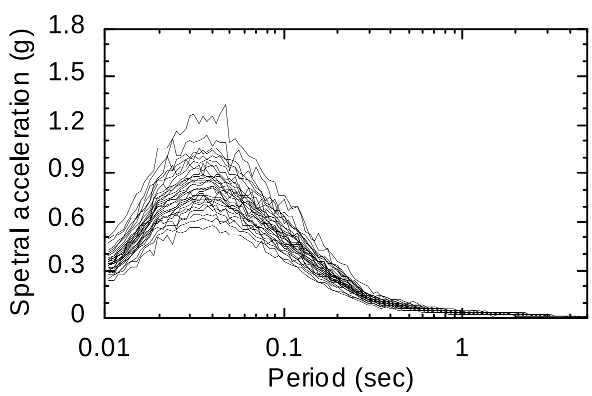

c. vertical component

Figure 3-6. Five-percent damped response spectra for the 30 sets of maximum-minimum DBE spectra-compatible ground motions for the North Anna site

spectral accelerations at orientations between 0° to 180° for a pair (the two orthogonal horizontal components) of ground motions. The solid curves of Figure 3-7a presents the 16th, 50th (median) and 84th percentiles of the ratio of the maximum demand to *GMRotI50*, which is an orientation-independent geomean demand defined in Boore et al. (2006). The median (θ) of the ratio varies between 1.25 and 1.35 at periods greater than 2 seconds. Figure 3-7b presents the logarithmic standard deviation (β) of the ratio, varying between 0.11 and 0.13 at periods greater than 2 seconds.

Beyer and Bommer (2006) investigated the ratio of the maximum to recorded geomean spectral demands using 949 earthquake records with moment magnitude ranging between 4.2 and 7.9 and hypocentral distance ranging between 5 and 200 km. They reported that the median of the ratio varied between 1.2 and 1.3, depending on the period (see the dotted line of Figure 3-7a): a similar result to that of Huang et al. (2008).

3.3 Analysis sets

Response-history analysis was performed for two intensities of shaking: 1) 100% DBE shaking using the 60 sets of ground motions of Figure 3-5 and Figure 3-6, and b) 150% DBE shaking using the ground motions of Figure 3-5 and Figure 3-6 but with the amplitude of the acceleration time series multiplied by 1.5.

At each intensity level, 4 sets of analyses were performed for each best-estimate model of Tables 2-1 through 2-3 and the 60 corresponding property-varied models to study the impact of variations in spectral demands and the mechanical properties of isolation systems on the response of isolated NPPs. Table 3-2 summarizes the 4 sets used for this study, denoted G0, M0, M1 and M2.

Set G0 involves response-history analysis of a best-estimate model subjected to 100% (150%) of the 30 sets of DBE spectrum-compatible ground motions of Figure 3-5 and produces 30 realizations for each of peak bearing displacement and shearing force in the horizontal plane. Here the letter G stands for geomean since the target horizontal DBE spectrum of Figure 3-1 is a geomean of two horizontal components and the number 0 is used to denote analysis performed using best-estimate models. The data developed from analysis of Set G0 is used to benchmark all other results.

Set M0 is similar to Set G0 but uses 30 maximum-minimum spectrum-compatible ground motions of Figure 3-6 for analysis of 100% and 150% DBE shaking. For Set M1 (M2), each of the 30 models associated with a given best-estimate model and scale factors in column F1 (F2) of Table 2-2 is analyzed

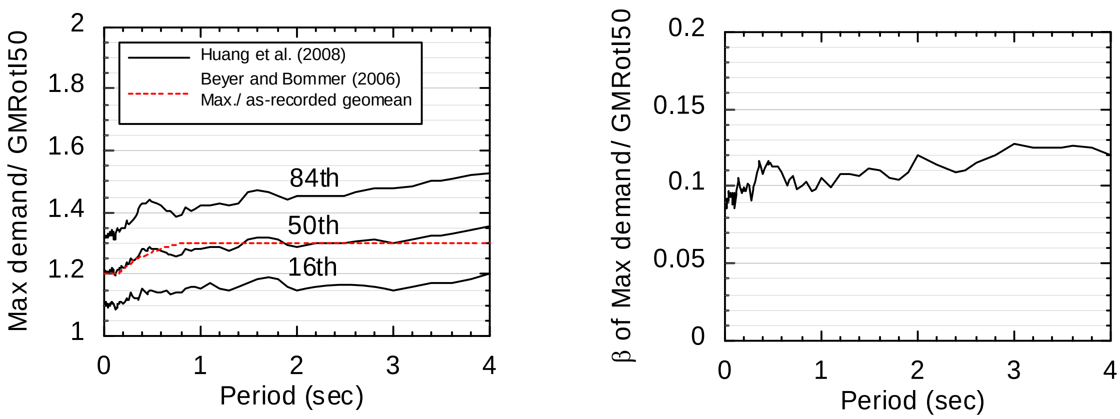

a. 16th, 50th and 84th percentiles

b. dispersion

Figure 3-7. Distribution of the ratio of maximum spectral demand and GMRotI50

using the 30 maximum-minimum spectrum-compatible ground motions of Figure 3-6 for 100% and 150% DBE shaking. At a given intensity, Sets M1 and M2 each produce 900 realizations (30 sets of ground motions × 30 models) for peak horizontal bearing displacement and transmitted shearing force.

3.4 Analysis results

3.4.1 Lead Rubber (LR) isolation systems

Goodness-of-fit test

All realizations in an analysis set are assumed to distribute lognormally with median (θ) and logarithmic standard deviation (β) computed using the following equations:

$$\theta = \exp\left(\frac{1}{n}\sum_{i=1}^{n}\ln y_i\right) \tag{3.1}$$

$$\beta = \sqrt{\frac{1}{n-1}\sum_{i=1}^{n}(\ln y_i - \ln\theta)^2} \tag{3.2}$$

where n is the total number of the realizations (peak displacement or force response) in an analysis set: 30 for Sets G0 and M0, and 900 for Sets M1 and M2. Variable y_i is the *i*th realization in an analysis set.

To verify the assumption for the distribution of the realizations, goodness-of-fit tests were performed and sample results are presented in Figure 3-8 using the realizations associated with Model LR_T3Q6 and 100% DBE shaking. Panels a, c and e present the results for peak displacement for Sets G0, M0 and M1, respectively, and panels b, d and f present results for peak transmitted shearing force. The results for Set M2 show a similar trend to those of Figure 3-8 and are not here. Each panel includes two curves. The solid curve is the cumulative distribution function (CDF) of the n realizations, which were sorted from smallest to largest and assigned a probability from $1/n$ to 1.0 in increments of $1/n$, and the dotted curve is the CDF of a lognormal distribution with the median and dispersion estimated using (3.1) and (3.2). Based on the results of the goodness-of-fit tests, we consider it acceptable to assume that the peak displacement and transmitted shearing force distribute lognormally.

Medians and logarithmic standard deviations of peak displacement and force

Table 3-3 presents θ and β of peak displacement and transmitted shearing force for each case, model and shaking intensity analyzed for LR isolation systems. Table 3-4 presents the ratio of θ and β

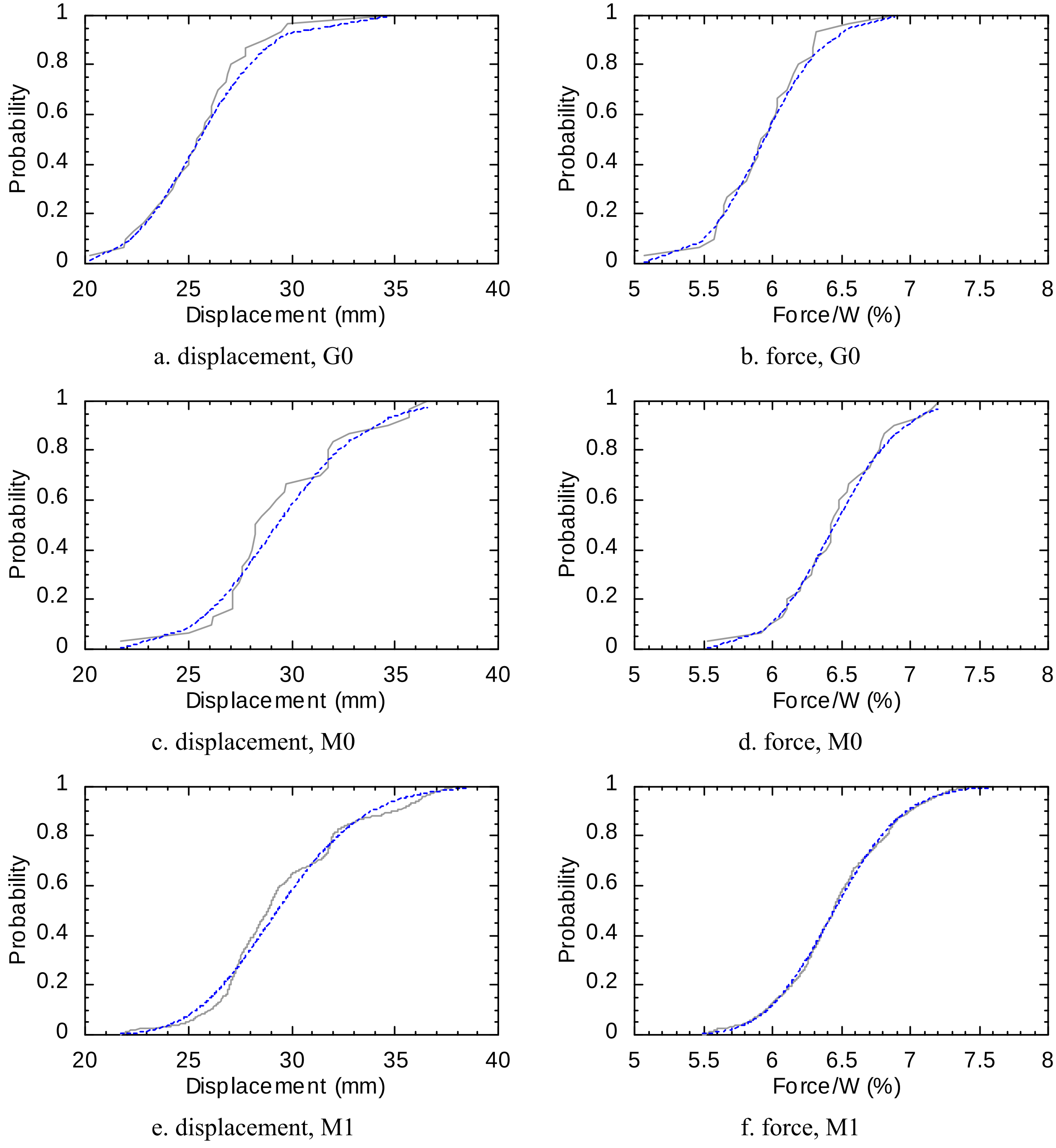

a. displacement, G0

b. force, G0

c. displacement, M0

d. force, M0

e. displacement, M1

f. force, M1

Figure 3-8. Goodness-of-fit tests for Model LR_T3Q6 subjected to 100% DBE shaking for Sets G0, M0 and M1

Table 3-3. Medians (θ) and dispersions (β) of peak displacement and shearing force for Sets G0, M0, M1 and M2 and 100% and 150% DBE shaking for LR systems

Model	100% DBE								150% DBE							
	θ (mm for displacement; %W for force)				β				θ (mm for displacement; %W for force)				β			
	G0	M0	M1	M2	G0	M0	M1	M2	G0	M0	M1	M2	G0	M0	M1	M2
Displacement																
LR_T2Q3	31	35	35	35	0.10	0.12	0.12	0.13	43	50	50	50	0.13	0.13	0.14	0.14
LR_T2Q6	23	26	26	26	0.09	0.09	0.10	0.11	32	37	37	37	0.09	0.12	0.12	0.13
LR_T2Q9	20	23	23	23	0.07	0.09	0.10	0.11	27	31	31	31	0.10	0.12	0.12	0.13
LR_T3Q3	35	40	40	40	0.11	0.13	0.13	0.14	50	58	58	58	0.13	0.17	0.17	0.18
LR_T3Q6	25	29	29	29	0.11	0.11	0.11	0.12	36	41	41	42	0.13	0.12	0.13	0.14
LR_T3Q9	21	24	24	24	0.10	0.12	0.12	0.12	29	33	33	33	0.12	0.13	0.13	0.14
LR_T4Q3	37	43	43	43	0.11	0.14	0.15	0.15	52	63	63	62	0.12	0.17	0.17	0.17
LR_T4Q6	27	30	30	31	0.11	0.11	0.11	0.12	38	43	43	43	0.14	0.14	0.14	0.14
LR_T4Q9	22	25	25	25	0.10	0.12	0.12	0.13	30	34	34	35	0.12	0.14	0.14	0.15
Force																
LR_T2Q3	5.7	6.3	6.3	6.3	0.07	0.08	0.09	0.09	7.2	8.0	8.0	8.0	0.09	0.09	0.09	0.10
LR_T2Q6	6.9	7.5	7.5	7.5	0.07	0.06	0.06	0.08	8.6	9.3	9.3	9.3	0.05	0.06	0.06	0.07
LR_T2Q9	8.3	9.1	9.1	9.1	0.06	0.06	0.07	0.09	10.3	11.0	11.0	11.0	0.05	0.07	0.07	0.09
LR_T3Q3	4.3	4.6	4.6	4.6	0.06	0.06	0.07	0.08	5.1	5.6	5.6	5.6	0.06	0.09	0.09	0.09
LR_T3Q6	5.9	6.5	6.4	6.4	0.06	0.06	0.06	0.08	7.1	7.5	7.5	7.5	0.05	0.05	0.05	0.07
LR_T3Q9	7.5	8.0	8.0	8.0	0.07	0.07	0.07	0.09	9.0	9.5	9.5	9.5	0.05	0.05	0.06	0.08
LR_T4Q3	3.7	4.0	4.0	4.0	0.04	0.05	0.06	0.08	4.2	4.5	4.5	4.5	0.04	0.06	0.07	0.10
LR_T4Q6	5.6	6.0	6.0	6.0	0.05	0.05	0.06	0.08	6.5	6.8	6.8	6.8	0.04	0.04	0.05	0.08
LR_T4Q9	7.2	7.7	7.7	7.7	0.06	0.06	0.07	0.09	8.5	9.0	9.0	9.0	0.05	0.05	0.05	0.08

Table 3-4. Ratios of median (θ) and dispersion (β) of peak displacement and shearing force for Sets G0, M0, M1 and M2 and 100% and 150% DBE shaking for LR systems

Model	100% DBE						150% DBE					
	Ratio of θ			Ratio of β			Ratio of θ			Ratio of β		
	$\frac{M0}{G0}$	$\frac{M1}{M0}$	$\frac{M2}{M1}$	$\frac{M0}{G0}$	$\frac{M1}{M0}$	$\frac{M2}{M1}$	$\frac{M0}{G0}$	$\frac{M1}{M0}$	$\frac{M2}{M1}$	$\frac{M0}{G0}$	$\frac{M1}{M0}$	$\frac{M2}{M1}$
Displacement												
LR_T2Q3	1.15	1.00	1.00	1.20	1.00	1.02	1.17	1.00	1.00	1.07	1.01	1.04
LR_T2Q6	1.14	1.00	1.00	1.03	1.06	1.11	1.16	1.00	1.00	1.36	1.00	1.08
LR_T2Q9	1.13	1.00	1.00	1.25	1.04	1.11	1.13	1.00	1.00	1.23	0.99	1.05
LR_T3Q3	1.14	1.00	1.01	1.18	1.01	1.06	1.18	1.00	1.00	1.37	0.99	1.02
LR_T3Q6	1.15	1.00	1.00	1.06	0.98	1.07	1.15	1.00	1.00	0.95	1.02	1.08
LR_T3Q9	1.12	1.00	1.00	1.17	0.97	1.02	1.14	1.00	1.01	1.11	0.99	1.07
LR_T4Q3	1.17	1.00	1.00	1.33	1.01	1.04	1.21	1.00	0.99	1.44	1.00	1.03
LR_T4Q6	1.13	1.00	1.00	1.05	1.04	1.09	1.15	1.00	1.00	1.01	1.01	1.04
LR_T4Q9	1.13	1.00	1.00	1.16	1.01	1.05	1.15	1.01	1.01	1.23	1.01	1.06
Force												
LR_T2Q3	1.10	1.00	1.00	1.16	1.02	1.07	1.11	1.00	1.00	1.04	1.03	1.11
LR_T2Q6	1.10	1.00	1.00	0.91	1.05	1.21	1.09	1.00	1.00	1.23	1.00	1.18
LR_T2Q9	1.09	1.00	1.00	1.18	1.11	1.23	1.07	1.00	1.00	1.23	1.08	1.20
LR_T3Q3	1.07	1.00	1.00	1.15	1.05	1.18	1.08	1.00	1.00	1.46	1.00	1.09
LR_T3Q6	1.09	1.00	1.00	0.98	1.05	1.24	1.06	1.00	1.00	0.88	1.14	1.38
LR_T3Q9	1.07	1.00	1.00	1.02	1.07	1.23	1.06	1.00	1.00	0.97	1.19	1.37
LR_T4Q3	1.06	1.00	1.00	1.30	1.14	1.39	1.08	1.00	0.99	1.56	1.12	1.35
LR_T4Q6	1.07	1.00	1.00	1.04	1.12	1.33	1.05	1.00	1.00	0.94	1.26	1.51
LR_T4Q9	1.07	1.00	1.00	0.98	1.12	1.29	1.06	1.00	1.00	0.95	1.21	1.48

between Sets M0 and G0, Sets M1 and M0 and Sets M2 and M1 for each model and shaking intensity. Table 3-5 presents the ratios of θ and β at 150% to 100% DBE shaking. The key observations include:

1) For 100% (150%) DBE shaking, the values of θ of Table 3-3 for displacement range between 20 (27) and 43 (63) mm and those for transmitted shearing force range between 3.7 (4.2) and 9.1 (11.0) percent of the supported weight. For 100% DBE shaking, the values of θ for the models with $Q_d = 0.09W$ and $0.06W$ are close to the yield displacement of the LR bearings (25 mm). Such isolation systems make little sense for rock sites in the CEUS and should not be used. The results for those isolation systems in Table 3-3 through Table 3-7 are shaded and not discussed further in this report.

2) In Table 3-4, the ratios of θ for M1/M0 and M2/M1 are equal to 1 for all models with $Q_d = 0.03W$ and shaking intensities. The median response for analyses accounting for variability in the mechanical properties of the isolation system (i.e., M1 and M2) can be estimated without bias using analysis of a best-estimate model (i.e. M0).

3) In Table 3-4, the ratios of θ for M0/G0 for displacement range between 1.14 and 1.21 and those for shearing force range between 1.06 and 1.11 for all models with $Q_d = 0.03W$, depending on the degree of nonlinearity. If analysis is performed using geomean-spectrum-compatible ground motions, the median displacement should be increased by 15% to 20% and the median shearing force should be increased by 10% to address variability in spectral demands.

4) In Table 3-5, the ratio of θ at 150% to 100% DBE shaking for a given model and analysis set (for example, the θ (= 43 mm) for LR_T2Q3 and G0 for 150% DBE shaking divided by θ (= 31 mm) for 100% DBE shaking[2]) ranges between 1.40 and 1.47 for displacement and between 1.13 and 1.26 for shearing force for all models with $Q_d = 0.03W$. The ratio of θ does not vary significantly for displacement but shows dependency on T_d for shearing force. Such ratios could be used to estimate median and other fractile isolator responses in the absence of computations for 150% DBE shaking as noted below.

[2] Each value of θ reported in Table 3-3 for displacement was rounded to the nearest mm. The ratios of θ in Table 3-5 were not computed using the rounded numbers. For example, the ratio of θ of Table 3-5 for displacement, LR_2Q3 and G0, equal to 1.41, was computed by dividing 43.1 mm by 30.6 mm.

Table 3-5. Ratios of the statistics of Table 3-3 at 150% to 100% DBE shaking

Model	θ				β			
	G0	M0	M1	M2	G0	M0	M1	M2
Displacement								
LR_T2Q3	1.41	1.43	1.43	1.43	1.21	1.08	1.09	1.12
LR_T2Q6	1.40	1.42	1.42	1.41	0.96	1.26	1.18	1.15
LR_T2Q9	1.35	1.36	1.36	1.37	1.32	1.29	1.23	1.17
LR_T3Q3	1.42	1.47	1.46	1.46	1.15	1.33	1.30	1.25
LR_T3Q6	1.42	1.41	1.42	1.42	1.21	1.08	1.12	1.13
LR_T3Q9	1.36	1.38	1.38	1.38	1.15	1.10	1.13	1.18
LR_T4Q3	1.40	1.45	1.44	1.43	1.07	1.16	1.15	1.14
LR_T4Q6	1.40	1.42	1.42	1.42	1.31	1.26	1.22	1.16
LR_T4Q9	1.36	1.39	1.39	1.40	1.12	1.18	1.19	1.21
Force								
LR_T2Q3	1.25	1.26	1.26	1.26	1.19	1.07	1.07	1.10
LR_T2Q6	1.24	1.23	1.23	1.23	0.77	1.05	1.00	0.97
LR_T2Q9	1.24	1.21	1.21	1.22	0.97	1.02	0.98	0.96
LR_T3Q3	1.18	1.20	1.20	1.20	1.07	1.36	1.30	1.20
LR_T3Q6	1.20	1.17	1.17	1.17	0.89	0.80	0.87	0.97
LR_T3Q9	1.20	1.19	1.19	1.19	0.79	0.75	0.83	0.92
LR_T4Q3	1.13	1.14	1.14	1.14	1.00	1.20	1.19	1.15
LR_T4Q6	1.16	1.14	1.14	1.14	0.85	0.77	0.87	0.98
LR_T4Q9	1.18	1.17	1.17	1.17	0.78	0.76	0.82	0.94

5) In Table 3-3, the values of β of Table 3-3 for displacement range between 0.10 and 0.18 and those for transmitted shearing force range between 0.04 and 0.10 for all models with $Q_d = 0.03W$. The dispersion in displacement is higher than for transmitted shearing force, which is an expected result. Although there are significant percentage differences between Sets G0 and M2 for β (e.g., the percentage increase in β is 150% between Sets G0 and M2 for transmitted shearing force for model LR_T4Q3 and 150% DBE shaking), all values of β are small.

The number of pairs of ground motions required to achieve a reliable estimate of median response depends on the dispersion in the response and the required precision and confidence level for the estimate. For a lognormal distribution with a median of θ and a logarithmic standard deviation of β, the number of realizations (n) required to estimate the median within a range of $\theta(1+X)$ with $Z\%$ of confidence can be computed as (Huang et al. 2008b)

$$n = \left(\frac{\Phi^{-1}(1-\frac{\alpha}{2}) \cdot \beta}{\ln(1+X)} \right)^2 \tag{3.3}$$

where Φ^{-1} is the inverse standardized normal distribution function and $\alpha = 1 - Z\%$. If we assume that the response-history analysis is performed using geomean-spectrum-compatible ground motions (i.e., Set G0) and the dispersion in the peak response is no greater than 0.15 per Table 3-3, the minimum number of pairs of ground motions per (3.3) to ensure a 90% confidence of the true median displacement being within ±10% of the estimated value is 7.

Scale factors for responses with 1% (10%) probability of exceedance at 100% (150%) DBE shaking

As noted previously, ASCE 43 writes that nuclear structures should achieve two performance goals: 1) less than 1% probability of unacceptable performance for DBE shaking, and 2) less than 10% probability of unacceptable performance for shaking equal to 150% of the DBE ground motion. The computation of the probability of unacceptable performance involves the development of the fragility curves for isolated nuclear structures (Reed and Kennedy 1994, Kennedy 1999), which is beyond the scope of this study. Instead of computing the probability of unacceptable performance, we present factors to scale the median responses for Sets G0 and M0 and 100% DBE shaking to the responses corresponding to 1) 1% probability of exceedance (PE) for Sets M1 and M2 for 100% DBE shaking, and 2) 10% PE for Sets M1 and M2 for 150% DBE shaking. The factors for isolation-system displacement and transmitted shearing force are presented in Table 3-6 and Table 3-7, respectively.

If response-history analysis is performed using only the DBE spectrum-compatible ground motions, the factors in the 2nd through 5th columns of Table 3-6 and Table 3-7 can be used to address the influence of both maximum-demand orientation and the variation in the material properties of isolation systems on responses. The factor for displacement (force) corresponding to 1% PE at 100% DBE shaking ranges between 1.54 (1.22) and 1.66 (1.36) and that corresponding to 10% PE at 150% DBE shaking ranges between 1.96 (1.33) and 2.10 (1.58) for all models with $Q_d = 0.03W$. The variation in the factors of each column of Table 3-6 and Table 3-7 is not significant and the factor for Set M1 (e.g., cell (2, 3) of Table 3-6) is similar to the corresponding factor for Set M2 (e.g., cell (2, 5) of Table 3-6).

If response-history analysis is performed using the maximum-minimum spectra compatible ground motions, the factors in the 6th through 9th columns of Table 3-6 and Table 3-7 can be used to address the impact of variation in isolator material properties on response. The factor for displacement (force) corresponding to 1% PE at 100% DBE shaking ranges between 1.34 (1.15) and 1.42 (1.24) and that corresponding to 10% PE at 150% DBE shaking ranges between 1.70 (1.25) and 1.84 (1.44) for all models with $Q_d = 0.03W$.

3.4.2 Friction Pendulum (FP) isolation systems

Medians and logarithmic standard deviations of peak displacement and force

The analyses of Table 3-3 through Table 3-5 were repeated for the FP isolation systems and results are presented in Table 3-8 through Table 3-10, respectively. The key observations include:

1) For 100% (150%) DBE shaking, the values of θ of Table 3-8 for displacement range between 5.2 (9.2) and 13 (25) mm and those for transmitted shearing force range between 3.7 and 4.3 (4.3 and 5.6), 7.2 and 7.6 (8.2 and 8.9), and 10.6 and 10.9 (12.2 and 12.6) percent of the supported weight for Q_d of $0.03W$, $0.06W$ and $0.09W$, respectively. Given the spectra of Figure 3-5 and Figure 3-6, the median peak displacements are smaller than and median peak transmitted shearing forces are comparable to those of the LR isolation systems (see Table 3-3). This observation is expected since the spectral demands as well as the responses of the isolation systems are

Table 3-6. Ratios of displacement for 1% (10%) exceedance probability at 100% (150%) DBE to $\theta_{G0,DBE}$ and $\theta_{M0,DBE}$ for LR systems

Model	$\frac{D_{M1,DBE,99th}}{\theta_{G0,DBE}}$	$\frac{D_{M1,150\%DBE,90th}}{\theta_{G0,DBE}}$	$\frac{D_{M2,DBE,99th}}{\theta_{G0,DBE}}$	$\frac{D_{M2,150\%DBE,90th}}{\theta_{G0,DBE}}$	$\frac{D_{M1,DBE,99th}}{\theta_{M0,DBE}}$	$\frac{D_{M1,150\%DBE,90th}}{\theta_{M0,DBE}}$	$\frac{D_{M2,DBE,99th}}{\theta_{M0,DBE}}$	$\frac{D_{M2,150\%DBE,90th}}{\theta_{M0,DBE}}$
LR_T2Q3	1.54	1.96	1.55	1.98	1.34	1.70	1.35	1.72
LR_T2Q6	1.45	1.89	1.49	1.91	1.26	1.65	1.30	1.67
LR_T2Q9	1.41	1.79	1.45	1.81	1.25	1.58	1.28	1.60
LR_T3Q3	1.56	2.09	1.59	2.10	1.36	1.83	1.40	1.84
LR_T3Q6	1.49	1.91	1.53	1.94	1.30	1.67	1.33	1.69
LR_T3Q9	1.47	1.83	1.49	1.87	1.31	1.63	1.32	1.66
LR_T4Q3	1.64	2.09	1.66	2.09	1.40	1.79	1.42	1.78
LR_T4Q6	1.48	1.92	1.52	1.94	1.30	1.69	1.34	1.71
LR_T4Q9	1.50	1.89	1.52	1.93	1.32	1.68	1.35	1.70

Table 3-7. Ratios of shearing force for 1% (10%) exceedance probability at 100% (150%) DBE to $\theta_{G0,DBE}$ and $\theta_{M0,DBE}$ for LR systems

Model	$\frac{F_{M1,DBE,99th}}{\theta_{G0,DBE}}$	$\frac{F_{M1,150\%DBE,90th}}{\theta_{G0,DBE}}$	$\frac{F_{M2,DBE,99th}}{\theta_{G0,DBE}}$	$\frac{F_{M2,150\%DBE,90th}}{\theta_{G0,DBE}}$	$\frac{F_{M1,DBE,99th}}{\theta_{M0,DBE}}$	$\frac{F_{M1,150\%DBE,90th}}{\theta_{M0,DBE}}$	$\frac{F_{M2,DBE,99th}}{\theta_{M0,DBE}}$	$\frac{F_{M2,150\%DBE,90th}}{\theta_{M0,DBE}}$
LR_T2Q3	1.35	1.56	1.36	1.58	1.22	1.42	1.24	1.44
LR_T2Q6	1.27	1.46	1.31	1.48	1.16	1.34	1.19	1.35
LR_T2Q9	1.29	1.45	1.34	1.48	1.18	1.33	1.22	1.35
LR_T3Q3	1.25	1.43	1.28	1.44	1.17	1.34	1.20	1.35
LR_T3Q6	1.25	1.36	1.29	1.39	1.15	1.25	1.19	1.28
LR_T3Q9	1.27	1.38	1.32	1.41	1.18	1.28	1.23	1.31
LR_T4Q3	1.22	1.33	1.29	1.36	1.15	1.25	1.21	1.28
LR_T4Q6	1.23	1.30	1.28	1.34	1.15	1.21	1.20	1.25
LR_T4Q9	1.25	1.34	1.31	1.39	1.17	1.25	1.22	1.30

Table 3-8. Medians (θ) and dispersions (β) of peak displacement and shearing force for Sets G0, M0, M1 and M2 and 100% and 150% DBE shaking for FP systems

Model	100% DBE								150% DBE							
	θ (mm for displacement; %W for force)				β				θ (mm for displacement; %W for force)				β			
	G0	M0	M1	M2	G0	M0	M1	M2	G0	M0	M1	M2	G0	M0	M1	M2
Displacement																
FP_T2Q3	9.4	11	11	11	0.18	0.25	0.24	0.25	18	23	23	23	0.19	0.23	0.23	0.25
FP_T2Q6	6.6	7.6	7.6	7.6	0.23	0.28	0.27	0.28	12	14	14	14	0.23	0.27	0.26	0.27
FP_T2Q9	5.2	5.9	5.9	5.9	0.23	0.29	0.29	0.29	9.2	11	11	11	0.25	0.28	0.28	0.29
FP_T3Q3	10	12	12	12	0.20	0.24	0.24	0.24	19	24	24	24	0.20	0.23	0.23	0.24
FP_T3Q6	7.1	8.0	8.0	8.1	0.24	0.29	0.29	0.30	12	15	15	15	0.23	0.27	0.27	0.27
FP_T3Q9	5.5	6.2	6.2	6.2	0.24	0.31	0.30	0.31	10	11	11	11	0.26	0.30	0.29	0.30
FP_T4Q3	11	13	13	13	0.21	0.23	0.23	0.24	20	25	25	25	0.21	0.23	0.23	0.25
FP_T4Q6	7.3	8.3	8.3	8.3	0.25	0.31	0.31	0.31	13	15	15	15	0.24	0.28	0.28	0.28
FP_T4Q9	5.7	6.3	6.3	6.4	0.25	0.31	0.31	0.32	10	12	12	12	0.28	0.31	0.31	0.32
Force																
FP_T2Q3	4.2	4.3	4.3	4.3	0.07	0.09	0.09	0.11	5.3	5.6	5.6	5.6	0.09	0.14	0.14	0.14
FP_T2Q6	7.5	7.6	7.6	7.6	0.05	0.06	0.07	0.10	8.8	8.9	8.9	8.9	0.07	0.08	0.09	0.11
FP_T2Q9	10.9	10.9	10.9	10.9	0.04	0.07	0.08	0.11	12.6	12.7	12.7	12.6	0.06	0.07	0.08	0.11
FP_T3Q3	3.8	3.9	3.9	3.9	0.06	0.06	0.07	0.10	4.5	4.6	4.6	4.6	0.07	0.09	0.10	0.12
FP_T3Q6	7.3	7.3	7.3	7.3	0.04	0.05	0.07	0.10	8.4	8.4	8.4	8.4	0.06	0.07	0.08	0.11
FP_T3Q9	10.7	10.8	10.7	10.7	0.04	0.07	0.08	0.11	12.4	12.4	12.4	12.3	0.06	0.08	0.09	0.12
FP_T4Q3	3.7	3.7	3.7	3.7	0.05	0.06	0.07	0.10	4.3	4.3	4.3	4.3	0.06	0.08	0.09	0.12
FP_T4Q6	7.2	7.2	7.2	7.2	0.04	0.05	0.07	0.11	8.3	8.3	8.3	8.2	0.06	0.07	0.08	0.12
FP_T4Q9	10.6	10.7	10.7	10.6	0.04	0.07	0.08	0.11	12.3	12.3	12.3	12.2	0.06	0.08	0.09	0.12

Table 3-9. Ratios of median (θ) and dispersion (β) of peak displacement and shearing force for Sets G0, M0, M1 and M2 and 100% and 150% DBE shaking for FP systems

Model	100% DBE						150% DBE					
	Ratio of θ			Ratio of β			Ratio of θ			Ratio of β		
	$\frac{M0}{G0}$	$\frac{M1}{M0}$	$\frac{M2}{M1}$	$\frac{M0}{G0}$	$\frac{M1}{M0}$	$\frac{M2}{M1}$	$\frac{M0}{G0}$	$\frac{M1}{M0}$	$\frac{M2}{M1}$	$\frac{M0}{G0}$	$\frac{M1}{M0}$	$\frac{M2}{M1}$
Displacement												
FP_T2Q3	1.20	1.00	1.00	1.36	0.99	1.03	1.29	1.00	1.00	1.24	1.00	1.06
FP_T2Q6	1.15	1.00	1.00	1.20	0.99	1.03	1.19	1.00	1.00	1.17	0.99	1.02
FP_T2Q9	1.13	1.00	1.00	1.25	0.99	1.01	1.15	1.00	1.00	1.16	0.99	1.03
FP_T3Q3	1.22	1.00	1.00	1.18	1.00	1.03	1.27	1.00	1.00	1.14	1.00	1.05
FP_T3Q6	1.14	1.00	1.00	1.21	0.99	1.03	1.19	1.00	1.00	1.17	0.99	1.02
FP_T3Q9	1.11	1.00	1.00	1.27	0.99	1.02	1.15	1.00	1.00	1.13	0.99	1.03
FP_T4Q3	1.22	1.00	1.00	1.09	1.00	1.04	1.25	1.00	1.00	1.13	1.00	1.05
FP_T4Q6	1.14	1.00	1.00	1.23	0.99	1.02	1.19	1.00	1.00	1.17	0.98	1.01
FP_T4Q9	1.11	1.00	1.00	1.26	0.99	1.02	1.15	1.00	1.00	1.12	1.00	1.03
Force												
FP_T2Q3	1.05	1.00	1.00	1.31	1.05	1.16	1.06	1.00	1.00	1.56	0.99	1.01
FP_T2Q6	1.01	1.00	1.00	1.15	1.23	1.44	1.02	1.00	1.00	1.07	1.11	1.28
FP_T2Q9	1.01	1.00	1.00	1.50	1.18	1.39	1.00	1.00	1.00	1.18	1.16	1.35
FP_T3Q3	1.02	1.00	1.00	1.07	1.17	1.38	1.03	1.00	1.00	1.32	1.07	1.19
FP_T3Q6	1.00	1.00	1.00	1.19	1.29	1.51	1.00	1.00	1.00	1.13	1.17	1.37
FP_T3Q9	1.01	1.00	1.00	1.53	1.19	1.40	1.00	1.00	1.00	1.34	1.15	1.34
FP_T4Q3	1.01	1.00	1.00	1.05	1.25	1.48	1.01	1.00	1.00	1.26	1.12	1.31
FP_T4Q6	1.00	1.00	1.00	1.23	1.30	1.53	1.00	1.00	1.00	1.22	1.17	1.38
FP_T4Q9	1.01	1.00	1.00	1.55	1.20	1.41	1.00	1.00	1.00	1.40	1.14	1.34

Table 3-10. Ratios of the statistics of Table 3-8 for 150% to 100% DBE shaking

Model	θ				β			
	G0	M0	M1	M2	G0	M0	M1	M2
Displacement								
FP_T2Q3	1.88	2.02	2.01	2.01	1.03	0.94	0.95	0.98
FP_T2Q6	1.74	1.80	1.80	1.80	0.99	0.96	0.96	0.95
FP_T2Q9	1.76	1.80	1.80	1.80	1.06	0.97	0.98	0.99
FP_T3Q3	1.90	1.97	1.97	1.98	1.00	0.97	0.97	0.99
FP_T3Q6	1.73	1.81	1.81	1.82	0.97	0.94	0.93	0.92
FP_T3Q9	1.76	1.81	1.81	1.81	1.10	0.97	0.97	0.98
FP_T4Q3	1.90	1.94	1.94	1.95	0.97	1.01	1.01	1.02
FP_T4Q6	1.74	1.81	1.82	1.82	0.97	0.92	0.91	0.90
FP_T4Q9	1.77	1.83	1.82	1.82	1.11	0.98	0.99	1.00
Force								
FP_T2Q3	1.27	1.29	1.29	1.30	1.32	1.57	1.48	1.29
FP_T2Q6	1.17	1.18	1.18	1.18	1.49	1.39	1.25	1.11
FP_T2Q9	1.16	1.16	1.16	1.16	1.40	1.10	1.08	1.05
FP_T3Q3	1.19	1.19	1.19	1.20	1.22	1.50	1.37	1.17
FP_T3Q6	1.15	1.15	1.15	1.15	1.39	1.32	1.19	1.08
FP_T3Q9	1.16	1.15	1.15	1.15	1.35	1.19	1.14	1.09
FP_T4Q3	1.17	1.17	1.17	1.16	1.19	1.44	1.30	1.14
FP_T4Q6	1.15	1.14	1.14	1.14	1.37	1.35	1.22	1.10
FP_T4Q9	1.15	1.15	1.15	1.15	1.35	1.22	1.16	1.11

insignificant in the long period range for the North Anna site and the FP isolation systems have a much higher pre-yield stiffness than the LR isolation systems.

2) In Table 3-9, the ratios of θ for M1/M0 and M2/M1 are equal to 1 for all models and shaking intensities. The median response for analyses accounting for the variability in the mechanical properties of the isolation system (i.e., M1 and M2) can be estimated without bias using analysis of a best-estimate model (i.e., M0).

3) In Table 3-9, the ratios of θ for M0/G0 for displacement range between 1.11 and 1.29 and are higher for the models with $Q_d = 0.03W$ than that for $Q_d = 0.06W$ and $0.09W$. The difference in the values of θ for shearing force between Sets G0 and M0 is insignificant. For FP isolation systems with $Q_d = 0.03W$, the median displacement computed using geomean-spectrum-compatible ground motions should be increased by 20% to 30% to address variability in spectral demands.

4) In Table 3-10, the ratios of θ at 150% to 100% DBE shaking range between 1.73 and 2.02 for displacement and between 1.14 and 1.29 for shearing force. The ratios for displacement are much greater than those for shearing force due to the nonlinear behavior of the isolation systems. The ratio for displacement is greater for FP isolation systems than for LR isolation systems (see Table 3-5) for a given Q_d and T_d but the difference in the ratio for shearing force between the FP and LR isolation systems for a given Q_d and T_d is insignificant.

5) In Table 3-8, the dispersions (β) in displacement are higher than those in transmitted shearing force. For displacement, the dispersion increases if the variability in the spectral demand is included in the analysis (see the ratio of β of Table 3-9 for M0/G0) and does not further increase as the variability in the bearing properties is considered (see the ratios of β of Table 3-9 for M1/M0 and M2/M1). For transmitted shearing force, although there are significant percentage differences in the dispersions between Sets G0 and M2, all values of β are small.

6) The dispersion in displacement for the FP isolation systems (Table 3-8) is much higher than that for LR isolation systems (Table 3-3), which results in a greater number of pairs of ground motions required in the response-history analysis to achieve a reliable estimate of median displacement. If we assume that the response-history analysis is performed for Set G0 using the models with $Q_d = 0.03W$ and the dispersion in the peak displacement is no greater than 0.21 per

Table 3-8, the minimum number of pairs of ground motions per (3.3) to ensure a 90% confidence of the true median displacement being within ±10% of the estimated value is 13.

Scale factors for responses with 1% (10%) probability of exceedance at 100% (150%) DBE shaking

The analyses of Table 3-6 and Table 3-7 were repeated for FP isolation systems and results are presented in Table 3-11 and Table 3-12, respectively. As noted above, the dispersion in displacement for FP isolation systems is higher than that for LR isolation systems and therefore the factors to scale the median displacements for Sets G0 and M0 to the displacements corresponding with 1% (10%) PE at 100% (150%) DBE shaking for Sets M1 and M2 are higher for FP isolation systems than for LR isolation systems.

If response-history analysis is performed using only the DBE spectrum-compatible ground motions, the scale factor for displacement (force) corresponding to 1% PE at 100% DBE shaking ranges between 2.09 (1.17) and 2.37 (1.35) and that corresponding to 10% PE at 150% DBE shaking ranges between 2.91 (1.27) and 3.35 (1.62) (see the 2nd through 5th columns of Table 3-11 and Table 3-12).

If response-history analysis is performed using the maximum-minimum spectra compatible ground motions, the factor for displacement (force) corresponding to 1% PE at 100% DBE shaking ranges between 1.73 (1.17) and 2.09 (1.29) and that corresponding to 10% PE at 150% DBE shaking ranges between 2.53 (1.27) and 2.78 (1.55) (see the 6th through 9th columns of Table 3-11 and Table 3-12).

The median displacements of Table 3-3 and Table 3-8 at 100% DBE shaking are very small. The median displacements of the LR isolation systems with $Q_d = 0.09W$ are either smaller than or barely equal to the yield displacement (24 mm). Analysis results for LDR isolation systems are presented in the following subsection.

3.4.3 Low Damping Rubber (LDR) isolation systems

Medians and logarithmic standard deviations of peak displacement and force

The analyses of Table 3-3 through Table 3-5 were repeated for LDR isolation systems and results are presented in Table 3-13 through Table 3-15, respectively. The key observations include:

1) For 100% DBE shaking, the values of θ of Table 3-13 for displacement range between 61 and 73 mm and those for transmitted shearing force range between (6.2 and 7.1), (2.8 and 3.2), and

Table 3-11. Ratios of displacement for 1% (10%) exceedance probability at 100% (150%) DBE to $\theta_{G0,DBE}$ and $\theta_{M0,DBE}$ for FP systems

Model	$\frac{D_{M1,DBE,99th}}{\theta_{G0,DBE}}$	$\frac{D_{M1,150\%DBE,90th}}{\theta_{G0,DBE}}$	$\frac{D_{M2,DBE,99th}}{\theta_{G0,DBE}}$	$\frac{D_{M2,150\%DBE,90th}}{\theta_{G0,DBE}}$	$\frac{D_{M1,DBE,99th}}{\theta_{M0,DBE}}$	$\frac{D_{M1,150\%DBE,90th}}{\theta_{M0,DBE}}$	$\frac{D_{M2,DBE,99th}}{\theta_{M0,DBE}}$	$\frac{D_{M2,150\%DBE,90th}}{\theta_{M0,DBE}}$
FP_T2Q3	2.13	3.28	2.18	3.35	1.77	2.72	1.81	2.78
FP_T2Q6	2.18	2.91	2.23	2.93	1.90	2.53	1.94	2.55
FP_T2Q9	2.21	2.92	2.24	2.95	1.96	2.59	1.98	2.61
FP_T3Q3	2.12	3.25	2.17	3.31	1.73	2.65	1.77	2.71
FP_T3Q6	2.23	2.92	2.28	2.95	1.96	2.56	2.00	2.59
FP_T3Q9	2.25	2.94	2.28	2.98	2.02	2.64	2.05	2.67
FP_T4Q3	2.09	3.20	2.14	3.26	1.71	2.62	1.75	2.67
FP_T4Q6	2.32	2.96	2.37	2.99	2.04	2.60	2.08	2.62
FP_T4Q9	2.29	3.00	2.32	3.03	2.06	2.71	2.09	2.74

Table 3-12. Ratios of shearing force for 1% (10%) exceedance probability at 100% (150%) DBE to $\theta_{G0,DBE}$ and $\theta_{M0,DBE}$ for FP systems

Model	$\frac{F_{M1,DBE,99th}}{\theta_{G0,DBE}}$	$\frac{F_{M1,150\%DBE,90th}}{\theta_{G0,DBE}}$	$\frac{F_{M2,DBE,99th}}{\theta_{G0,DBE}}$	$\frac{F_{M2,150\%DBE,90th}}{\theta_{G0,DBE}}$	$\frac{F_{M1,DBE,99th}}{\theta_{M0,DBE}}$	$\frac{F_{M1,150\%DBE,90th}}{\theta_{M0,DBE}}$	$\frac{F_{M2,DBE,99th}}{\theta_{M0,DBE}}$	$\frac{F_{M2,150\%DBE,90th}}{\theta_{M0,DBE}}$
FP_T2Q3	1.30	1.61	1.35	1.62	1.24	1.54	1.29	1.55
FP_T2Q6	1.18	1.33	1.27	1.37	1.17	1.32	1.26	1.36
FP_T2Q9	1.20	1.30	1.28	1.35	1.19	1.29	1.28	1.34
FP_T3Q3	1.21	1.39	1.29	1.42	1.19	1.36	1.26	1.39
FP_T3Q6	1.17	1.28	1.27	1.33	1.17	1.28	1.27	1.33
FP_T3Q9	1.20	1.30	1.29	1.34	1.20	1.29	1.28	1.34
FP_T4Q3	1.19	1.32	1.28	1.37	1.18	1.31	1.27	1.35
FP_T4Q6	1.17	1.27	1.28	1.32	1.17	1.27	1.28	1.32
FP_T4Q9	1.21	1.30	1.29	1.35	1.20	1.29	1.29	1.34

(1.6 and 1.8) percent of the supported weight for isolation systems with periods of 2, 3 and 4 seconds, respectively. The median responses for 150% DBE shaking are 150% of those for 100% DBE shaking since the isolation systems are modeled using linear springs and linear viscous damping. The median transmitted shearing forces of Table 3-13 are small because the spectral demands in the long period range of the horizontal DBE spectrum of Figure 3-1 are small: the 5%-damping spectral ordinates at periods of 2, 3 and 4 seconds are 0.045, 0.022 and 0.012 g, respectively.

2) In Table 3-14, the trend in the ratios of θ for M1/M0 and M2/M1 is the same as that in Table 3-4 and Table 3-9; namely, the median response for analyses where the variability in material properties of isolators is included can be estimated without bias using a best-estimate model.

3) In Table 3-14, the ratios of θ for M0/G0 are independent of the isolation period and between 1.14 and 1.16 for both displacement and shearing force. If analysis is performed using geomean-spectrum-compatible ground motions, the median response should be increased by 15% to address variability in spectral demands.

4) In Table 3-13, the dispersions β in peak response range between 0.1 and 0.16. If we assume that the response-history analysis is performed using geomean-spectrum-compatible ground motions and the dispersion in the peak response is no greater than 0.12 per Table 3-13, the minimum number of pairs of ground motions required to estimate the median response within ±10% of the *true* value with 90% confidence per (3.3) is 4.

Scale factors for responses with 1% (10%) probability of exceedance at 100% (150%) DBE shaking

The analyses of Table 3-6 and Table 3-7 were repeated for the LDR isolation systems and results are presented in Table 3-15 and Table 3-16, where the corresponding scale factors for displacement and shearing force for a given model are similar. For example, the factors $D_{M1,DBE,99th} / \theta_{G0,DBE}$ and $F_{M1,DBE,99th} / \theta_{G0,DBE}$ for Model LDR_T2 are 1.43 and 1.44, respectively. The increase in the dispersion in the mechanical properties of the isolation system does not have a significant impact on the scale factors; for example, the factors $D_{M1,150\%DBE,90th} / \theta_{G0,DBE}$ and $D_{M2,150\%DBE,90th} / \theta_{G0,DBE}$ for Model LDR_T2 are both 1.94.

If the response-history analysis is performed using only the DBE spectrum-compatible ground motions, the scale factor for response corresponding to 1% (10%) PE at 100% (150%) DBE shaking ranges between 1.43 (1.94) and 1.67 (2.12). If the response-history analysis is performed using the maximum-minimum spectra compatible ground motions, the scale factor ranges between 1.25 (1.70) and 1.44 (1.83).

Table 3-13. Medians (θ) and dispersions (β) of peak displacement and shearing force for Sets G0, M0, M1 and M2 and 100% and 150% DBE shaking for LDR systems

Model	100% DBE								150% DBE							
	θ (mm for displacement; %W for force)				β				θ (mm for displacement; %W for force)				β			
	G0	M0	M1	M2	G0	M0	M1	M2	G0	M0	M1	M2	G0	M0	M1	M2
Displacement																
LDR_T2	61	70	70	69	0.12	0.10	0.10	0.10	92	105	105	104	0.12	0.10	0.10	0.10
LDR_T3	63	72	72	72	0.11	0.10	0.10	0.10	94	109	109	108	0.11	0.10	0.10	0.10
LDR_T4	63	73	73	73	0.12	0.12	0.12	0.12	95	110	110	110	0.12	0.12	0.12	0.12
Force																
LDR_T2	6.2	7.1	7.0	7.0	0.12	0.10	0.10	0.12	9.3	10.6	10.5	10.4	0.12	0.10	0.10	0.12
LDR_T3	2.8	3.2	3.2	3.2	0.11	0.10	0.11	0.14	4.2	4.9	4.9	4.8	0.11	0.10	0.11	0.14
LDR_T4	1.6	1.8	1.8	1.8	0.12	0.12	0.13	0.16	2.4	2.8	2.8	2.7	0.12	0.12	0.13	0.16

Table 3-14. Ratios of median (θ) and dispersion (β) of peak displacement and shearing force for Sets G0, M0, M1 and M2 and 100% and 150% DBE shaking for LDR systems

Model	100% DBE						150% DBE					
	Ratio of θ			Ratio of β			Ratio of θ			Ratio of β		
	$\frac{M0}{G0}$	$\frac{M1}{M0}$	$\frac{M2}{M1}$	$\frac{M0}{G0}$	$\frac{M1}{M0}$	$\frac{M2}{M1}$	$\frac{M0}{G0}$	$\frac{M1}{M0}$	$\frac{M2}{M1}$	$\frac{M0}{G0}$	$\frac{M1}{M0}$	$\frac{M2}{M1}$
Displacement												
LDR_T2	1.14	1.00	0.99	0.81	1.02	1.06	1.14	1.00	0.99	0.81	1.02	1.06
LDR_T3	1.16	1.00	1.00	0.91	1.00	1.04	1.16	1.00	1.00	0.91	1.00	1.04
LDR_T4	1.16	1.00	1.00	0.96	0.99	1.02	1.16	1.00	1.00	0.96	0.99	1.02
Force												
LDR_T2	1.14	1.00	0.99	0.81	1.05	1.17	1.14	1.00	0.99	0.81	1.05	1.17
LDR_T3	1.16	1.00	0.99	0.91	1.12	1.30	1.16	1.00	0.99	0.91	1.12	1.30
LDR_T4	1.16	1.00	0.99	0.96	1.09	1.26	1.16	1.00	0.99	0.96	1.09	1.26

Table 3-15. Ratios of displacement for 1% (10%) exceedance probability at 100% (150%) DBE to $\theta_{G0,DBE}$ and $\theta_{M0,DBE}$ for LDR systems

Model	$\frac{D_{M1,DBE,99th}}{\theta_{G0,DBE}}$	$\frac{D_{M1,150\%DBE,90th}}{\theta_{G0,DBE}}$	$\frac{D_{M2,DBE,99th}}{\theta_{G0,DBE}}$	$\frac{D_{M2,150\%DBE,90th}}{\theta_{G0,DBE}}$	$\frac{D_{M1,DBE,99th}}{\theta_{M0,DBE}}$	$\frac{D_{M1,150\%DBE,90th}}{\theta_{M0,DBE}}$	$\frac{D_{M2,DBE,99th}}{\theta_{M0,DBE}}$	$\frac{D_{M2,150\%DBE,90th}}{\theta_{M0,DBE}}$
LDR_T2	1.43	1.94	1.44	1.94	1.25	1.70	1.26	1.70
LDR_T3	1.46	1.97	1.47	1.98	1.26	1.70	1.27	1.71
LDR_T4	1.52	2.02	1.52	2.02	1.31	1.74	1.31	1.74

Table 3-16. Ratios of shearing force for 1% (10%) exceedance probability at 100% (150%) DBE to $\theta_{G0,DBE}$ and $\theta_{M0,DBE}$ for LDR systems

Model	$\frac{F_{M1,DBE,99th}}{\theta_{G0,DBE}}$	$\frac{F_{M1,150\%DBE,90th}}{\theta_{G0,DBE}}$	$\frac{F_{M2,DBE,99th}}{\theta_{G0,DBE}}$	$\frac{F_{M2,150\%DBE,90th}}{\theta_{G0,DBE}}$	$\frac{F_{M1,DBE,99th}}{\theta_{M0,DBE}}$	$\frac{F_{M1,150\%DBE,90th}}{\theta_{M0,DBE}}$	$\frac{F_{M2,DBE,99th}}{\theta_{M0,DBE}}$	$\frac{F_{M2,150\%DBE,90th}}{\theta_{M0,DBE}}$
LDR_T2	1.44	1.94	1.48	1.96	1.26	1.70	1.30	1.72
LDR_T3	1.50	2.00	1.61	2.08	1.29	1.72	1.39	1.79
LDR_T4	1.56	2.05	1.67	2.12	1.34	1.76	1.44	1.83

SECTION 4
STUDIES FOR CEUS SOIL SITES

4.1 Design basis earthquake

The site of the Vogtle nuclear power plant (NPP) in Waynesboro, Georgia, is a representative soil site for NPPs in the Central and Eastern US (CEUS). The Design Basis Earthquake (DBE) used for the study at the Vogtle site is introduced in this subsection.

Figure 4-1 presents the horizontal DBE spectrum developed by the Southern Nuclear Operating Company for the Vogtle Early Site Permit (ESP) Application (SNOC 2008). The spectrum is a site-specific uniform risk spectrum at the ground-surface level. The development of the spectrum of Figure 4-1 involves probabilistic seismic hazard analysis (PSHA), site response analysis and the conversion of a uniform hazard spectrum (UHS) to a uniform risk spectrum (URS). The procedure used to develop the spectrum of Figure 4-1 is documented in the Vogtle ESP application and is summarized by step below:

1. PSHA was performed for hard rock conditions at seven structural periods, 0, 0.04, 0.1, 0.2, 0.4, 1 and 2 seconds, using the attenuation relationship of McCann et al. (2004).The seven spectral ordinates associated with a mean annual frequency of exceedance (MAFE) of 10^{-4} are presented in Figure 4-2 using the symbol "×".

2. The seismic hazard of Step 1 was deaggregated at MAFEs of 10^{-4} and 10^{-5} per USNRC Regulatory Guide 1.165 (USNRC 1997) for two sets of structural frequencies, namely, a *high-frequency* set bracketing 10 and 5 Hz and a *low-frequency* set bracketing 2.5 and 1 Hz. The controlling pair of magnitude (M_w) and distance (r) was identified to be 5.6 and 12 km for the high-frequency set and 7.2 and 130 km for the low-frequency set.

3. For a given MAFE, the spectral shapes for each of the high- and low-frequency sets were developed using the controlling [M_w - r] pairs of Step 2 and the attenuation relationship of McGuire et al. (2001) for the Central and Eastern United States. The resultant spectral shapes were scaled to target spectral ordinates at 7.5 Hz (0.133 second) and 1.75 Hz (0.57 second) for the high- and low-frequency cases, respectively, and the target spectral ordinates at 7.5 and 1.75 Hz were obtained through the interpolation of the spectral ordinates of Step 1 for the corresponding MAFE. The scaled spectra for the high- and low-frequency cases for a MAFE of 10^{-4} are presented in Figure 4-2 using the red and blue curves, respectively.

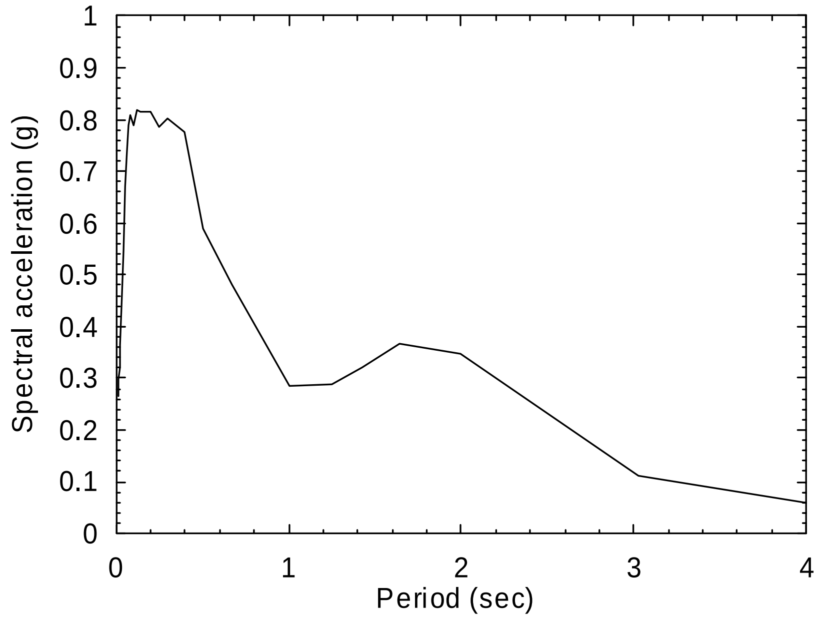

Figure 4-1. Five-percent damped horizontal DBE spectrum for the Vogtle site (SNOC 2008)

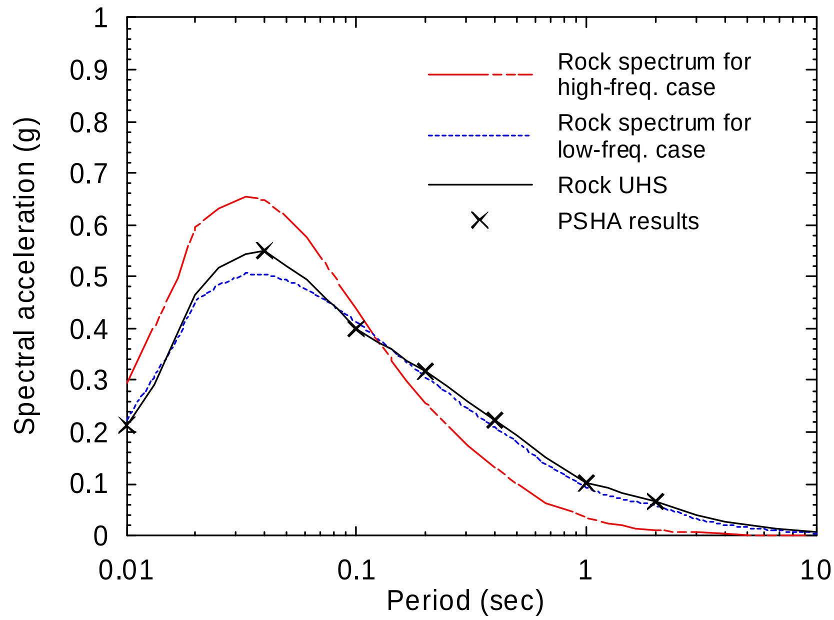

Figure 4-2. Five-percent damped spectral accelerations for a MAFE of 10^{-4} and hard rock

4. For a given MAFE, the scaled spectra of Step 3 for the high- and low-frequency cases were used as target rock spectra to develop 60 spectrally matched ground motions (30 per case) for site response analysis. The spectral matching was performed in the time domain using 60 seed ground motions selected based on the controlling [M_w - r] pair of Step 2 and average shear-wave velocity in the 30 meters below the ground surface (V_{S30}) of 600+ m/s. Due to the lack of strong ground motion records in the Eastern North America (ENA), 58 of the 60 selected seed ground motions were recorded in the regions other than ENA.

5. Site-response analysis was performed to characterize the amplification of rock motion to the free-field ground surface. Site investigations were conducted to identify soil parameters. The variations in shear modulus and damping of the soil were developed using two sets of soil degradation relationships developed for EPRI (1993) and the Savannah River site (Lee 1996). Sixty soil profiles were developed for each set of degradation relationships. For each target spectrum developed in Step 3, the 60 soil profiles were paired with 30 spectrally matched ground motions (one ground motion for two soil profiles) and analyzed using the computer program SHAKE (Deng and Ostadan 2000). For each analysis, the site amplification factor at a given period was computed using the spectral acceleration for soil response divided by the target rock spectral acceleration. The mean of the site amplification factors obtained from the analyses for each target spectrum of Step 3 was used to develop the soil spectrum for the Vogtle ESP site.

   Figure 4-3 presents the site amplification factors developed for a MAFE of 10^{-4}. The results of Figure 4-3 indicate a mode at a period of 1.6 second (0.6 Hz) for the soil columns developed by site-response analysis. The site amplification factor at 1.6 seconds is 3.9 for the low-frequency case, which is substantially greater than the corresponding value in ASCE 7-05 (ASCE 2006).

6. For a given MAFE, the site-class factors for the high- and low-frequency cases were merged into one set of factors, where the factor at a given period was chosen from either case. The controlling case at a period is that with a higher mean soil response in the analysis of Step 5. At periods smaller than 0.125 second (i.e., frequencies greater than 8 Hz), the high-frequency case governs; at periods greater than 0.5 second (i.e., frequencies smaller than 2 Hz), the low-frequency case governs. At periods between 0.125 and 0.5 second (i.e., frequencies between 2 and 8 Hz), the controlling case depends on the period and MAFE.

7. The site amplification factors of Step 6 were used to scale the rock UHS for MAFEs of 10^{-4} and 10^{-5} to site-specific UHS. The rock UHS for a MAFE of 10^{-4} is presented in Figure 4-2 using the solid black line. The development of the rock UHS of Figure 4-2 started from the seven PSHA spectral ordinates of Figure 4-2 presented using the symbol "×". The target rock spectrum of Figure 4-2 for the high- or low-frequency case was scaled to match the seven spectral ordinates of Step 1 to develop the rock UHS. The choice of the high- or low-frequency case depended on the controlling case determined in Step 6. At periods smaller than 0.125 second, the rock spectral shape for the high-frequency case was used; at periods greater than 0.5 second, that for the low-frequency case was used.

   For example, the spectral ordinates of Step 1 for a MAFE of 10^{-4} are 0.1 and 0.065 g at periods of 1 and 2 seconds, respectively, where the low-frequency case controls the spectral demand. The spectral ordinates for the target rock spectrum of Figure 4-2 for the low-frequency case at periods of 1 and 2 seconds are 0.09 and 0.06 g, respectively, and were scaled by factors of 1.11 and 1.08 to be 0.1 and 0.065 g. The scale factors for periods between 1 and 2 seconds were developed by linear interpolation.

   Note that the rock UHS of Figure 4-2 is not consistent with the definition of the SSE per USNRC Regulatory Guide 1.165, where the SSE is required to envelop high- and low-frequency spectra for a MAFE of 10^{-5}. The rock UHS of Figure 4-2 was developed for the purpose of generating a performance-based URS per ASCE 43-05 (ASCE 2005).

   The rock UHS of Figure 4-2 is re-plotted in Figure 4-4 together with the corresponding site-specific UHS developed using the rock UHS of Figure 4-2 and the site amplification factors of Step 6 for a MAFE of 10^{-4}. A peak can be observed in the site-specific UHS of Figure 4-4 at a period of 1.6 second that corresponds to the peak in the site amplification spectrum of Figure 4-3 at the same period.

8. The conversion of a UHS to a URS was performed per ASCE 43-05. The ratio of the spectral ordinates of the site-specific UHS for MAFEs of 10^{-5} and 10^{-4} for each period was computed and termed AR. The site-specific UHS for a MAFE of 10^{-4} was converted to a URS using the following equation:

$$\text{URS} = \text{UHS}_{\text{Soil},10^{-4}} \times \max(1.0 \text{ or } 0.6 \cdot \text{AR}^{0.8}) \tag{4.1}$$

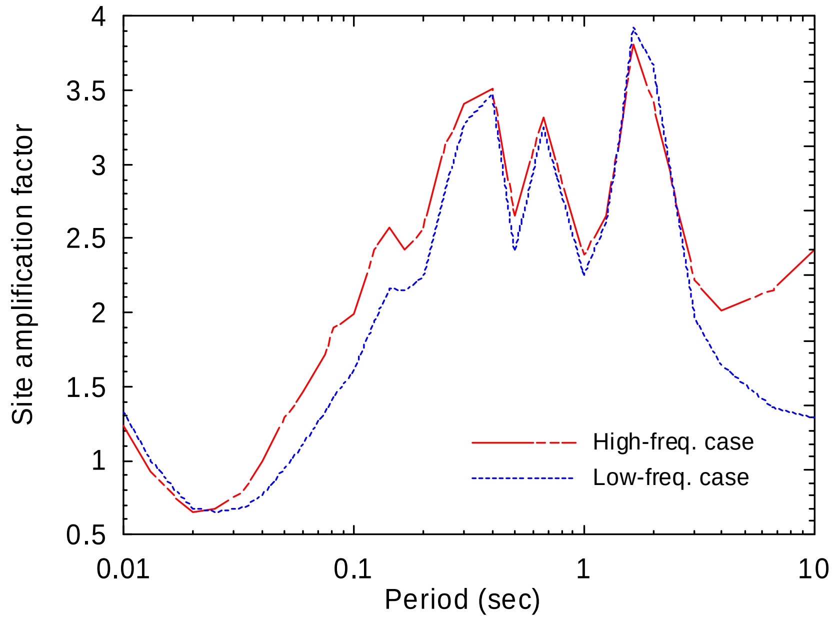

Figure 4-3. Site amplification factors for a MAFE of 10^{-4} for high- and low-frequency cases

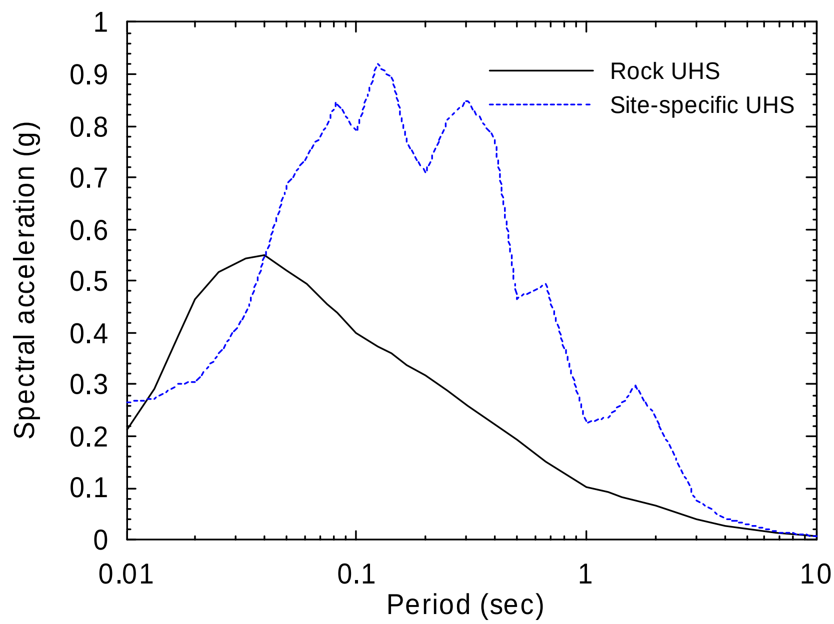

Figure 4-4. Five-percent damped rock and site-specific UHS for a MAFE of 10^{-4}

where $\mathrm{UHS}_{\mathrm{Soil},10^{-4}}$ is the spectral ordinate of the site-specific UHS for a MAFE of 10^{-4} at a given period. The spectrum so developed is termed the baseline DBE spectrum. The site-specific UHS for a MAFE of 10^{-4} and the baseline DBE spectrum are presented in Figure 4-5. The baseline DBE spectrum was smoothed by a running average filter, which smoothed out the peaks and troughs in the raw spectrum at periods smaller than 1 second but maintains the peak at a period of 1.6 seconds representing a long-period mode of the soil column used in the analysis. The smoothed DBE spectrum of Figure 4-1 is also presented in Figure 4-5.

The horizontal and vertical DBE spectra developed by the Southern Nuclear Operating Company for the Vogtle site are presented in Figure 4-6, where the vertical DBE spectral ordinates were developed by scaling the horizontal DBE spectral ordinates using a V/H scale factor of 0.9 at periods smaller than 0.07 second (15 Hz) and 0.5 at periods greater than 1 second. Interpolation was used to determine the scale factors at periods between 0.07 and 1 second. The technical basis for the V/H scale factors for the spectra of Figure 4-6 is provided in SNOC (2008). The DBE spectra of Figure 4-6 were used in this study.

4.2 Selection and scaling of ground motions

The two-step approach described in Section 3.2 was used to developed synthetic ground motions for the Vogtle study. In the first step, the computer code "Strong Ground Motion Simulation" (SGMS, Halldorsson 2004) was used to generate 30 sets of CEUS-type seed ground motions. Each set of ground motions includes two horizontal components and a vertical component. The $[M_w - r]$ pair used to generate seed ground motions was the controlling pair for the low-frequency hazard identified in Step 2 of Section 4.1, namely, M_w = 7.2 and r = 130 km. In the second step, each set of the seed ground motions was spectrally matched to the DBE spectra of Figure 4-6 using the computer code RSPMATCH (Abrahamson 1998).

Panels a, c and e of Figure 4-7 present a sample set of DBE spectrum-compatible ground motions and panels b, d and f present the target and achieved spectral accelerations for the time series of panels a, c and e, respectively. Panels a, b and c of Figure 4-8 present the spectral accelerations for the horizontal components 1 and 2 and vertical component, respectively, of all 30 sets of DBE spectrum-compatible ground motions. Each spectrum of Figure 4-8 closely matches the target.

The 30 sets of DBE spectrum-compatible ground motions of Figure 4-8 were amplitude scaled to develop the maximum-minimum spectra compatible ground motions. The scaling procedure was the same as that

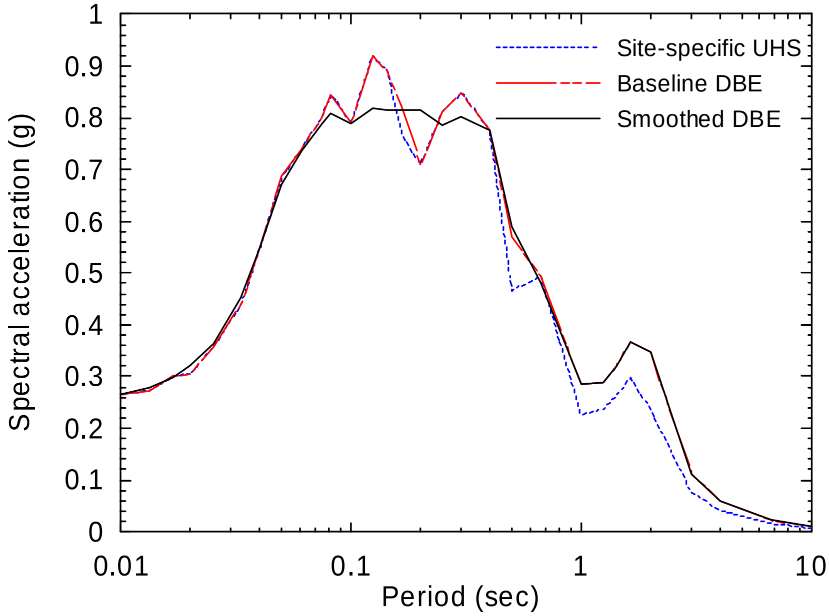

Figure 4-5. Site-specific UHS of Figure 4-4 and the raw and smoothed SNOC DBE spectra for the Vogtle site

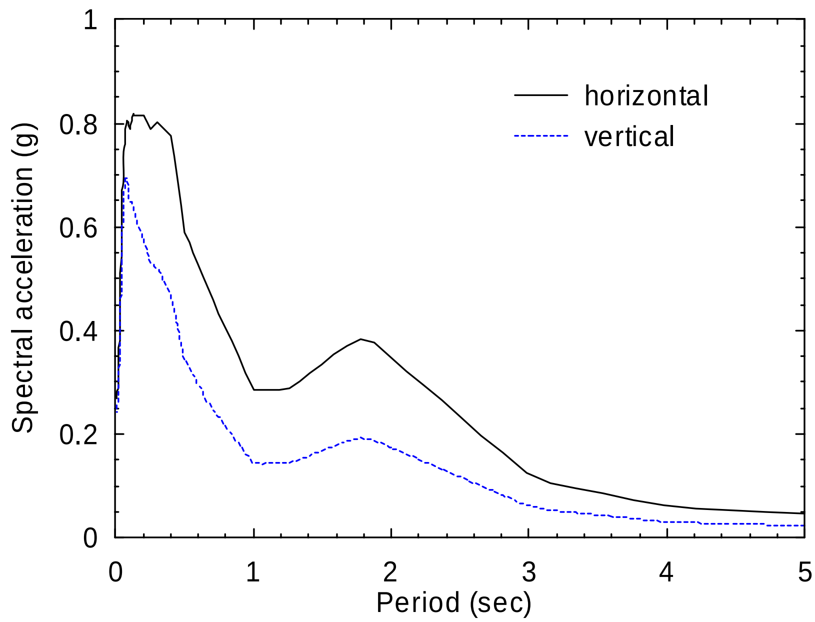

Figure 4-6. Five-percent damped horizontal and vertical DBE spectra for the Vogtle site

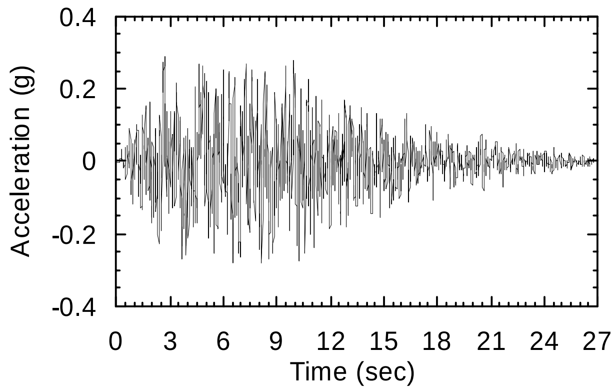

a. horizontal component 1

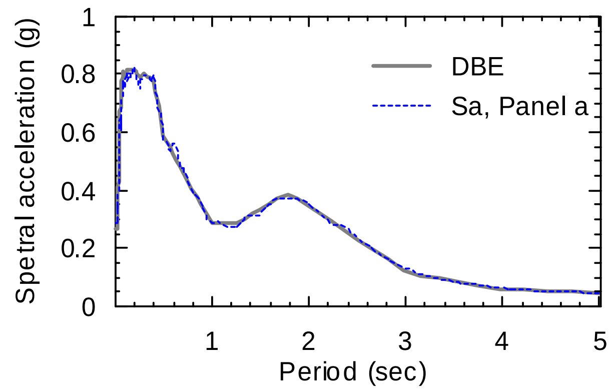

b. response spectrum of the time series of panel a

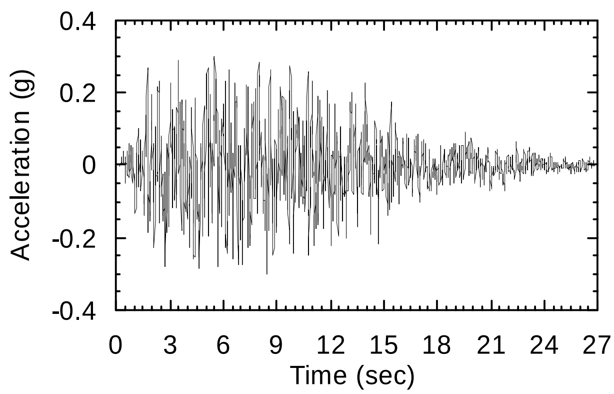

c. horizontal component 2

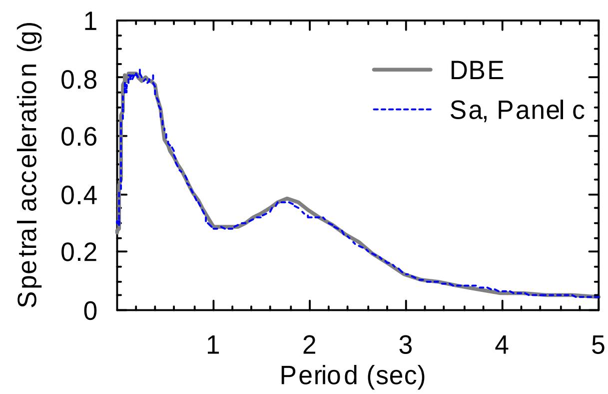

d. response spectrum of the time series of panel c

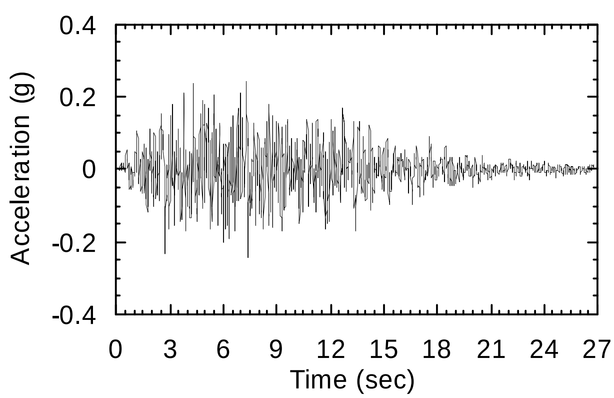

e. vertical component

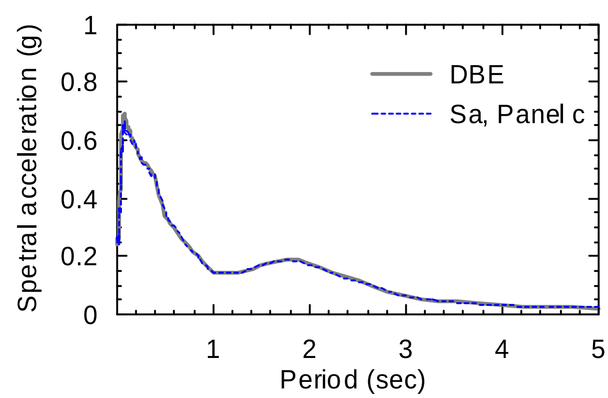

f. response spectrum of the time series of panel e

Figure 4-7. Sample spectrally matched acceleration time series and the corresponding 5% damped response spectra

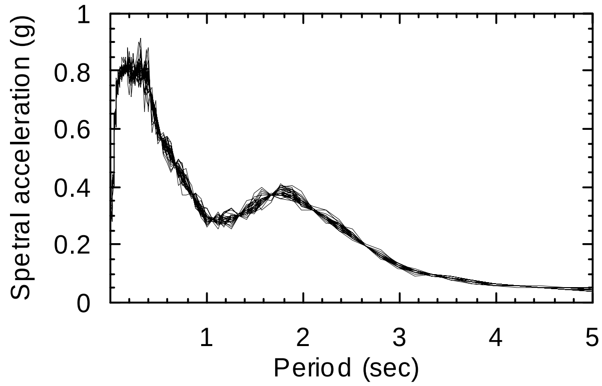

a. horizontal component 1

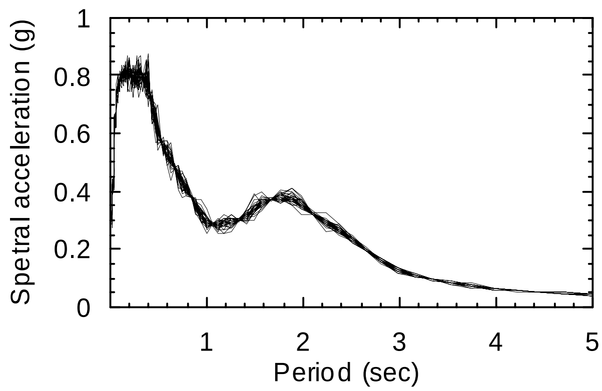

b. horizontal component 2

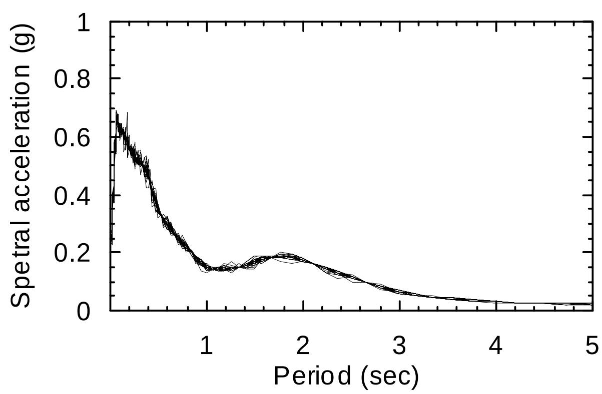

c. vertical component

Figure 4-8. Five-percent damped response spectra for the 30 sets of DBE spectrum-compatible ground motions for the Vogtle site

described in Section 3.2.2 and is not repeated here. Panels a, b and c of Figure 4-9 present the spectral accelerations for the horizontal components 1 and 2 and vertical component, respectively, of all 30 sets of DBE spectrum-compatible ground motions.

4.3 Analysis sets

The analysis described in Section 3.3 was repeated using the ground motions developed for the Vogtle NPP site. Response-history analysis was performed for two intensities of shaking: 1) 100% DBE shaking using the 60 sets of ground motions of Figure 4-8 and Figure 4-9, and b) 150% DBE shaking using the ground motions of Figure 4-8 and Figure 4-9 but with the amplitude of the acceleration time series multiplied by 1.5.

At each intensity level, the 4 sets of analyses of Table 3-2, namely, Sets G0, M0, M1 and M2, were performed for each best-estimate model of Tables 2-1 through 2-3 and the 60 corresponding property-varied models to study the impact of variations in spectral demand and mechanical properties of the isolation system on the response of isolated NPPs.

4.4 Analysis results

4.4.1 Lead Rubber (LR) isolation systems

Medians and logarithmic standard deviations of peak displacement and force

Table 4-1 presents θ and β of peak displacement and transmitted shear force for each case, model and shaking intensity analyzed LR isolation systems. Table 4-2 presents the ratios of θ and β between Sets M0 and G0, Sets M1 and M0 and Sets M2 and M1 for each model and shaking intensity. Table 4-3 presents the ratios of θ and β at 150% to 100% DBE shaking. The key observations include:

1) For 100% (150%) DBE shaking, the values of θ of Table 4-1 for displacement range between 101 (251) and 401 (686) mm and those for transmitted shearing force range between 8.4 (11.3) and 42.8 (71.1) percent of the supported weight. The median shearing forces for the models associated with T_d = 2 seconds are greater than those with T_d = 3 and 4 seconds. For the spectral shape of Figure 4-1 where a local peak is evident at a period of 1.6 seconds, the use of an isolation period of 2 seconds makes no practical sense. Accordingly, the results for the isolation systems with T_d = 2 seconds in Table 4-1 through Table 4-5 are shaded and not used again in this report.

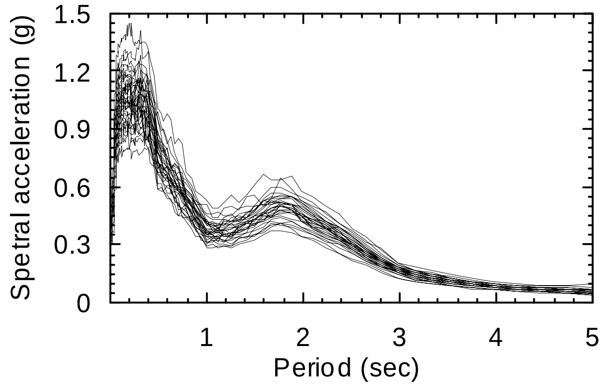

a. maximum component

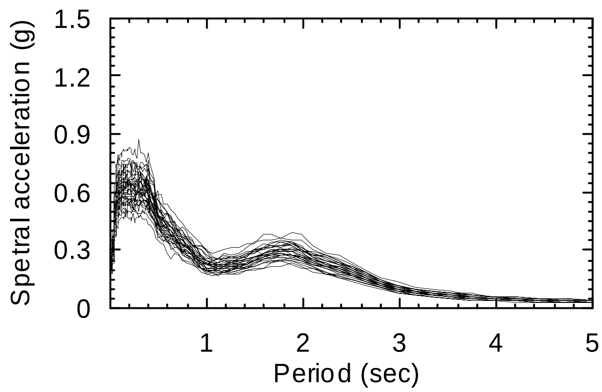

b. minimum component

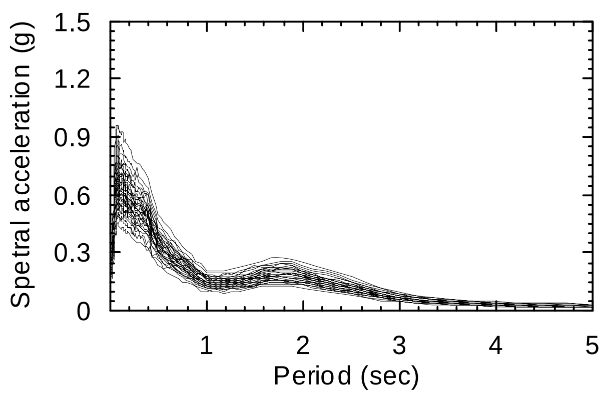

c. vertical component

Figure 4-9. Five-percent damped response spectra for the 30 sets of maximum-minimum DBE spectra-compatible ground motions for the Vogtle site

Table 4-1. Medians (θ) and dispersions (β) of peak displacement and shearing force for Sets G0, M0, M1 and M2 and 100% and 150% DBE shaking for LR systems

Model	100% DBE								150% DBE							
	θ (mm for displacement; %W for force)				β				θ (mm for displacement; %W for force)				β			
	G0	M0	M1	M2	G0	M0	M1	M2	G0	M0	M1	M2	G0	M0	M1	M2
Displacement																
LR_T2Q3	322	401	400	398	0.15	0.15	0.15	0.15	571	686	686	683	0.13	0.14	0.14	0.14
LR_T2Q6	179	248	248	246	0.19	0.19	0.20	0.23	389	506	504	499	0.16	0.16	0.16	0.18
LR_T2Q9	101	140	141	142	0.19	0.28	0.28	0.30	251	351	351	348	0.20	0.20	0.21	0.24
LR_T3Q3	289	349	348	347	0.13	0.18	0.18	0.19	467	558	557	555	0.12	0.15	0.15	0.16
LR_T3Q6	204	264	263	263	0.16	0.24	0.23	0.24	368	456	455	454	0.15	0.21	0.21	0.22
LR_T3Q9	133	183	183	183	0.19	0.25	0.25	0.27	277	366	366	365	0.17	0.25	0.24	0.25
LR_T4Q3	227	274	274	274	0.13	0.20	0.20	0.20	352	425	426	427	0.11	0.18	0.18	0.18
LR_T4Q6	195	238	238	238	0.15	0.23	0.23	0.23	309	373	374	374	0.16	0.23	0.23	0.23
LR_T4Q9	143	188	187	187	0.15	0.24	0.24	0.25	265	332	332	331	0.15	0.23	0.23	0.23
Force																
LR_T2Q3	34.6	42.8	42.6	42.3	0.14	0.15	0.15	0.17	59.2	71.1	71.0	70.5	0.13	0.14	0.14	0.16
LR_T2Q6	23.2	30.3	30.2	30.0	0.16	0.17	0.17	0.18	43.7	55.9	55.6	55.0	0.15	0.15	0.16	0.17
LR_T2Q9	18.8	22.9	23.0	23.2	0.11	0.18	0.17	0.17	33.0	43.2	43.1	42.9	0.16	0.17	0.17	0.19
LR_T3Q3	15.3	18.1	18.1	18.0	0.11	0.16	0.17	0.21	23.0	27.3	27.2	27.1	0.11	0.15	0.16	0.21
LR_T3Q6	14.6	17.5	17.5	17.4	0.10	0.16	0.16	0.17	21.5	25.6	25.6	25.5	0.11	0.18	0.18	0.20
LR_T3Q9	14.6	17.0	17.0	17.0	0.09	0.12	0.12	0.13	20.5	24.9	24.8	24.7	0.10	0.17	0.17	0.18
LR_T4Q3	8.4	9.6	9.6	9.6	0.09	0.15	0.16	0.18	11.3	13.3	13.3	13.3	0.09	0.16	0.16	0.18
LR_T4Q6	10.6	11.8	11.8	11.7	0.07	0.12	0.12	0.13	13.1	15.0	15.0	15.0	0.10	0.15	0.15	0.16
LR_T4Q9	12.3	13.6	13.6	13.6	0.05	0.09	0.09	0.10	15.2	16.9	16.9	16.9	0.07	0.12	0.12	0.13

Table 4-2. Ratios of median (θ) and dispersion (β) of peak displacement and shearing force for Sets G0, M0, M1 and M2 and 100% and 150% DBE shaking for LR systems

Model	100% DBE						150% DBE					
	Ratio of θ			Ratio of β			Ratio of θ			Ratio of β		
	M0/G0	M1/M0	M2/M1	M0/G0	M1/M0	M2/M1	M0/G0	M1/M0	M2/M1	M0/G0	M1/M0	M2/M1
Displacement												
LR_T2Q3	1.25	1.00	0.99	1.02	1.00	1.04	1.20	1.00	1.00	1.04	1.01	1.04
LR_T2Q6	1.39	1.00	0.99	0.98	1.02	1.15	1.30	1.00	0.99	0.99	1.01	1.09
LR_T2Q9	1.39	1.00	1.01	1.49	1.00	1.08	1.40	1.00	0.99	0.98	1.03	1.15
LR_T3Q3	1.21	1.00	1.00	1.38	1.00	1.04	1.20	1.00	1.00	1.25	1.02	1.08
LR_T3Q6	1.29	1.00	1.00	1.47	0.99	1.01	1.24	1.00	1.00	1.41	1.00	1.03
LR_T3Q9	1.38	1.00	1.00	1.32	1.02	1.09	1.32	1.00	1.00	1.49	0.99	1.03
LR_T4Q3	1.21	1.00	1.00	1.58	0.99	1.01	1.21	1.00	1.00	1.65	0.99	1.00
LR_T4Q6	1.22	1.00	1.00	1.50	0.99	1.01	1.21	1.00	1.00	1.49	0.98	1.00
LR_T4Q9	1.32	1.00	1.00	1.56	1.00	1.05	1.25	1.00	1.00	1.50	0.99	1.02
Force												
LR_T2Q3	1.24	1.00	0.99	1.06	1.02	1.12	1.20	1.00	0.99	1.08	1.04	1.13
LR_T2Q6	1.30	1.00	0.99	1.08	1.01	1.07	1.28	1.00	0.99	1.01	1.03	1.10
LR_T2Q9	1.22	1.00	1.01	1.56	0.97	1.01	1.31	1.00	1.00	1.08	1.00	1.07
LR_T3Q3	1.19	1.00	0.99	1.44	1.06	1.18	1.19	1.00	0.99	1.30	1.12	1.28
LR_T3Q6	1.20	1.00	1.00	1.60	1.01	1.06	1.20	1.00	1.00	1.55	1.03	1.11
LR_T3Q9	1.16	1.00	1.00	1.36	1.00	1.06	1.21	1.00	1.00	1.65	1.01	1.07
LR_T4Q3	1.15	1.00	1.00	1.64	1.03	1.13	1.17	1.00	1.00	1.85	1.03	1.13
LR_T4Q6	1.11	1.00	1.00	1.76	1.01	1.09	1.14	1.00	1.00	1.58	1.00	1.07
LR_T4Q9	1.10	1.00	1.00	1.60	1.01	1.11	1.12	1.00	1.00	1.84	1.02	1.09

Table 4-3. Ratios of the statistics of Table 4-1 at 150% to 100% DBE shaking

Model	θ				β			
	G0	M0	M1	M2	G0	M0	M1	M2
Displacement								
LR_T2Q3	1.78	1.71	1.71	1.72	0.91	0.93	0.93	0.93
LR_T2Q6	2.17	2.04	2.03	2.03	0.84	0.84	0.83	0.79
LR_T2Q9	2.49	2.51	2.49	2.45	1.08	0.71	0.74	0.78
LR_T3Q3	1.61	1.60	1.60	1.60	0.92	0.83	0.85	0.88
LR_T3Q6	1.80	1.73	1.73	1.73	0.93	0.89	0.89	0.91
LR_T3Q9	2.08	2.00	2.00	2.00	0.89	1.00	0.97	0.91
LR_T4Q3	1.55	1.55	1.55	1.56	0.86	0.90	0.89	0.89
LR_T4Q6	1.59	1.57	1.57	1.58	1.04	1.03	1.02	1.02
LR_T4Q9	1.86	1.77	1.77	1.77	0.99	0.95	0.95	0.92
Force								
LR_T2Q3	1.71	1.66	1.67	1.67	0.94	0.96	0.97	0.98
LR_T2Q6	1.88	1.85	1.84	1.83	0.95	0.90	0.92	0.94
LR_T2Q9	1.76	1.88	1.88	1.85	1.42	0.99	1.02	1.08
LR_T3Q3	1.50	1.50	1.50	1.50	0.98	0.89	0.94	1.01
LR_T3Q6	1.47	1.47	1.47	1.47	1.12	1.09	1.11	1.16
LR_T3Q9	1.40	1.46	1.46	1.45	1.13	1.37	1.37	1.39
LR_T4Q3	1.36	1.38	1.38	1.38	0.91	1.03	1.03	1.03
LR_T4Q6	1.24	1.28	1.28	1.28	1.42	1.27	1.25	1.23
LR_T4Q9	1.23	1.25	1.25	1.25	1.22	1.41	1.41	1.39

Table 4-4. Ratios of displacement for 1% (10%) exceedance probability at 100% (150%) DBE to $\theta_{G0,DBE}$ and $\theta_{M0,DBE}$ for LR systems

Model	$\frac{D_{M1,DBE,99th}}{\theta_{G0,DBE}}$	$\frac{D_{M1,150\%DBE,90th}}{\theta_{G0,DBE}}$	$\frac{D_{M2,DBE,99th}}{\theta_{G0,DBE}}$	$\frac{D_{M2,150\%DBE,90th}}{\theta_{G0,DBE}}$	$\frac{D_{M1,DBE,99th}}{\theta_{M0,DBE}}$	$\frac{D_{M1,150\%DBE,90th}}{\theta_{M0,DBE}}$	$\frac{D_{M2,DBE,99th}}{\theta_{M0,DBE}}$	$\frac{D_{M2,150\%DBE,90th}}{\theta_{M0,DBE}}$
LR_T2Q3	1.76	2.55	1.77	2.55	1.41	2.04	1.42	2.05
LR_T2Q6	2.18	3.46	2.32	3.50	1.57	2.50	1.67	2.52
LR_T2Q9	2.67	4.53	2.85	4.68	1.93	3.26	2.05	3.37
LR_T3Q3	1.83	2.34	1.85	2.37	1.51	1.94	1.53	1.96
LR_T3Q6	2.22	2.91	2.24	2.93	1.72	2.26	1.73	2.27
LR_T3Q9	2.47	3.75	2.59	3.77	1.79	2.73	1.88	2.74
LR_T4Q3	1.92	2.36	1.93	2.37	1.60	1.96	1.60	1.96
LR_T4Q6	2.06	2.58	2.07	2.58	1.69	2.11	1.69	2.11
LR_T4Q9	2.29	3.10	2.34	3.11	1.74	2.36	1.78	2.36

Table 4-5. Ratios of shearing force for 1% (10%) exceedance probability at 100% (150%) DBE to $\theta_{G0,DBE}$ and $\theta_{M0,DBE}$ for LR systems

Model	$\frac{F_{M1,DBE,99th}}{\theta_{G0,DBE}}$	$\frac{F_{M1,150\%DBE,90th}}{\theta_{G0,DBE}}$	$\frac{F_{M2,DBE,99th}}{\theta_{G0,DBE}}$	$\frac{F_{M2,150\%DBE,90th}}{\theta_{G0,DBE}}$	$\frac{F_{M1,DBE,99th}}{\theta_{M0,DBE}}$	$\frac{F_{M1,150\%DBE,90th}}{\theta_{M0,DBE}}$	$\frac{F_{M2,DBE,99th}}{\theta_{M0,DBE}}$	$\frac{F_{M2,150\%DBE,90th}}{\theta_{M0,DBE}}$
LR_T2Q3	1.74	2.47	1.80	2.52	1.41	2.00	1.46	2.03
LR_T2Q6	1.93	2.92	1.97	2.95	1.48	2.24	1.51	2.26
LR_T2Q9	1.82	2.87	1.84	2.90	1.49	2.35	1.51	2.38
LR_T3Q3	1.78	2.20	1.91	2.32	1.50	1.85	1.61	1.95
LR_T3Q6	1.76	2.22	1.80	2.27	1.47	1.85	1.50	1.90
LR_T3Q9	1.55	2.10	1.57	2.13	1.33	1.81	1.35	1.83
LR_T4Q3	1.67	1.96	1.74	2.01	1.45	1.70	1.51	1.75
LR_T4Q6	1.47	1.72	1.51	1.74	1.32	1.55	1.36	1.57
LR_T4Q9	1.35	1.61	1.38	1.63	1.22	1.46	1.25	1.48

2) In Table 4-2, the ratios of θ for M1/M0 and M2/M1 are equal to 1 for all models with T_d = 3 and 4 seconds and shaking intensities. The median response for analyses accounting for the variability in isolation-system material properties (i.e., Sets M1 and M2) can be estimated without bias using analysis of a best-estimate model (i.e., Set M0).

3) In Table 4-2, the ratios of θ for M0/G0 for displacement range between 1.20 and 1.38 and those for shearing force range between 1.10 and 1.21 for all models with T_d = 3 and 4 seconds. If analysis is performed using geomean-spectrum-compatible ground motions, the median displacement should be increased by 20% to 40% and the median shearing force should be increased by 20% to address variability in spectral demands.

4) In Table 4-3, the ratio of θ at 150% to 100% DBE shaking for a given model and analysis set ranges between 1.55 and 2.08 for bearing displacement and between 1.23 and 1.50 for shearing force all models with T_d = 3 and 4 seconds. At a given T_d, the ratio of θ for bearing displacement increases as Q_d increases and that for shearing force decreases as Q_d increases.

5) In Table 4-1, the values of β of Table 4-1 for displacement range between 0.11 and 0.27 and those for transmitted shearing force range between 0.05 and 0.21 for all models with T_d = 3 and 4 seconds. The dispersion in displacement is higher than for transmitted shearing force. The percentage increase in β due to variability in spectral demand is higher than that due to the variability in the mechanical properties of the isolation system.

6) If we assume that the response-history analysis is performed for Set G0 using the models associated with T_d = 3 and 4 seconds and the dispersion in the peak bearing displacement is no greater than 0.19 per Table 4-1, the minimum number of pairs of ground motions per (3.3) to ensure a 90% confidence of the true median displacement being within ±10% of the estimated value is 11.

Scale factors for responses with 1% (10%) probability of exceedance at 100% (150%) DBE shaking

The analyses of Table 3-6 and Table 3-7 were repeated for the Vogtle NPP site to compute the factors to scale the median responses for Sets G0 and M0 and 100% DBE shaking to the responses corresponding to 1) 1% probability of exceedance (PE) for Sets M1 and M2 for 100% DBE shaking, and 2) 10% PE for Sets M1 and M2 for 150% DBE shaking. The results are presented in Table 4-4 and Table 4-5 for displacement and shearing force, respectively. The scale factor for displacement is greater than the corresponding factor for shearing force. For example, the factors $D_{M1,DBE,99th}/\theta_{G0,DBE}$ and $F_{M1,DBE,99th}/\theta_{G0,DBE}$ for Model LR_T3Q6 are 2.22 and 1.76, respectively. The factors for 10% PE and 150% DBE shaking are greater than the corresponding factors for 1% PE and 100% DBE shaking: $D_{M1,150\%DBE,90th}/\theta_{G0,DBE}$ and $D_{M1,DBE,99th}/\theta_{G0,DBE}$ for Model LR_T3Q6 are 2.91 and 2.22, respectively.

If response-history analysis is performed using only the DBE spectrum-compatible ground motions, the scale factor for displacement (force) corresponding to 1% PE at 100% DBE shaking ranges between 1.83 (1.35) and 2.59 (1.91) and that corresponding to 10% PE at 150% DBE shaking ranges between 2.34 (1.61) and 3.77 (2.32) for all models associated with T_d = 3 and 4 seconds (see the 2nd through 5th columns of Table 4-4 and Table 4-5).

If response-history analysis is performed using the maximum-minimum spectra compatible ground motions, the factor for displacement (force) corresponding to 1% PE at 100% DBE shaking ranges between 1.51 (1.22) and 1.88 (1.61) and that corresponding to 10% PE at 150% DBE shaking ranges between 1.94 (1.46) and 2.74 (1.95) for all models associated with T_d = 3 and 4 seconds (see the 6th through 9th columns of Table 4-4 and Table 4-5).

4.4.2 Friction Pendulum (FP) isolation systems

Medians and logarithmic standard deviations of peak displacement and force

The analyses of Table 4-1 through Table 4-3 were repeated for the FP isolation systems and results are presented in Table 4-6 through Table 4-8, respectively. The key observations include:

1) For 100% (150%) DBE shaking, the values of θ of Table 4-6 for displacement range between 71 (191) and 379 (674) mm and those for transmitted shearing force range between 8.4 (12.6) and 44.3 (81.4) percent of the supported weight. Similar to the presentation of Section 4.4.1, the shape of the spectrum at the Vogtle site per the dashed line in Figure 4-4 should preclude the use of isolation systems with T_d = 2 seconds. Accordingly, the results for the isolation systems with T_d = 2 seconds are shaded in Table 4-6 through Table 4-10 not used further in this report.

2) In Table 4-7, the ratios of θ for M1/M0 and M2/M1 are equal to 1 for all models and shaking intensities. The median response for analyses accounting for variability in the mechanical

Table 4-6. Medians (θ) and dispersions (β) of peak displacement and shearing force for Sets G0, M0, M1 and M2 and 100% and 150% DBE shaking for FP systems

Model	100% DBE								150% DBE							
	θ (mm for displacement; %W for force)				β				θ (mm for displacement; %W for force)				β			
	G0	M0	M1	M2	G0	M0	M1	M2	G0	M0	M1	M2	G0	M0	M1	M2
Displacement																
FP_T2Q3	303	379	379	379	0.14	0.15	0.15	0.15	559	674	674	674	0.13	0.14	0.14	0.14
FP_T2Q6	145	208	208	208	0.21	0.22	0.23	0.26	363	474	474	473	0.16	0.16	0.16	0.18
FP_T2Q9	71	105	105	105	0.21	0.33	0.34	0.37	217	311	311	310	0.21	0.22	0.23	0.26
FP_T3Q3	246	303	303	303	0.14	0.20	0.19	0.20	433	523	523	523	0.12	0.15	0.15	0.15
FP_T3Q6	140	190	190	189	0.21	0.30	0.30	0.31	308	391	391	391	0.18	0.25	0.24	0.25
FP_T3Q9	76	105	106	106	0.22	0.32	0.32	0.35	208	282	282	281	0.22	0.30	0.30	0.31
FP_T4Q3	193	240	240	240	0.15	0.22	0.22	0.22	325	403	403	403	0.12	0.19	0.19	0.19
FP_T4Q6	128	168	168	168	0.20	0.29	0.28	0.29	255	319	319	319	0.18	0.26	0.25	0.26
FP_T4Q9	79	107	107	107	0.21	0.31	0.31	0.33	191	250	249	249	0.21	0.29	0.28	0.29
Force																
FP_T2Q3	35.2	44.3	44.2	44.2	0.14	0.17	0.17	0.17	67.2	81.4	81.4	81.4	0.14	0.16	0.16	0.16
FP_T2Q6	21.5	28.5	28.5	28.6	0.16	0.22	0.22	0.23	46.9	60.5	60.5	60.6	0.14	0.20	0.19	0.20
FP_T2Q9	17.1	21.2	21.2	21.4	0.10	0.21	0.20	0.21	34.2	45.2	45.2	45.3	0.16	0.23	0.23	0.24
FP_T3Q3	14.8	17.9	17.9	17.9	0.13	0.21	0.21	0.21	25.6	30.6	30.6	30.6	0.12	0.18	0.18	0.18
FP_T3Q6	12.7	15.4	15.4	15.4	0.11	0.19	0.19	0.19	22.0	26.4	26.5	26.5	0.13	0.24	0.24	0.23
FP_T3Q9	13.4	15.0	15.0	15.0	0.06	0.10	0.10	0.11	20.3	24.4	24.3	24.4	0.11	0.20	0.20	0.19
FP_T4Q3	8.4	9.8	9.8	9.8	0.11	0.17	0.17	0.17	12.6	15.0	15.0	15.0	0.12	0.17	0.17	0.17
FP_T4Q6	9.9	11.1	11.1	11.1	0.07	0.14	0.14	0.14	14.2	16.4	16.4	16.4	0.11	0.18	0.18	0.18
FP_T4Q9	12.2	13.0	13.0	13.0	0.05	0.07	0.07	0.09	15.9	17.8	17.8	17.9	0.08	0.15	0.15	0.15

Table 4-7. Ratios of median (θ) and dispersion (β) of peak displacement and shearing force for Sets G0, M0, M1 and M2 and 100% and 150% DBE shaking for FP systems

Model	100% DBE						150% DBE					
	Ratio of θ			Ratio of β			Ratio of θ			Ratio of β		
	$\frac{M0}{G0}$	$\frac{M1}{M0}$	$\frac{M2}{M1}$	$\frac{M0}{G0}$	$\frac{M1}{M0}$	$\frac{M2}{M1}$	$\frac{M0}{G0}$	$\frac{M1}{M0}$	$\frac{M2}{M1}$	$\frac{M0}{G0}$	$\frac{M1}{M0}$	$\frac{M2}{M1}$
Displacement												
FP_T2Q3	1.25	1.00	1.00	1.03	1.00	1.05	1.20	1.00	1.00	1.11	0.99	1.02
FP_T2Q6	1.43	1.00	1.00	1.03	1.03	1.13	1.31	1.00	1.00	0.99	1.01	1.08
FP_T2Q9	1.47	1.00	1.00	1.56	1.02	1.10	1.43	1.00	1.00	1.04	1.03	1.13
FP_T3Q3	1.23	1.00	1.00	1.36	0.99	1.02	1.21	1.00	1.00	1.23	0.99	1.01
FP_T3Q6	1.36	1.00	1.00	1.40	1.00	1.04	1.27	1.00	1.00	1.38	0.99	1.02
FP_T3Q9	1.40	1.00	1.01	1.48	1.02	1.09	1.36	1.00	1.00	1.39	1.00	1.04
FP_T4Q3	1.25	1.00	1.00	1.53	0.99	1.01	1.24	1.00	1.00	1.54	0.99	1.01
FP_T4Q6	1.31	1.00	1.00	1.41	0.99	1.02	1.25	1.00	1.00	1.47	0.99	1.01
FP_T4Q9	1.36	1.00	1.00	1.50	1.00	1.06	1.31	1.00	1.00	1.36	0.99	1.02
Force												
FP_T2Q3	1.26	1.00	1.00	1.23	0.99	1.03	1.21	1.00	1.00	1.18	0.99	1.01
FP_T2Q6	1.32	1.00	1.00	1.36	1.00	1.04	1.29	1.00	1.00	1.39	1.00	1.04
FP_T2Q9	1.24	1.00	1.01	2.07	0.99	1.02	1.32	1.00	1.00	1.49	1.00	1.04
FP_T3Q3	1.21	1.00	1.00	1.63	0.98	1.00	1.19	1.00	1.00	1.48	0.98	1.00
FP_T3Q6	1.21	1.00	1.00	1.77	0.98	0.99	1.20	1.00	1.00	1.87	0.98	0.99
FP_T3Q9	1.12	1.00	1.00	1.62	1.01	1.05	1.20	1.00	1.00	1.89	0.98	1.00
FP_T4Q3	1.17	1.00	1.00	1.59	0.99	1.00	1.19	1.00	1.00	1.47	0.98	1.00
FP_T4Q6	1.12	1.00	1.00	1.95	0.98	1.00	1.15	1.00	1.00	1.68	0.98	1.00
FP_T4Q9	1.07	1.00	1.00	1.43	1.06	1.20	1.12	1.00	1.00	1.97	0.98	1.00

Table 4-8. Ratios of the statistics of Table 4-6 for 150% to 100% DBE shaking

Model	θ				β			
	G0	M0	M1	M2	G0	M0	M1	M2
Displacement								
FP_T2Q3	1.85	1.78	1.78	1.78	0.92	0.99	0.98	0.95
FP_T2Q6	2.49	2.28	2.28	2.28	0.76	0.73	0.71	0.68
FP_T2Q9	3.05	2.97	2.97	2.95	1.01	0.67	0.68	0.69
FP_T3Q3	1.76	1.72	1.72	1.72	0.86	0.77	0.77	0.77
FP_T3Q6	2.20	2.06	2.06	2.07	0.84	0.83	0.82	0.80
FP_T3Q9	2.75	2.67	2.66	2.64	1.01	0.95	0.93	0.89
FP_T4Q3	1.69	1.68	1.68	1.68	0.83	0.84	0.83	0.83
FP_T4Q6	1.99	1.90	1.90	1.90	0.86	0.90	0.90	0.89
FP_T4Q9	2.43	2.34	2.34	2.33	1.02	0.93	0.92	0.89
Force								
FP_T2Q3	1.91	1.84	1.84	1.84	0.99	0.96	0.95	0.94
FP_T2Q6	2.18	2.12	2.12	2.12	0.87	0.89	0.88	0.88
FP_T2Q9	2.00	2.13	2.13	2.12	1.57	1.13	1.13	1.15
FP_T3Q3	1.74	1.71	1.71	1.71	0.94	0.86	0.86	0.86
FP_T3Q6	1.72	1.71	1.72	1.72	1.17	1.24	1.24	1.23
FP_T3Q9	1.52	1.63	1.63	1.62	1.64	1.91	1.86	1.77
FP_T4Q3	1.51	1.53	1.53	1.53	1.08	1.00	1.00	1.00
FP_T4Q6	1.43	1.47	1.47	1.47	1.48	1.27	1.28	1.28
FP_T4Q9	1.31	1.37	1.37	1.37	1.64	2.25	2.08	1.72

properties of the isolation system (i.e., M1 and M2) can be estimated without bias using analysis of a best-estimate model.

3) In Table 4-7, the ratios of θ for M0/G0 for displacement range between 1.21 and 1.40 and those for shearing force range between 1.07 and 1.21 for all models with T_d = 3 and 4 seconds. If the analysis is performed using geomean-spectrum-compatible ground motions, the median displacement should be increased by 20% to 40% and the median shearing force should be increased by 10% to 20% to address variability in spectral demand.

4) In Table 4-8, the ratios of θ at 150% to 100% DBE shaking range between 1.68 and 2.75 for bearing displacement and between 1.31 and 1.74 for shearing force for all models with T_d = 3 and 4 seconds. At a given T_d, the ratio of θ for displacement increases as Q_d increases and that for shearing force decreases as Q_d increases.

5) In Table 4-6, the values of β for displacement range between 0.14 and 0.35 and those for transmitted shearing force range between 0.05 and 0.21 for all models with T_d = 3 and 4 seconds. The dispersion in displacement is generally higher than for transmitted shearing force. The percentage increase in β due to the variability in spectral demand is higher than that due to the variability in the mechanical properties of the isolation system.

6) If we assume that the response-history analysis is performed for Set G0 using the models with T_d = 3 and 4 seconds and the dispersion in the peak displacement is no greater than 0.22 per Table 4-6, the minimum number of pairs of ground motions per (3.3) to ensure a 90% confidence of the true median displacement being within ±10% of the estimated value is about 14.

Scale factors for responses with 1% (10%) probability of exceedance at 100% (150%) DBE shaking

The analyses of Table 4-4 and Table 4-5 were repeated for the FP isolation systems and results are presented in Table 4-9 and Table 4-10, respectively. For all models with T_d = 3 and 4 seconds, the scale factor for displacement is generally greater than the corresponding factor for shearing force except for Model FP_T3Q3. The factor for 10% PE and 150% DBE shaking is greater than the corresponding factor for 1% PE and 100% DBE shaking: a trend similar to that observed in Table 4-4 and Table 4-5 for LR bearings.

Table 4-9. Ratios of displacement for 1% (10%) exceedance probability at 100% (150%) DBE to $\theta_{G0,DBE}$ and $\theta_{M0,DBE}$ for FP systems

Model	$\frac{D_{M1,DBE,99th}}{\theta_{G0,DBE}}$	$\frac{D_{M1,150\%DBE,90th}}{\theta_{G0,DBE}}$	$\frac{D_{M2,DBE,99th}}{\theta_{G0,DBE}}$	$\frac{D_{M2,150\%DBE,90th}}{\theta_{G0,DBE}}$	$\frac{D_{M1,DBE,99th}}{\theta_{M0,DBE}}$	$\frac{D_{M1,150\%DBE,90th}}{\theta_{M0,DBE}}$	$\frac{D_{M2,DBE,99th}}{\theta_{M0,DBE}}$	$\frac{D_{M2,150\%DBE,90th}}{\theta_{M0,DBE}}$
FP_T2Q3	1.75	2.67	1.78	2.68	1.40	2.13	1.42	2.14
FP_T2Q6	2.43	4.01	2.59	4.08	1.70	2.81	1.81	2.85
FP_T2Q9	3.23	5.86	3.51	6.08	2.19	3.98	2.39	4.13
FP_T3Q3	1.93	2.57	1.95	2.58	1.57	2.09	1.58	2.09
FP_T3Q6	2.72	3.83	2.80	3.85	2.00	2.82	2.06	2.83
FP_T3Q9	2.98	5.49	3.20	5.57	2.13	3.93	2.29	3.99
FP_T4Q3	2.09	2.65	2.10	2.66	1.68	2.13	1.68	2.13
FP_T4Q6	2.52	3.44	2.56	3.45	1.93	2.63	1.96	2.64
FP_T4Q9	2.78	4.56	2.91	4.59	2.05	3.36	2.14	3.38

Table 4-10. Ratios of shearing force for 1% (10%) exceedance probability at 100% (150%) DBE to $\theta_{G0,DBE}$ and $\theta_{M0,DBE}$ for FP systems

Model	$\frac{F_{M1,DBE,99th}}{\theta_{G0,DBE}}$	$\frac{F_{M1,150\%DBE,90th}}{\theta_{G0,DBE}}$	$\frac{F_{M2,DBE,99th}}{\theta_{G0,DBE}}$	$\frac{F_{M2,150\%DBE,90th}}{\theta_{G0,DBE}}$	$\frac{F_{M1,DBE,99th}}{\theta_{M0,DBE}}$	$\frac{F_{M1,150\%DBE,90th}}{\theta_{M0,DBE}}$	$\frac{F_{M2,DBE,99th}}{\theta_{M0,DBE}}$	$\frac{F_{M2,150\%DBE,90th}}{\theta_{M0,DBE}}$
FP_T2Q3	1.85	2.83	1.87	2.84	1.47	2.25	1.49	2.26
FP_T2Q6	2.21	3.61	2.27	3.64	1.67	2.73	1.71	2.75
FP_T2Q9	1.99	3.55	2.03	3.59	1.61	2.87	1.64	2.91
FP_T3Q3	1.97	2.61	1.97	2.61	1.63	2.16	1.63	2.16
FP_T3Q6	1.89	2.81	1.89	2.81	1.56	2.33	1.56	2.33
FP_T3Q9	1.42	2.33	1.45	2.33	1.28	2.09	1.30	2.09
FP_T4Q3	1.74	2.23	1.74	2.23	1.48	1.91	1.48	1.91
FP_T4Q6	1.55	2.07	1.55	2.07	1.39	1.85	1.39	1.85
FP_T4Q9	1.26	1.77	1.30	1.77	1.18	1.66	1.22	1.66

If response-history analysis is performed using only the DBE spectrum-compatible ground motions, the scale factor for displacement (force) corresponding to 1% PE at 100% DBE shaking ranges between 1.93 (1.26) and 3.20 (1.97) and that corresponding to 10% PE at 150% DBE shaking ranges between 2.57 (1.77) and 5.57 (2.81) (see the 2nd through 5th columns of Table 4-9 and Table 4-10). The values of $D_{M1,150\%DBE,90th}/\theta_{G0,DBE}$ and $D_{M2,150\%DBE,90th}/\theta_{G0,DBE}$ for the models with $Q_d = 0.09W$ are much higher than those with $Q_d = 0.03W$ and $0.06W$. For example, the value of $D_{M2,150\%DBE,90th}/\theta_{G0,DBE}$ for Model FP_T3Q9 is 5.57, which is the product of 1.4 (see Table 4-7 for the ratio of median displacement for Model FP_T3Q9, M0/G0 and 100% DBE shaking), 2.67 (see Table 4-8 for the ratio of median displacement for Model FP_T3Q9 and Set M0 for 150% to 100% DBE shaking) and 1.5 (the ratio of the 90^{th}- to 50^{th}-percentile value of a lognormal distribution with a β of 0.31, presented in Table 4-6 for displacement, Model FP_T3Q9, Set M2 and 150% DBE shaking). The value of $D_{M2,150\%DBE,90th}/\theta_{G0,DBE}$ for Model FP_T3Q3 is 2.58, which is the product of 1.23, 1.72 and 1.22, where the third value is the ratio of the 90^{th}- to 50^{th}-percentile value of a lognormal distribution with a β of 0.15 (see Table 4-6 for displacement, Model FP_T3Q3, Set M2 and 150% DBE shaking).

If response-history analysis is performed using the maximum-minimum spectra compatible ground motions, the factor for displacement (force) corresponding to 1% PE at 100% DBE shaking ranges between 1.57 (1.18) and 2.29 (1.63) and that corresponding to 10% PE at 150% DBE shaking ranges between 2.09 (1.66) and 3.99 (2.33) (see the 6th through 9th columns of Table 4-9 and Table 4-10).

SECTION 5
STUDIES FOR WUS ROCK SITES

5.1 Design basis earthquake

The site of the Diablo Canyon nuclear power plant (NPP) in San Luis Obispo County, California, is a representative rock site for a NPP in the Western US (WUS). The Design Basis Earthquake (DBE) used for the study at the Diablo Canyon site, which was provided by staff at the United States Nuclear Regulatory Commission (USNRC), is introduced in this subsection.

The horizontal and vertical DBE spectra for the Diablo Canyon study are presented in Figure 5-1 using both normal and logarithmic scales. The horizontal DBE spectrum transmitted to the authors is truncated at a period of 2 seconds with the spectral ordinates at periods of 1, 1.5 and 2 seconds equal to 0.9, 0.59 and 0.4 g, respectively. Since the spectral ordinates at periods greater than 1 second is close to the function of $0.9/T$, where T is period, the horizontal spectral ordinates at periods greater than 1 second were replaced by $0.9/T$ at periods between 1 and 5 seconds. The vertical DBE spectrum provided to the authors was truncated at a period of 1 second. The spectral ordinates of $0.9/T$ at periods between 1 and 5 seconds were scaled by the ratio of the ordinates of the original vertical and horizontal DBE spectra at a period of 1 second to develop the vertical spectra of Figure 5-1.

5.2 Selection and scaling of ground motions

Panels a and b of Figure 5-2 present the deaggregation of the seismic hazard at periods of 2 and 3 seconds, respectively, and an annual frequency of exceedance of 10^{-4} for the Diablo Canyon NPP site. The deaggregation results were generated using USGS interactive deaggregation tool (USGS 2009a). The magnitude (M_w) and distance (r) for the modal and mean events, which are indentified in Figure 5-2, range between 7.5 and 7.8 (M_w) and 10 and 20 km (r).

The seed ground motions used to develop the DBE spectrum-compatible ground motions for the Diablo Canyon study were selected from the PEER NGA Database (http://peer.berkeley.edu/nga/). The number of rock-site records in the PEER NGA Database within the ranges of M_w and r listed above is less than 30. To select 30 sets of seed ground motions, we expanded the range to M_w greater than 6.6, r less than 32 km and V_{S30} (the average shear-wave velocity to 30-meter depth) greater than 700 m/s. Table 5-1 presents the 30 sets of seed ground motions used for the Diablo Canyon study. Each set of the seed

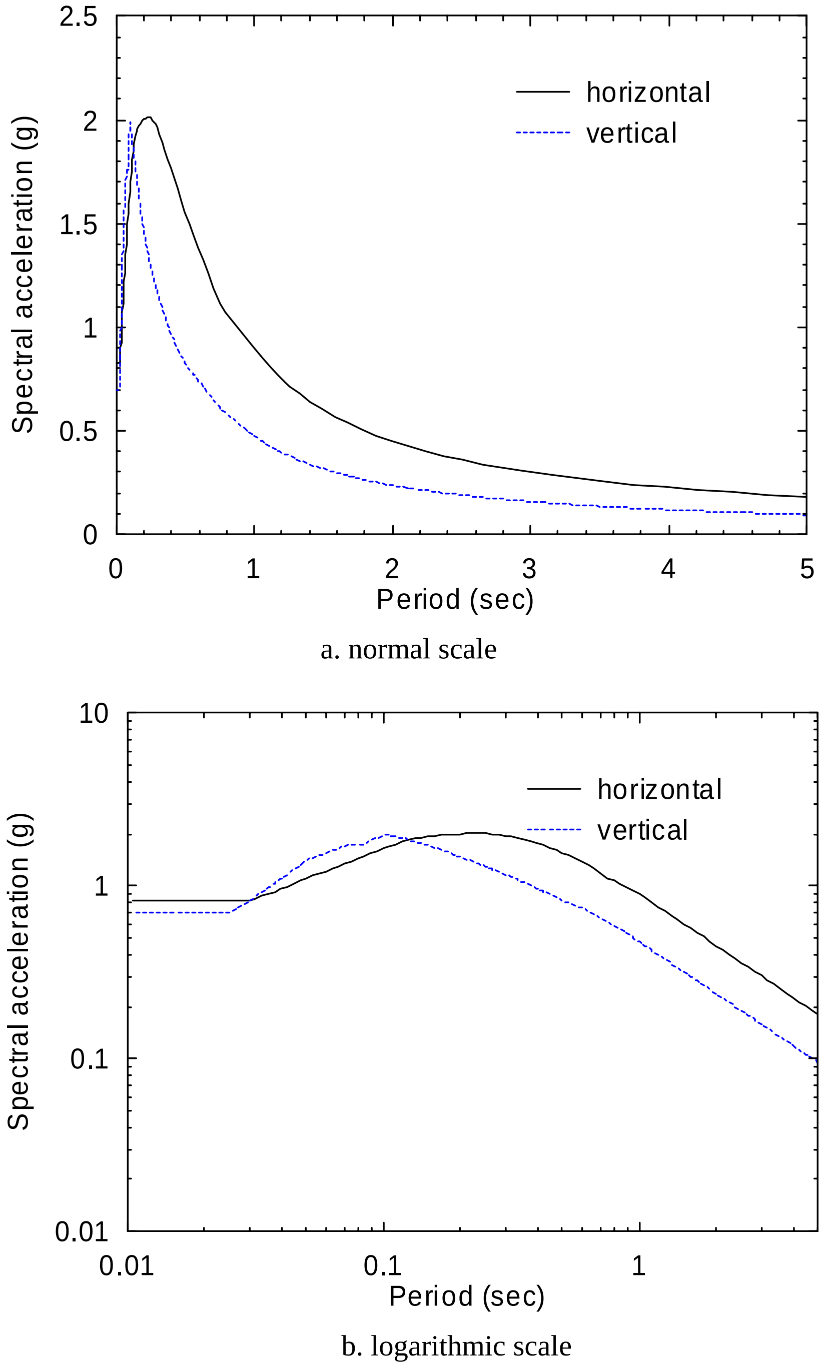

Figure 5-1. Horizontal and vertical DBE spectra for the Diablo Canyon NPP site and 5% damping in normal and logarithmic scales

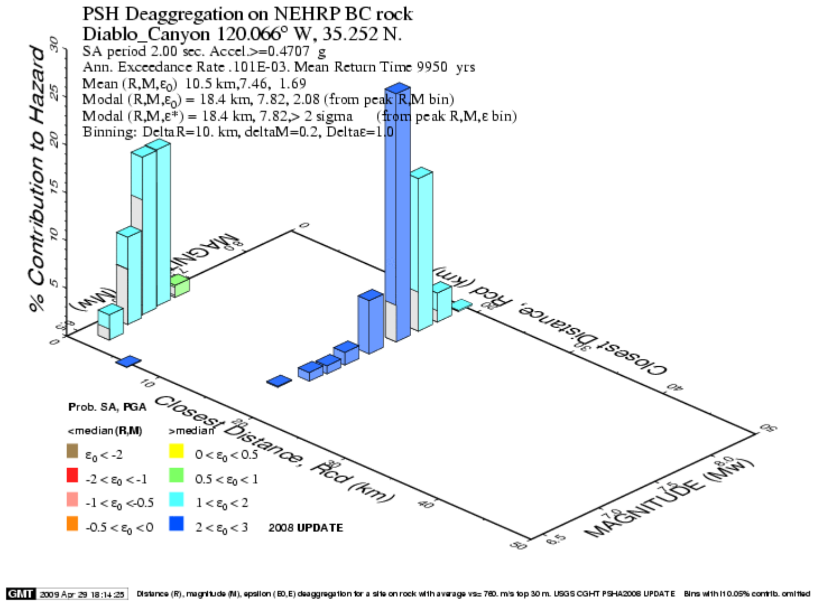

a. 2 seconds

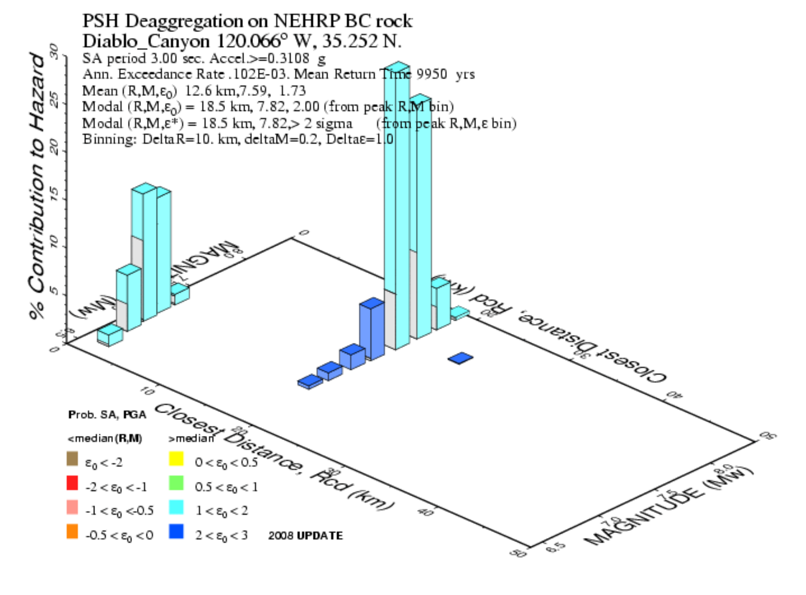

b. 3 seconds

Figure 5-2. Deaggregation of the seismic hazard at periods of 2 and 3 seconds at an annual frequency of exceedance of 10^{-4} for the Diablo Canyon NPP site (USGS 2009a)

ground motions was spectrally matched to the DBE spectra of Figure 5-1 using the computer code RSPMATCH (Abrahamson 1998).

Panels a, c and e of Figure 5-3 present a sample set of DBE spectrum-compatible ground motions and panels b, d and f present the target and achieved spectral accelerations for the time series of panels a, c and e, respectively. The spectrum-compatible ground motions of Figure 5-3 were developed using the third set of seed motions in Table 5-1. Panels a, b and c of Figure 5-4 present the spectral accelerations for horizontal components 1 and 2 and the vertical component, respectively, of all 30 sets of DBE spectrum-compatible ground motions. Each spectrum of Figure 5-4 closely matches the target.

The 30 sets of DBE spectrum-compatible ground motions of Figure 5-4 were amplitude scaled to develop the maximum-minimum spectra compatible ground motions. The scaling procedure was the same as that described in Section 3.2.2 and is not repeated herein. Panels a, b and c of Figure 5-5 present the spectral accelerations for the horizontal components 1 and 2 and vertical component, respectively, of all 30 sets of DBE spectrum-compatible ground motions.

5.3 Analysis sets and discussion

The analysis described in Section 3.3 was repeated using the ground motions developed for the Diablo Canyon NPP site. Response-history analysis was performed for two intensities of shaking: 1) 100% DBE shaking using the 60 sets of ground motions of Figure 5-4 and Figure 5-5, and b) 150% DBE shaking using the ground motions of Figure 5-4 and Figure 5-5 but with the acceleration amplitudes multiplied by 1.5. At each intensity level, the 4 sets of analyses of Table 3-2, namely, Sets G0, M0, M1 and M2, were performed for each best-estimate model of Tables 2-1 through 2-3 and the 60 corresponding property-varied models to study the impact of variations in spectral demand and mechanical properties of the isolation system on the response of isolated NPPs.

The amplitude of the spectral response in the vertical direction for 100% DBE (and 150% DBE) shaking is such that separation of the containment vessel from the foundation is possible in either conventional or isolated configurations. Although disengagement of the containment vessel from the foundation could be accommodated, alternate analysis tools and numerical models from those described in Section 2 would be required for response computations. Analysis codes and component models would have address disengagement and re-contact for conventional and FP-isolated containment vessels and differences in compressive and tensile isolator axial stiffness for LR-isolated containment vessels.

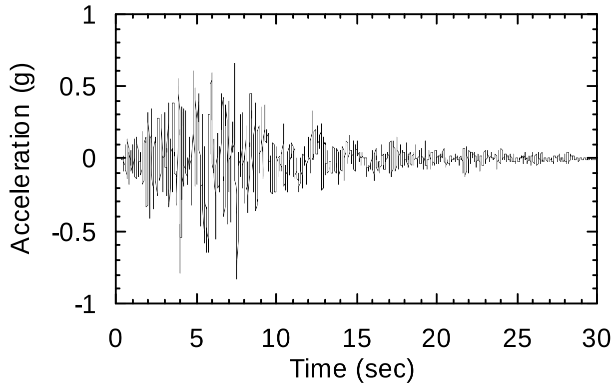

a. horizontal component 1

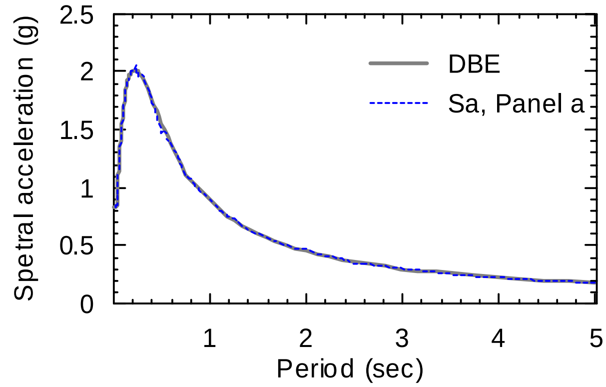

b. response spectrum of the time series of panel a

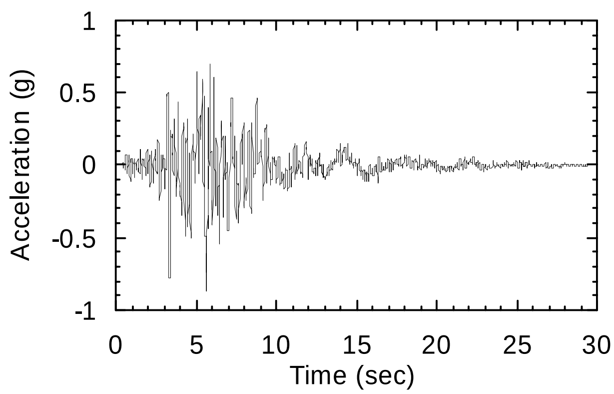

c. horizontal component 2

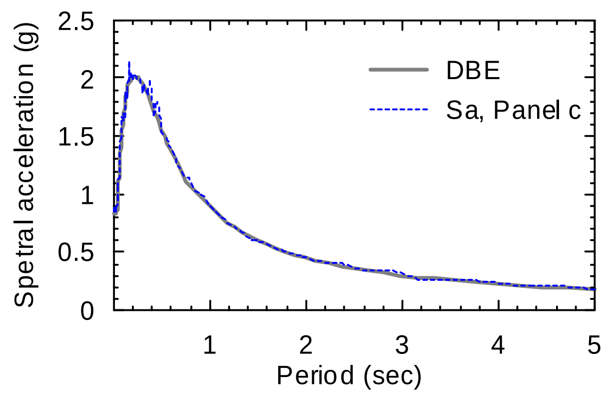

d. response spectrum of the time series of panel c

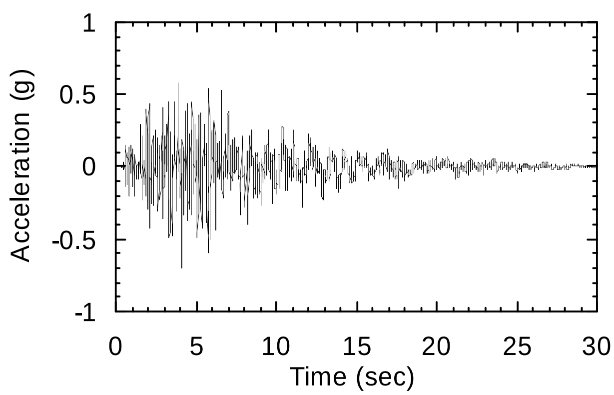

e. vertical component

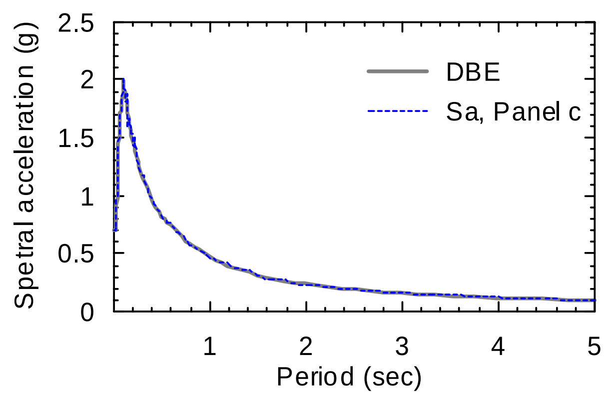

f. response spectrum of the time series of panel e

Figure 5-3. Sample spectrally matched acceleration time series and the corresponding 5% damped response spectra

Table 5-1. Seed ground motions for the Diablo Canyon study

No.	Event	Station	Date	M_w	r (km)	V_{S30} (m/s)
1	San Fernando	Lake Hughes #4	1971/02/09	6.61	25.1	821.7
2	San Fernando	Pacoima Dam (upper left)	1971/02/09	6.61	1.8	2016.1
3	San Fernando	Pasadena	1971/02/09	6.61	21.5	969.1
4	Tabas, Iran	Tabas	1978/09/16	7.35	2.1	766.8
5	Irpinia, Italy	Auletta	1980/11/23	6.90	9.6	1000.0
6	Irpinia, Italy	Bagnoli Irpinio	1980/11/23	6.90	8.2	1000.0
7	Irpinia, Italy	Bisaccia	1980/11/23	6.90	21.3	1000.0
8	Irpinia, Italy	Sturno	1980/11/23	6.90	10.8	1000.0
9	Loma Prieta	Gilroy - Gavilan Coll.	1989/10/18	6.93	10.0	729.7
10	Loma Prieta	Gilroy Array #1	1989/10/18	6.93	9.6	1428.0
11	Loma Prieta	UCSC	1989/10/18	6.93	18.5	714.0
12	Loma Prieta	UCSC Lick Observatory	1989/10/18	6.93	18.4	714.0
13	Cape Mendocino	Petrolia	1992/04/25	7.01	8.2	712.8
14	Northridge	Burbank - Howard Rd.	1994/01/17	6.69	16.9	821.7
15	Northridge	Chalon Rd	1994/01/17	6.69	20.5	740.1
16	Northridge	Griffith Park Observatory	1994/01/17	6.69	23.8	1015.9
17	Northridge	Wonderland Ave	1994/01/17	6.69	20.3	1222.5
18	Northridge	LA 00	1994/01/17	6.69	19.1	706.2
19	Northridge	Lake Hughes #4	1994/01/17	6.69	31.7	821.7
20	Northridge	Pacoima Dam (downstr)	1994/01/17	6.69	7.0	2016.1
21	Northridge	Pacoima Dam (upper left)	1994/01/17	6.69	7.0	2016.1
22	Northridge	Santa Susana Ground	1994/01/17	6.69	16.7	715.1
23	Northridge	Vasquez Rocks Park	1994/01/17	6.69	23.6	996.4
24	Kocaeli, Turkey	Gebze	1999/08/17	7.51	10.9	792.0
25	Kocaeli, Turkey	Izmit	1999/08/17	7.51	7.2	811.0
26	Chi-Chi, Taiwan	TCU045	1999/09/20	7.62	26.0	704.6
27	Chi-Chi, Taiwan	TCU102	1999/09/20	7.62	1.5	714.3
28	Duzce, Turkey	Lamont 1060	1999/11/12	7.14	25.9	782.0
29	Manjil, Iran	Abbar	1990/06/20	7.37	12.6	724.0
30	Loma Prieta	Los Gatos - Lexington Dam	1989/10/18	6.93	5.0	1070.3

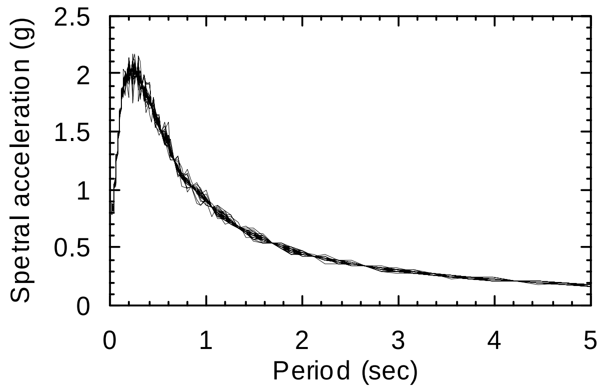

a. horizontal component 1

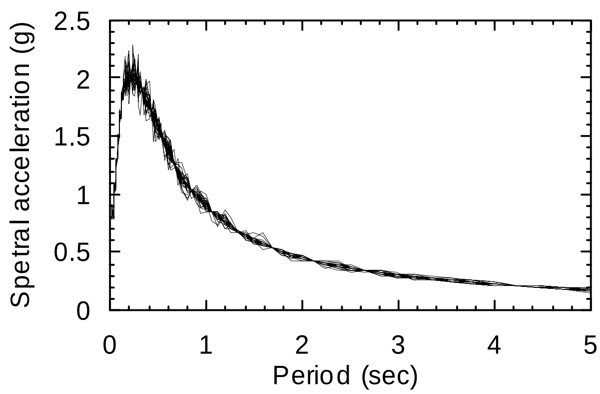

b. horizontal component 2

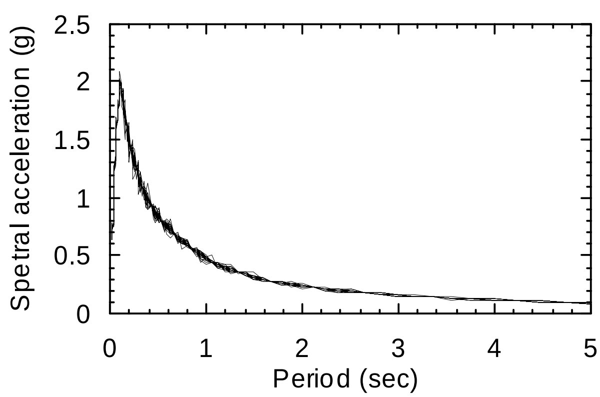

c. vertical component

Figure 5-4. Five-percent damped response spectra of the 30 sets of DBE spectrum-compatible ground motions for the Diablo Canyon site

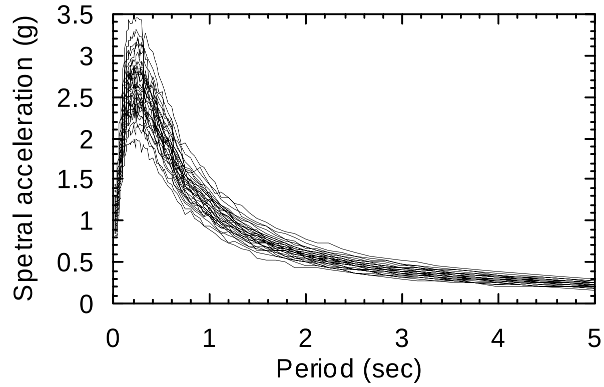

a. maximum component

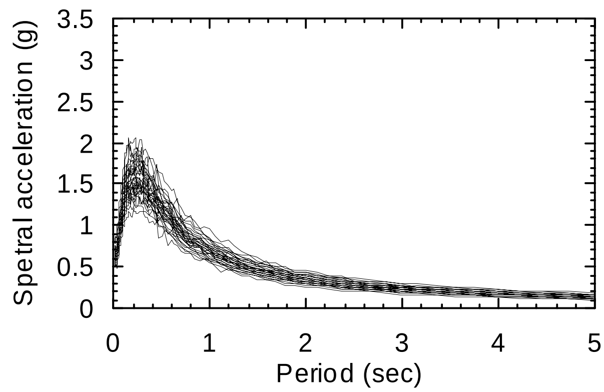

b. minimum component

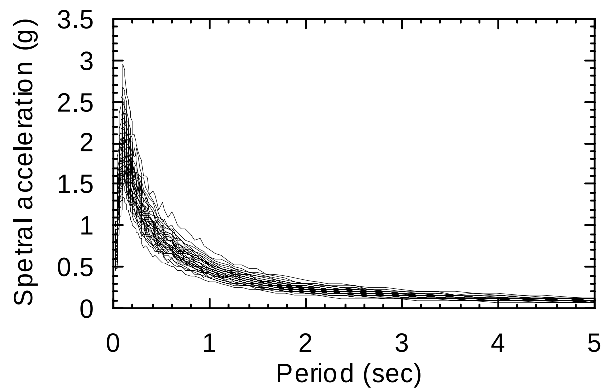

c. vertical component

Figure 5-5. Five-percent damped response spectra of the 30 sets of maximum-minimum DBE spectra-compatible ground motions for the Diablo Canyon site

Numerical and experimental studies have shown that vertical earthquake shaking does not affect the displacement response of either elastomeric or sliding isolation systems (e.g., Zayas et al, 1987, Mosqueda et al. 2004, Morgan 2007, Fenz and Constantinou, 2008b). The effects of vertical earthquake shaking on transmitted shearing forces in elastomeric isolation systems will be small. Experiments on FP-isolated models using recorded ground motions have shown only modest percent changes in transmitted shearing forces resulting from the application of vertical earthquake shaking, although significant percent increases have been observed for some combinations of near-fault ground motions, structural systems and isolator characteristics (Zayas et al, 1987, Fenz and Constantinou, 2008b). Given that the numerical tools of Chapter 2 may not reliably capture the effects of the intense vertical shaking expected at the Diablo Canyon site for 100% and 150% DBE shaking, the discussion that follows focuses solely on displacements of the isolation system.

5.4 Analysis results

5.4.1 Lead Rubber (LR) isolation systems

Medians and logarithmic standard deviations of peak displacement

Table 5-2 presents θ and β of peak displacement for each case, model and shaking intensity analyzed for LR isolation systems. Table 5-3 presents the ratios of θ and β for Set M0 to Set G0, Set M1 to Set M0, and Set M2 to Set M1, for each model and shaking intensity. Table 5-4 presents the ratios of θ and β at 150% to 100% DBE shaking. The key observations include:

1) For 100% (150%) DBE shaking, the values of θ of Table 5-2 for displacement range between 338 (595) and 940 (1621) mm.

2) In Table 5-3, the ratios of θ for M1/M0 and M2/M1 are equal to 1 for all models and shaking intensities. The median response for analyses accounting for the variability in the mechanical properties of isolation systems (i.e., Sets M1 and M2) can be estimated without bias using analysis of a best-estimate model (i.e., Set M0).

3) In Table 5-3, the ratios of θ for M0/G0 for displacement range between 1.17 and 1.22. If the analysis is performed using geomean-spectrum-compatible ground motions, the median displacement should be increased by 20% to address variability in spectral demands.

Table 5-2. Medians (θ) and dispersions (β) of peak displacement for Sets G0, M0, M1 and M2 and 100% and 150% DBE shaking for LR systems

Model	100% DBE								150% DBE							
	θ (mm)				β				θ (mm)				β			
	G0	M0	M1	M2	G0	M0	M1	M2	G0	M0	M1	M2	G0	M0	M1	M2
LR_T2Q3	488	572	573	576	0.10	0.13	0.13	0.14	792	932	932	936	0.09	0.12	0.12	0.13
LR_T2Q6	401	473	473	472	0.14	0.20	0.20	0.21	678	797	797	798	0.12	0.16	0.16	0.17
LR_T2Q9	338	404	404	405	0.19	0.25	0.25	0.25	595	703	703	702	0.14	0.21	0.21	0.21
LR_T3Q3	643	774	774	776	0.15	0.18	0.18	0.18	1086	1300	1300	1303	0.12	0.16	0.16	0.16
LR_T3Q6	494	584	585	585	0.19	0.26	0.25	0.25	862	1039	1039	1041	0.18	0.22	0.22	0.22
LR_T3Q9	404	471	472	472	0.20	0.28	0.28	0.28	729	863	864	865	0.20	0.26	0.26	0.26
LR_T4Q3	785	940	938	937	0.14	0.16	0.16	0.17	1359	1621	1618	1619	0.13	0.14	0.14	0.14
LR_T4Q6	527	642	642	642	0.19	0.24	0.24	0.24	1011	1220	1219	1217	0.15	0.19	0.19	0.20
LR_T4Q9	418	493	493	495	0.21	0.29	0.29	0.29	779	951	951	950	0.19	0.24	0.24	0.24

Table 5-3. Ratios of median (θ) and dispersion (β) of peak displacement for Sets G0, M0, M1 and M2 and 100% and 150% DBE shaking for LR systems

Model	100% DBE						150% DBE					
	Ratio of θ			Ratio of β			Ratio of θ			Ratio of β		
	$\frac{M0}{G0}$	$\frac{M1}{M0}$	$\frac{M2}{M1}$	$\frac{M0}{G0}$	$\frac{M1}{M0}$	$\frac{M2}{M1}$	$\frac{M0}{G0}$	$\frac{M1}{M0}$	$\frac{M2}{M1}$	$\frac{M0}{G0}$	$\frac{M1}{M0}$	$\frac{M2}{M1}$
LR_T2Q3	1.17	1.00	1.00	1.27	1.01	1.06	1.18	1.00	1.00	1.33	1.01	1.09
LR_T2Q6	1.18	1.00	1.00	1.46	1.00	1.03	1.18	1.00	1.00	1.34	1.01	1.04
LR_T2Q9	1.19	1.00	1.00	1.29	0.99	1.01	1.18	1.00	1.00	1.47	1.00	1.03
LR_T3Q3	1.20	1.00	1.00	1.23	0.99	1.01	1.20	1.00	1.00	1.34	1.00	1.03
LR_T3Q6	1.18	1.00	1.00	1.35	0.98	1.01	1.21	1.00	1.00	1.22	0.98	0.99
LR_T3Q9	1.17	1.00	1.00	1.40	0.99	1.01	1.18	1.00	1.00	1.32	0.98	1.01
LR_T4Q3	1.20	1.00	1.00	1.16	1.01	1.05	1.19	1.00	1.00	1.07	1.00	1.06
LR_T4Q6	1.22	1.00	1.00	1.25	0.99	1.03	1.21	1.00	1.00	1.31	0.99	1.03
LR_T4Q9	1.18	1.00	1.00	1.41	0.99	1.01	1.22	1.00	1.00	1.26	1.00	1.03

Table 5-4. Ratios of the statistics of Table 5-2 at 150% to 100% DBE shaking

Model	θ				β			
	G0	M0	M1	M2	G0	M0	M1	M2
LR_T2Q3	1.62	1.63	1.62	1.63	0.83	0.87	0.87	0.89
LR_T2Q6	1.69	1.68	1.69	1.69	0.86	0.80	0.80	0.81
LR_T2Q9	1.76	1.74	1.74	1.73	0.73	0.83	0.84	0.85
LR_T3Q3	1.69	1.68	1.68	1.68	0.80	0.87	0.88	0.89
LR_T3Q6	1.75	1.78	1.78	1.78	0.97	0.87	0.87	0.86
LR_T3Q9	1.81	1.83	1.83	1.83	0.98	0.92	0.92	0.92
LR_T4Q3	1.73	1.73	1.72	1.73	0.94	0.86	0.86	0.86
LR_T4Q6	1.92	1.90	1.90	1.90	0.76	0.80	0.80	0.80
LR_T4Q9	1.87	1.93	1.93	1.92	0.90	0.81	0.82	0.84

4) In Table 5-4, the ratio of θ at 150% to 100% DBE shaking for a given model and analysis set ranges between 1.62 and 1.93. The variation in the ratio of θ is no more than 20%.

5) The values of β of Table 5-2 range between 0.09 and 0.29. The percentage increase in β due to the variability in spectral demand is higher than that due to the variability in the mechanical properties of the isolation system.

6) If we assume that the response-history analysis is performed for Set G0 and the dispersion in the peak displacement is no greater than 0.21 per Table 5-2, the minimum number of pairs of ground motions per (3.3) to ensure a 90% confidence of the true median displacement being within ±10% of the estimated value is 13.

Scale factors for responses with 1% (10%) probability of exceedance at 100% (150%) DBE shaking

The analyses of Table 3-6 and Table 3-7 were repeated for the Diablo Canyon NPP site to compute the factors to scale the median responses for Sets G0 and M0 and 100% DBE shaking to the responses corresponding to 1) 1% probability of exceedance (PE) for Sets M1 and M2 for 100% DBE shaking, and 2) 10% PE for Sets M1 and M2 for 150% DBE shaking. Results are presented in Table 5-5. The factor for 10% PE and 150% DBE shaking is greater than the corresponding factor for 1% PE and 100% DBE shaking for all cases of Table 5-5.

If the response-history analysis is performed using only the DBE spectrum-compatible ground motions, the scale factor for displacement corresponding to 1% PE at 100% DBE shaking ranges between 1.60 and 2.33 and that corresponding to 10% PE at 150% DBE shaking ranges between 2.22 and 3.11 (see the 2nd through 5th columns of Table 5-5).

If the response-history analysis is performed using the maximum-minimum spectra compatible ground motions, the factor for displacement corresponding to 1% PE at 100% DBE shaking ranges between 1.37 and 1.97 and that corresponding to 10% PE at 150% DBE shaking ranges between 1.89 and 2.64 (see the 6th through 9th columns of Table 5-5).

5.4.2 Friction Pendulum (FP) isolation systems

Medians and logarithmic standard deviations of peak displacement

Table 5-5. Ratios of the displacement for 1% (10%) exceedance probability at 100% (150%) DBE to $\theta_{G0,DBE}$ and $\theta_{M0,DBE}$ for LR systems

Model	$\frac{D_{M1,DBE,99th}}{\theta_{G0,DBE}}$	$\frac{D_{M1,150\%DBE,90th}}{\theta_{G0,DBE}}$	$\frac{D_{M2,DBE,99th}}{\theta_{G0,DBE}}$	$\frac{D_{M2,150\%DBE,90th}}{\theta_{G0,DBE}}$	$\frac{D_{M1,DBE,99th}}{\theta_{M0,DBE}}$	$\frac{D_{M1,150\%DBE,90th}}{\theta_{M0,DBE}}$	$\frac{D_{M2,DBE,99th}}{\theta_{M0,DBE}}$	$\frac{D_{M2,150\%DBE,90th}}{\theta_{M0,DBE}}$
LR_T2Q3	1.60	2.22	1.64	2.26	1.37	1.89	1.40	1.92
LR_T2Q6	1.88	2.44	1.91	2.47	1.59	2.07	1.62	2.09
LR_T2Q9	2.13	2.71	2.14	2.73	1.78	2.27	1.79	2.28
LR_T3Q3	1.82	2.47	1.84	2.49	1.52	2.05	1.53	2.07
LR_T3Q6	2.12	2.79	2.13	2.79	1.79	2.35	1.80	2.35
LR_T3Q9	2.24	2.98	2.26	2.99	1.92	2.55	1.94	2.56
LR_T4Q3	1.73	2.45	1.75	2.48	1.44	2.05	1.47	2.07
LR_T4Q6	2.12	2.95	2.15	2.97	1.74	2.42	1.76	2.43
LR_T4Q9	2.31	3.08	2.33	3.11	1.96	2.61	1.97	2.64

The analyses of Table 5-2 through Table 5-4 were repeated for FP isolation systems and results are presented in Table 5-6 through Table 5-8, respectively. The key observations include:

1) For 100% (150%) DBE shaking, the values of θ of Table 5-6 range between 321 (593) and 923 (1276) mm. For a given model and analysis set, the median displacement for FP isolation systems is comparable to that for LR isolation systems (see Table 5-2).

2) In Table 5-7, the ratios of θ for M1/M0 and M2/M1 are equal to 1 for all models and shaking intensities.

3) In Table 5-7, the ratios of θ for M0/G0 range between 1.16 and 1.23. If analysis is performed using geomean-spectrum-compatible ground motions, the median displacement and shearing force should be increased by 20% to address the variability in spectral demands

4) In Table 5-8, the ratios of θ at 150% to 100% DBE shaking range between 1.67 and 2.0. For a given Q_d and T_d , the ratio for displacement is comparable for FP and LR isolation systems.

5) If we assume that the response-history analysis is performed for Set G0 and the dispersion in the peak displacement is no greater than 0.24 per Table 5-6, the minimum number of pairs of ground motions per (3.3) to ensure a 90% confidence of the true median displacement being within ±10% of the estimated value is 17.

Scale factors for responses with 1% (10%) probability of exceedance at 100% (150%) DBE shaking

The analyses of Table 5-5 were repeated for FP isolation systems and results are presented in Table 5-9.

If the response-history analysis is performed using only the DBE spectrum-compatible ground motions, the scale factor for displacement corresponding to 1% PE at 100% DBE shaking ranges between 1.60 and 2.49 and that corresponding to 10% PE at 150% DBE shaking ranges between 2.29 and 3.31 (see the 2nd through 5th columns of Table 5-9).

If response-history analysis is performed using the maximum-minimum spectra compatible ground motions, the factor for displacement corresponding to 1% PE at 100% DBE shaking ranges between 1.38 and 2.06 and that corresponding to 10% PE at 150% DBE shaking ranges between 1.98 and 2.74 (see the 6th through 9th columns of Table 5-9).

Table 5-6. Medians (θ) and dispersions (β) of peak displacement for Sets G0, M0, M1 and M2 and 100% and 150% DBE shaking for FP systems

Model	100% DBE								150% DBE							
	θ (mm)				β				θ (mm)				β			
	G0	M0	M1	M2	G0	M0	M1	M2	G0	M0	M1	M2	G0	M0	M1	M2
FP_T2Q3	492	571	571	572	0.11	0.14	0.14	0.14	819	953	953	953	0.11	0.13	0.13	0.13
FP_T2Q6	392	461	461	461	0.15	0.22	0.21	0.22	686	800	801	801	0.13	0.17	0.17	0.17
FP_T2Q9	321	385	385	384	0.21	0.26	0.26	0.27	593	697	697	697	0.16	0.22	0.22	0.22
FP_T3Q3	632	751	752	752	0.15	0.19	0.18	0.19	1080	1275	1275	1276	0.12	0.16	0.16	0.16
FP_T3Q6	471	555	556	557	0.21	0.28	0.27	0.28	852	1006	1006	1007	0.18	0.23	0.23	0.23
FP_T3Q9	374	442	443	443	0.23	0.29	0.29	0.30	707	832	833	834	0.21	0.28	0.27	0.27
FP_T4Q3	769	923	923	923	0.14	0.17	0.17	0.17	1354	1617	1617	1617	0.13	0.14	0.14	0.14
FP_T4Q6	503	617	617	619	0.20	0.23	0.23	0.24	988	1197	1197	1198	0.16	0.19	0.19	0.19
FP_T4Q9	382	462	462	463	0.24	0.31	0.31	0.31	756	925	925	928	0.20	0.24	0.23	0.24

Table 5-7. Ratios of median (θ) and dispersion (β) of peak displacement for Sets G0, M0, M1 and M2 and 100% and 150% DBE shaking for FP systems

Model	100% DBE						150% DBE					
	Ratio of θ			Ratio of β			Ratio of θ			Ratio of β		
	$\frac{M0}{G0}$	$\frac{M1}{M0}$	$\frac{M2}{M1}$	$\frac{M0}{G0}$	$\frac{M1}{M0}$	$\frac{M2}{M1}$	$\frac{M0}{G0}$	$\frac{M1}{M0}$	$\frac{M2}{M1}$	$\frac{M0}{G0}$	$\frac{M1}{M0}$	$\frac{M2}{M1}$
FP_T2Q3	1.16	1.00	1.00	1.29	0.99	1.01	1.16	1.00	1.00	1.16	0.99	1.01
FP_T2Q6	1.18	1.00	1.00	1.40	0.99	1.01	1.17	1.00	1.00	1.25	0.99	1.01
FP_T2Q9	1.20	1.00	1.00	1.24	0.99	1.02	1.18	1.00	1.00	1.34	0.99	1.01
FP_T3Q3	1.19	1.00	1.00	1.24	0.99	1.02	1.18	1.00	1.00	1.33	0.99	1.01
FP_T3Q6	1.18	1.00	1.00	1.30	0.99	1.01	1.18	1.00	1.00	1.28	0.98	1.01
FP_T3Q9	1.18	1.00	1.00	1.30	0.99	1.02	1.18	1.00	1.00	1.31	0.99	1.01
FP_T4Q3	1.20	1.00	1.00	1.20	0.99	1.03	1.19	1.00	1.00	1.10	0.99	1.02
FP_T4Q6	1.23	1.00	1.00	1.19	1.00	1.03	1.21	1.00	1.00	1.21	1.00	1.03
FP_T4Q9	1.21	1.00	1.00	1.30	0.98	1.01	1.22	1.00	1.00	1.19	0.99	1.03

Table 5-8. Ratios of the statistics of Table 5-6 for 150% to 100% DBE shaking

Model	θ				β			
	G0	M0	M1	M2	G0	M0	M1	M2
FP_T2Q3	1.67	1.67	1.67	1.67	1.07	0.96	0.96	0.96
FP_T2Q6	1.75	1.74	1.74	1.74	0.87	0.78	0.78	0.78
FP_T2Q9	1.85	1.81	1.81	1.81	0.77	0.84	0.83	0.83
FP_T3Q3	1.71	1.70	1.70	1.70	0.80	0.86	0.85	0.85
FP_T3Q6	1.81	1.81	1.81	1.81	0.85	0.84	0.83	0.83
FP_T3Q9	1.89	1.88	1.88	1.88	0.93	0.94	0.93	0.92
FP_T4Q3	1.76	1.75	1.75	1.75	0.93	0.86	0.85	0.85
FP_T4Q6	1.97	1.94	1.94	1.94	0.79	0.81	0.81	0.81
FP_T4Q9	1.98	2.00	2.00	2.00	0.82	0.76	0.76	0.78

Table 5-9. Ratios of the displacement for 1% (10%) exceedance probability at 100% (150%) DBE to $\theta_{G0,DBE}$ and $\theta_{M0,DBE}$ for FP systems

Model	$\frac{D_{M1,DBE,99th}}{\theta_{G0,DBE}}$	$\frac{D_{M1,150\%DBE,90th}}{\theta_{G0,DBE}}$	$\frac{D_{M2,DBE,99th}}{\theta_{G0,DBE}}$	$\frac{D_{M2,150\%DBE,90th}}{\theta_{G0,DBE}}$	$\frac{D_{M1,DBE,99th}}{\theta_{M0,DBE}}$	$\frac{D_{M1,150\%DBE,90th}}{\theta_{M0,DBE}}$	$\frac{D_{M2,DBE,99th}}{\theta_{M0,DBE}}$	$\frac{D_{M2,150\%DBE,90th}}{\theta_{M0,DBE}}$
FP_T2Q3	1.60	2.29	1.61	2.30	1.38	1.98	1.38	1.98
FP_T2Q6	1.93	2.52	1.94	2.53	1.64	2.15	1.65	2.15
FP_T2Q9	2.20	2.87	2.22	2.88	1.83	2.39	1.85	2.40
FP_T3Q3	1.82	2.47	1.84	2.47	1.53	2.08	1.55	2.08
FP_T3Q6	2.23	2.86	2.24	2.87	1.89	2.43	1.90	2.43
FP_T3Q9	2.33	3.16	2.36	3.17	1.97	2.67	2.00	2.68
FP_T4Q3	1.77	2.52	1.78	2.53	1.47	2.10	1.49	2.11
FP_T4Q6	2.12	3.03	2.16	3.06	1.72	2.47	1.76	2.49
FP_T4Q9	2.47	3.27	2.49	3.31	2.05	2.71	2.06	2.74

SECTION 6
SUMMARY, CONCLUSIONS AND RECOMMENDATIONS

6.1 Summary

Two ASCE standards are used for the analysis and design of nuclear power plants (NPPs): ASCE 4-98, *Seismic Analysis of Safety-related Nuclear Structures and Commentary* (ASCE 2000) and ASCE 43-05, *Seismic Design Criteria for Structures, Systems and Components in Nuclear Facilities* (ASCE 2005). Section 1.3 of ASCE 43-05 presents dual performance objectives for nuclear structures: 1) 1% probability of unacceptable performance for 100% Design Basis Earthquake (DBE) shaking, and 2) 10% probability of unacceptable performance for 150% DBE shaking. ASCE Standard 4-98, which includes provisions for the analysis and design of seismic isolation systems, is being updated at the time of this writing, and the studies reported herein are undertaken by the authors to provide the technical basis for proposed changes to the 2010 edition of the standard.

In base-isolated nuclear structures, the accelerations and deformations in structures, systems and components (SSCs) are relatively small. The SSCs are expected to remain elastic for both DBE shaking and beyond design basis shaking. As such, unacceptable performance of an isolated nuclear structure will most likely involve either the failure of isolation bearings or impact of the isolated superstructure and surrounding building or geotechnical structures. Three performance statements for achieving the above two performance objectives of ASCE 43-05 were used for this study, namely, 1) individual isolators shall suffer no damage in DBE shaking, 2) the probability of the isolated nuclear structure impacting surrounding structure (moat) for 100% (150%) DBE shaking is 1% (10%) or less, and 3) individual isolators sustain gravity and earthquake-induced axial loads at 90th percentile lateral displacements consistent with 150% DBE shaking. Performance statement 1 can be realized by production testing of each isolator supplied to a project for median DBE displacements and co-existing gravity and earthquake-induced axial forces. Analysis can be used in support of performance statement 2 provided that the isolators are modeled correctly and the ground motion representations are reasonable. Performance statement 3 can be realized by prototype testing of a limited number of isolators for mean displacements and co-existing axial forces consistent with 150% of the DBE, noting that an isolation system is composed of 10’s to 100’s of isolators and that failure of the isolation system would have to involve the simultaneous failure of a significant percentage of the isolators in the system. Nonlinear response-history analysis was performed in this study in support of performance statements 2 and 3, accounting for the variability in both earthquake ground motion and the mechanical properties of the isolation system.

The mechanical properties of low-damping rubber (LDR), lead-rubber (LR) and Friction Pendulum (FP) seismic isolation bearings will tend to vary from the values assumed for design both a) at the time of fabrication due to variability in basic material properties, and b) over the lifespan of the nuclear structure due to aging, contamination, ambient temperature, etc. The variability of the mechanical properties of an assembly of isolators (the isolation system) will be smaller than the variability of individual isolators. Two levels of variability were considered for these studies: Bin F1 assumed that the probability of the values of the key parameters of the isolation system being within $\pm 10\%$ of the best-estimate values was 95%; Bin F2 assumed that the probability of the values of the key parameters of the isolation system being within $\pm 20\%$ of the best-estimate values was 95%.

The goals of the study were three-fold, namely, for representative rock and soil sites in the Central and Eastern United States (CEUS) and a rock site in the Western United States (WUS), 1) determine the ratio of the 99%-ile estimate of the displacement (force) computed using a distribution of DBE spectral demands and distributions of isolator mechanical properties to the median isolator displacement (force) computed using best-estimate properties and spectrum-compatible DBE shaking; 2) determine the ratio of the 90%-ile estimate of the displacement (force) computed using a distribution of 150% DBE spectral demands and distributions of isolator mechanical properties to the median isolator displacement (force) computed using best-estimate properties and spectrum-compatible DBE shaking, and 3) determine the number of sets of three-component ground motions to be used for response-history analysis to develop a reliable estimate of the median displacement (force).

Computations were performed for three sites (North Anna, Vogtle and Diablo Canyon), three types of isolators (LR and FP bearings for all three sites and LDR bearings for North Anna only), and realistic mechanical properties for the isolators. Three-component sets of ground motions scaled to a) an appropriate distribution of spectral demand (denoted by the prefix M) and b) a geomean spectrum (denoted by the prefix G) were used to represent the seismic hazard at each site. For each isolation model, four sets of analysis were performed. Set G0 involves the use of ground motions scaled per b) and best-estimate isolator properties and Sets M0, M1 and M2 involve the use of ground motions scaled per a) and isolation systems with best-estimate properties (Set M0), the properties of Bins F1 (Set M1) and Bin F2 (Set M2). The Latin Hypercube Sampling procedure was used to reduce the computational effort.

The mechanical properties of LR and FP bearings will change with repeated cycling to large displacements as energy is dissipated by the lead core and by sliding friction, respectively. The heating of the lead core in the LR bearing and of the sliding surface (FP bearing) will reduce the energy dissipated by the isolation system at a given displacement and loading frequency. The thermo-mechanical response of seismic isolation bearings is not addressed here.

The analyses presented in this report do not consider torsional response of the isolated nuclear structure. If the increment in displacement response due to torsion is a significant percentage of the displacement at the center of mass of the isolated superstructure, the conclusions and recommendations presented below must be used with care.

Table 6-1 presents the isolation-system displacement and transmitted shearing force for the most demanding scenario considered in this study, namely, the response associated with 10% PE and 150% DBE shaking in analysis set M2. Values for transmitted shearing force for the Diablo Canyon site are not presented for the reasons given in Chapter 5. Those isolation systems that make little practical sense are shaded and not considered further. We note that for each representative site and type of isolation system, one or more combinations of isolation-system mechanical properties are suitable. Importantly, we note that the single concave FP bearing could be replaced with the triple concave FP bearing to produce responses similar to those of the LR bearing.

At the North Anna site, the results for models with $Q_d = 0.06W$ and $0.09W$ are shaded because the isolation-system displacements are tiny: the LR models subjected to 100% DBE shaking did not or barely achieved the yield displacement of the lead core. At the Vogtle site, the results for models with $T_d = 2$ seconds are shaded because such an isolation system would not be used at a site with the DBE spectrum of Figure 4-1; the results for $Q_d = 0.09W$ are also shaded because the scale factors of Figures 4-4 and 4-9 for displacement with 10% PE in 150% DBE shaking are much higher than the factors for the models with $Q_d = 0.03W$ and $0.06W$. At the Diablo Canyon site, the results for the models with displacements greater than 1500 mm (60 inches) are shaded because better isolation systems could be used.

Table 6-1. Bearing displacement and shearing force for 10% PE and 150% DBE shaking

Type of isolator	Model	Displacement (mm)			Shearing Force (%W)	
		North Anna	Vogtle	Diablo Canyon	North Anna	Vogtle
Lead Rubber	LR_T2Q3	60	821	1100	9	87
	LR_T2Q6	44	627	990	10	68
	LR_T2Q9	36	472	922	12	55
	LR_T3Q3	73	686	1603	6	35
	LR_T3Q6	50	598	1375	8	33
	LR_T3Q9	40	502	1207	11	31
	LR_T4Q3	77	537	1945	5	17
	LR_T4Q6	52	503	1562	8	18
	LR_T4Q9	42	444	1300	10	20
Friction Pendulum	FP_T2Q3	31	811	1131	7	100
	FP_T2Q6	19	593	993	10	78
	FP_T2Q9	15	432	924	15	62
	FP_T3Q3	33	635	1564	5	39
	FP_T3Q6	21	538	1351	10	36
	FP_T3Q9	17	420	1185	14	31
	FP_T4Q3	34	512	1946	5	19
	FP_T4Q6	22	444	1537	10	21
	FP_T4Q9	17	361	1266	14	22
Low Damping Rubber	LDR_T2	121			12	
	LDR_T3	124			5	
	LDR_T4	127			3	

6.2 Conclusions

The key conclusions of the study presented in this report are:

1. At a period of 0.1 (0.2) second, the 150% DBE spectral demand in the horizontal direction is 0.9 (0.5), 1.2 (1.2) and 2.6 (3.0) g, for the North Anna, Vogtle and Diablo Canyon sites, respectively. The reduction in horizontal seismic force on the supported structure due to the implementation of seismic isolation is significant, even for the worse-case scenarios of Table 6-1.

2. For a given model, the ratio of median responses for Set M0 to Set G0 generally ranges between 1.1 and 1.3. The median responses for analyses using geomean spectrum-compatible ground motions in both horizontal directions should be amplified to address the known variability in spectral demands.

3. The ratios of median responses for Set M1 to Set M0 and those for Set M2 to Set M1 are either equal to or very close to 1 for all cases considered in this study. The median response for analyses accounting for the variability in isolator material properties (i.e., M1 and M2) can be estimated without bias using analysis of a best-estimate model (i.e. M0).

4. Table 6-2 presents the lower and upper bounds on the factors to scale the median displacements for Sets G0 and M0 and 100% DBE shaking to the displacements corresponding to 1) 1% PE for Sets M1 and M2 for 100% DBE shaking and 2) 10% PE for Sets M1 and M2 for 150% DBE shaking. Only the cases not shaded in Table 6-1 are considered in the analysis of Table 6-2.

   For a given site, type of isolator and analysis set (G0 or M0), the factor for 10% PE and 150% DBE shaking is greater than that for 1% PE and 100% DBE shaking. For a given site and type of isolator, the factor for Set G0 is always greater than that for Set M0 since the ratio of median displacement for Set M0 to Set G0 is always greater than 1. For Set G0, 10% PE and 150% DBE shaking, the upper bound of the scale factor for LR (FP) bearings is 2.1 (3.3) at the North Anna site, 2.9 (3.8) at the Vogtle site, and 3.1 (3.3) at the Diablo Canyon site. At the Diablo Canyon site, the spectral demand is much higher than that at the two CEUS sites and the difference in the scale factors for the LR and FP bearings is insignificant.

5. Table 6-2 presents the lower and upper bounds for β in displacement for Sets G0 and M0 and 100% DBE shaking, together with the corresponding number of sets of ground motions required in the

Table 6-2. Lower and upper bounds for 1) scale factors for displacement associated with (1% PE, 100% DBE) and (10% PE, 150% DBE), 2) β in displacement and 3) n [1]

Site	Type of Isolator	Scale factor for 1% PE 100% DBE		Scale factor for 10% PE 150% DBE		β		n	
		Lower[2]	Upper[3]	Lower	Upper	Lower	Upper	Lower	Upper
G0									
North Anna	LR	1.5	1.7	2.0	2.1	0.10	0.11	3	4
	FP	2.1	2.2	3.2	3.3	0.18	0.21	10	13
	LDR	1.4	1.5	1.9	2.0	0.11	0.12	4	4
Vogtle	LR	1.8	2.2	2.3	2.9	0.13	0.16	5	8
	FP	1.9	2.8	2.6	3.8	0.14	0.21	6	14
Diablo Canyon	LR	1.6	2.3	2.2	3.1	0.10	0.21	3	13
	FP	1.6	2.5	2.3	3.3	0.11	0.24	3	17
M0									
North Anna	LR	1.3	1.4	1.7	1.8	0.12	0.14	5	6
	FP	1.7	1.8	2.6	2.8	0.23	0.25	16	18
	LDR	1.3	1.3	1.7	1.7	0.10	0.12	3	5
Vogtle	LR	1.5	1.7	1.9	2.3	0.18	0.24	10	17
	FP	1.6	2.1	2.1	2.8	0.20	0.30	11	27
Diablo Canyon	LR	1.4	2.0	1.9	2.6	0.13	0.29	5	25
	FP	1.4	2.1	2.0	2.7	0.14	0.31	6	29

1. The number of sets of ground motions required to achieve a 90% confidence level that the true median displacement is within ±10% of the estimated value
2. Lower bound
3. Upper bound

response-history analysis to ensure a 90% confidence of the true median displacement being within ±10% of the estimated value. Only those cases not shaded in Table 6-1 are considered. The number of sets of ground motions required for Set M0 is always greater than for Set G0 because β is greater for Set M0.

6.3 Recommendations

The three key recommendations of this study are listed below and can be used in support of performance statements 2 and 3 identified in Section 6.1.

1. The bearing displacement for 1% PE for DBE shaking is smaller than that for 10% PE for 150% DBE shaking for the three NPP sites considered here. Analysis of isolator capacity and clearance to surrounding structure can be based on 10% PE for 150% DBE shaking.

2. Two levels of variability in isolation-system mechanical properties were considered: Bin F1 assumed that the probability of the values of the key parameters being within $\pm 10\%$ of the best-estimate values is 95% and Bin F2 assumed that the probability of the values of the key parameters being within $\pm 20\%$ of the best-estimate values is 95%. The difference in the factors to scale the results of analysis of best-estimate models and DBE shaking to 10% PE and 150% DBE shaking for Bins F1 and F2 is negligible. The recommended procedures presented below can be applied to both bins with no loss of accuracy.

3. Two approaches are presented below aiming to determine the displacement associated with 10% PE in 150% DBE shaking.

   Approach I involves the use of geomean spectrum-compatible ground motions. The analysis for Approach I is performed for 100% DBE shaking only, which is consistent with design practice for conventional nuclear structures. Approach II involves the use of maximum-minimum spectrum-compatible ground motions for 150% DBE shaking and requires more sets of ground motions for analysis than Approach I. The recommendations presented herein are based on the data of Table 6-2. The horizontal design force for the supported structure should be determined using the isolation-system displacement, the best-estimate force-displacement relationships of the isolation system, and an estimate of the sustained dead and live axial load and earthquake-induced axial load on the isolators. The default multipliers on isolation-system displacement presented below can be set aside by site-specific analysis for 150% DBE shaking using Approach II.

Approach I:

i. Select or generate n sets of seed ground motions appropriate for the site condition and controlling magnitude-distance pair(s) for the site. Each set of seed ground motions should include two horizontal components and one vertical component. The value of n should not be less than the corresponding upper bound value of n presented in Table 6-2 for Set G0. In lieu of calculation, use $n = 11$.

ii. Spectrally match each set of seed ground motions to the horizontal and vertical DBE spectra.

iii. Perform n response-history analyses using the best-estimate model and the n sets of spectrum-compatible ground motions of step ii.

iv. Compute the maximum horizontal displacement of the isolation system (i.e., vector sum at each time step) for each set of analyses. Sort the n maximum displacements and determine the median value.

v. Multiply the median value of step iv by the corresponding upper-bound scale factor of Table 6-2 for Set G0, 10% PE and 150% DBE shaking. In lieu of calculation, use a factor of 3.

Approach II:

i. Select or generate 30 sets of seed ground motions appropriate for the site condition and controlling magnitude-distance pair(s) for the site. Each set of seed ground motions should include two horizontal components and one vertical component.

ii. Develop 30 sets of maximum-minimum spectrum-compatible ground motions for 150% DBE shaking per the procedure of Section 3.2.2.

iii. For a given type of isolator (i.e., LDR, LR or FP) and user-selected range of isolator properties (i.e., Bin F1, Bin F2 or alternate), use the Latin Hypercube Sampling procedure of Section 2.3 to generate 30 models of the isolator.

iv. Using the Latin Hypercube sampling procedure, perform 30 response-history analyses using the 30 sets of ground motions of step ii and the 30 mathematical models of step iii. (Alternately, 900 analyses can be performed using each set of ground motions and each mathematical model, per Section 3.3 for Set M1 or M2.)

v. Compute the maximum horizontal displacement of the isolation system (vector sum at each time step) for each analysis. Assume that the displacements distribute lognormally and compute the median displacement, the logarithmic standard deviation and the 10% PE (90th percentile) displacement.

SECTION 7
REFERENCES

Abrahamson, N.A. (1998). "Non-stationary spectral matching program RSPMATCH." PG&E, Internal Report.

American Association of State Highway and Transportation Officials (AASHTO). (1999). "Guide specification for seismic isolation design." Washington, D.C.

American Society of Civil Engineers (ASCE). (2000). "Seismic analysis of safety-related nuclear structures and commentary." *ASCE 4-98*, ASCE, Reston, VA.

American Society of Civil Engineers (ASCE). (2005). "Seismic design criteria for structures, systems, and components in nuclear facilities." *ASCE/SEI 43-05*, ASCE, Reston, VA.

American Society of Civil Engineers (ASCE). (2006). "Minimum design loads for buildings and other structures." *ASCE/SEI 7-05*, ASCE, Reston, VA.

Beyer, K., and Bommer, J. J., 2006. Relationships between median values and between aleatory variabilities for different definitions of the horizontal component of motion, *Bulletin of the Seismological Society of America*, 96(4A), 1512-1522.

Boore, D. M., Watson-Lamprey, J., and Abrahamson, N. A., 2006. Orientation-independent measures of ground motion, *Bulletin of the Seismological Society of America*, 96(4A), 1502-1511.

Bozorgnia, Y., and Campbell, K. W. (2004). "The vertical-to-horizontal response spectral ratio and tentative procedures for developing simplified V/H and vertical design spectra." *Journal of Earthquake Engineering*, 8(2), 175-207.

Computers and Structures, Inc. (CSI). (2007). *SAP2000 user's manual – version 11.0*. Berkeley, CA.

Constantinou, M. C., Tsopelas, P., Kasalanati, A., and Wolff, E. D. (1999). "Property modification factors for seismic isolation bearings." *MCEER-99-0012*, Multidisciplinary Center for Earthquake Engineering Research, State University of New York, Buffalo, NY.

Constantinou, M. C., Whittaker, A. S., Kalpakidis, Y., Fenz, D. M., and Warn, G. P. (2007) "Performance of seismic isolation hardware under service and seismic loading." *MCEER-07-0012*, Multidisciplinary Center for Earthquake Engineering Research, State University of New York, Buffalo, NY.

Deng, N. and Ostadan, F. (2000). *Theoretical and User's Manual for SHAKE 2000*. Bechtel Power Corporation, San Francisco, CA.

Dominion Nuclear North Anna, LLC. (2006). "North Anna Early Site Permit Application (Revision 9)." <http://www.nrc.gov/reactors/new-reactors/esp/north-anna.html>

Electric Power Research Institute (EPRI). (1993). "Guidelines for determining design basis ground motions. Volume 5: Quantification of Seismic source effects." *TR-102293*, EPRI, Palo Alto, CA.

Federal Emergency Management Agency (FEMA). (2004). "NEHRP recommended provisions for seismic regulations for new buildings and other structures." *FEMA 450-1/2003 Edition (Provisions) and 450-2/2003 Edition (Commentary)*, FEMA, Washington, D.C.

Fenz, D. M., and Constantinou, M. C. (2008a). "Mechanical behavior of multi-spherical sliding bearings." *MCEER-08-0007*, Multidisciplinary Center for Earthquake Engineering Research, State University of New York, Buffalo, NY.

Fenz, D. M., and Constantinou, M. C. (2008b). "Development, implementation, and verification of dynamic analysis models for multi-spherical sliding bearings." *MCEER-08-0018*, Multidisciplinary Center for Earthquake Engineering Research, State University of New York, Buffalo, NY.

Fenz, D. M., and Constantinou, M. C. (2008c). "Spherical sliding isolation bearings with adaptive behavior: Experimental verification." *Earthquake Engineering and Structural Dynamics*, 37(2), 185-205.

Mosqueda, G., Whittaker, A. S., Fenves, G. L., and Mahin, S. A. (2004). "Experimental and analytical studies of the friction pendulum system for the seismic protection of simple bridges." *EERC 2004-01*, Earthquake Engineering Research Center, University of California, Berkeley, CA.

Halldorsson, B. (2004). <http://civil.eng.buffalo.edu/engseislab/products.htm> Engineering Seismology Laboratory, State University of New York, Buffalo, NY.

Halldorsson, B., and Papageorgiou, A. S. (2005). "Calibration of the specific barrier model to earthquakes of different tectonic regions." *Bulletin of the Seismological Society of America*, 93(3), 1099-1131.

Huang, Y.-N., Whittaker, A. S., and Luco, N. (2007). "Maximum and geometric-mean spectral demands in the near-fault region." *Proceedings*, 19th International Conference on Structural Mechanics in Reactor Technology, Toronto, Canada.

Huang, Y.-N., Whittaker, A. S., and Luco, N. (2008a). "Maximum spectral demands in the near-fault region." *Earthquake Spectra*, 24(1), 319-341.

Huang, Y.-N., Whittaker, A. S., and Luco, N. (2008b). "Performance assessment of conventional and base-isolated nuclear power plants for earthquake and blast loadings." *MCEER-08-0019*, Multidisciplinary Center for Earthquake Engineering Research, State University of New York, Buffalo, NY.

Huang, Y.-N., Whittaker, A. S., and Luco, N. (2009). "Seismic performance assessment for safety-related nuclear structures." *Proceedings*, 20th International Conference on Structural Mechanics in Reactor Technology, Helsinki, Finland.

Kalpakidis, I. V. (2008). "Effects of heating and load history on the behavior of lead-rubber bearings." *Ph.D. dissertation*, Department of Civil, Structural and Environmental Engineering, State University of New York, Buffalo, NY.

Kasalanti, A. (2009). Personal communication.

Kennedy, R. P. (1999). "Overview of methods for seismic PRA and margin analysis including recent innovations." *Proceedings*, The OECD-NEA Workshop on Seismic Risk, Nuclear Energy Agency, Tokyo, Japan.

Kennedy, R. P. (2007). "Performance-goal based (risk informed) approach for establishing the SSE site specific response spectrum for future nuclear power plants." *Proceedings*, 19th International Conference on Structural Mechanics in Reactor Technology, Toronto, Canada.

Lee, R. C. (1996). "Investigations of nonlinear dynamic properties at the Savannah River site." *WSRC-TR-96-0062*, Rev. 1, Westinghouse Savannah River Company, Aiken, SC.

Mayes, R. L., Button, M. R. and Jones, D. M. (1998) "Design issues for base isolated bridges: 1997 revised AASHTO code requirements." *Proceedings*, Structural Engineering World Congress, San Francisco, CA.

Mayes, R. L. (2006). "Implementation of higher performance structural systems in the United States." *Proceedings*, 8th National Conference on Earthquake Engineering, Earthquake Engineering Research Institute, San Francisco, CA.

McGuire, R. K., Silva, W. J. and Costantino, C. J. (2001). "Technical basis for revision of regulatory guidance on design ground motions: hazard- and risk- consistent ground motion spectra guidelines." *NUREG/CR-6728*, U.S. Nuclear Regulatory Commission, Washington, D.C.

McCann, M., Marrone, J., Youngs, R., Electric Power Research Institute and Jack R. Benjamin & Associates. (2004). "CEUS ground motion project." *Report 1009684*, Electric Power Research Institute, Palo Alto, CA.

Morgan, T. (2007). "The use of innovative base isolation systems to achieve complex seismic performance objectives."*Ph.D. dissertation*, Department of Civil and Environmental Engineering, University of California, Berkeley, CA.

Mosqueda, G., Whittaker, A. S., Fenves, G. L., and Mahin, S. A. (2004). "Experimental and analytical studies of the friction pendulum system for the seismic protection of simple bridges." *EERC 2004-01*, Earthquake Engineering Research Center, University of California, Berkeley, CA.

Naeim, F., and Kelly, J. M. (1999). *Design of seismic isolated structures: from theory to practice*, John Wiley, NY.

Nowak, A. S., and Collins, K. R. (2000). *Reliability of structures*, McGraw-Hill, Boston.

Reed, J. W., and Kennedy, R. P. (1994). "Methodology for developing seismic fragilities." *TR-103959*, Electric Power Research Institute, Palo Alto, CA.

Southern Nuclear Operating Company (SNOC). (2008). *Vogtle Early Site Permit Application*, SNOC. < http://adamswebsearch2.nrc.gov/idmws/ViewDocByAccession.asp?AccessionNumber=ML081020073 >

U.S. Geological Survey (USGS). (2008). "2002 Interactive Deaggregations." < http://eqint.cr.usgs.gov/deaggint/2002/index.php>

U.S. Geological Survey (USGS). (2009a). "2008 Interactive Deaggregations (Beta)." < http://eqint.cr.usgs.gov/deaggint/2008/index.php>

U.S. Geological Survey (USGS). (2009b). "Java ground motion parameter calculator - version 5.0.9." <http://earthquake.usgs.gov/research/hazmaps/design/>

U.S. Nuclear Regulatory Commission (USNRC). (1997). "Identification and characterization of seismic sources and determination of safe shutdown earthquake ground motion." *Regulatory Guide 1.165*, USNRC, Washington, D.C.

U.S. Nuclear Regulatory Commission (USNRC). (2007). "A performance-based approach to define the site-specific earthquake ground motion." *Regulatory Guide 1.208*, USNRC, Washington, D.C.

Zayas, V. A., Low, S. A., and Mahin, S. A. (1987). "The FPS earthquake resisting system: experimental report." *UCB/EERC-87/01*, Earthquake Engineering Research Center, University of California, Berkeley, CA.

MCEER Technical Reports

MCEER publishes technical reports on a variety of subjects written by authors funded through MCEER. These reports are available from both MCEER Publications and the National Technical Information Service (NTIS). Requests for reports should be directed to MCEER Publications, MCEER, University at Buffalo, State University of New York, Red Jacket Quadrangle, Buffalo, New York 14261. Reports can also be requested through NTIS, 5285 Port Royal Road, Springfield, Virginia 22161. NTIS accession numbers are shown in parenthesis, if available.

NCEER-87-0001 "First-Year Program in Research, Education and Technology Transfer," 3/5/87, (PB88-134275, A04, MF-A01).

NCEER-87-0002 "Experimental Evaluation of Instantaneous Optimal Algorithms for Structural Control," by R.C. Lin, T.T. Soong and A.M. Reinhorn, 4/20/87, (PB88-134341, A04, MF-A01).

NCEER-87-0003 "Experimentation Using the Earthquake Simulation Facilities at University at Buffalo," by A.M. Reinhorn and R.L. Ketter, to be published.

NCEER-87-0004 "The System Characteristics and Performance of a Shaking Table," by J.S. Hwang, K.C. Chang and G.C. Lee, 6/1/87, (PB88-134259, A03, MF-A01). This report is available only through NTIS (see address given above).

NCEER-87-0005 "A Finite Element Formulation for Nonlinear Viscoplastic Material Using a Q Model," by O. Gyebi and G. Dasgupta, 11/2/87, (PB88-213764, A08, MF-A01).

NCEER-87-0006 "Symbolic Manipulation Program (SMP) - Algebraic Codes for Two and Three Dimensional Finite Element Formulations," by X. Lee and G. Dasgupta, 11/9/87, (PB88-218522, A05, MF-A01).

NCEER-87-0007 "Instantaneous Optimal Control Laws for Tall Buildings Under Seismic Excitations," by J.N. Yang, A. Akbarpour and P. Ghaemmaghami, 6/10/87, (PB88-134333, A06, MF-A01). This report is only available through NTIS (see address given above).

NCEER-87-0008 "IDARC: Inelastic Damage Analysis of Reinforced Concrete Frame - Shear-Wall Structures," by Y.J. Park, A.M. Reinhorn and S.K. Kunnath, 7/20/87, (PB88-134325, A09, MF-A01). This report is only available through NTIS (see address given above).

NCEER-87-0009 "Liquefaction Potential for New York State: A Preliminary Report on Sites in Manhattan and Buffalo," by M. Budhu, V. Vijayakumar, R.F. Giese and L. Baumgras, 8/31/87, (PB88-163704, A03, MF-A01). This report is available only through NTIS (see address given above).

NCEER-87-0010 "Vertical and Torsional Vibration of Foundations in Inhomogeneous Media," by A.S. Veletsos and K.W. Dotson, 6/1/87, (PB88-134291, A03, MF-A01). This report is only available through NTIS (see address given above).

NCEER-87-0011 "Seismic Probabilistic Risk Assessment and Seismic Margins Studies for Nuclear Power Plants," by Howard H.M. Hwang, 6/15/87, (PB88-134267, A03, MF-A01). This report is only available through NTIS (see address given above).

NCEER-87-0012 "Parametric Studies of Frequency Response of Secondary Systems Under Ground-Acceleration Excitations," by Y. Yong and Y.K. Lin, 6/10/87, (PB88-134309, A03, MF-A01). This report is only available through NTIS (see address given above).

NCEER-87-0013 "Frequency Response of Secondary Systems Under Seismic Excitation," by J.A. HoLung, J. Cai and Y.K. Lin, 7/31/87, (PB88-134317, A05, MF-A01). This report is only available through NTIS (see address given above).

NCEER-87-0014 "Modelling Earthquake Ground Motions in Seismically Active Regions Using Parametric Time Series Methods," by G.W. Ellis and A.S. Cakmak, 8/25/87, (PB88-134283, A08, MF-A01). This report is only available through NTIS (see address given above).

NCEER-87-0015 "Detection and Assessment of Seismic Structural Damage," by E. DiPasquale and A.S. Cakmak, 8/25/87, (PB88-163712, A05, MF-A01). This report is only available through NTIS (see address given above).

NCEER-87-0016 "Pipeline Experiment at Parkfield, California," by J. Isenberg and E. Richardson, 9/15/87, (PB88-163720, A03, MF-A01). This report is available only through NTIS (see address given above).

NCEER-87-0017 "Digital Simulation of Seismic Ground Motion," by M. Shinozuka, G. Deodatis and T. Harada, 8/31/87, (PB88-155197, A04, MF-A01). This report is available only through NTIS (see address given above).

NCEER-87-0018 "Practical Considerations for Structural Control: System Uncertainty, System Time Delay and Truncation of Small Control Forces," J.N. Yang and A. Akbarpour, 8/10/87, (PB88-163738, A08, MF-A01). This report is only available through NTIS (see address given above).

NCEER-87-0019 "Modal Analysis of Nonclassically Damped Structural Systems Using Canonical Transformation," by J.N. Yang, S. Sarkani and F.X. Long, 9/27/87, (PB88-187851, A04, MF-A01).

NCEER-87-0020 "A Nonstationary Solution in Random Vibration Theory," by J.R. Red-Horse and P.D. Spanos, 11/3/87, (PB88-163746, A03, MF-A01).

NCEER-87-0021 "Horizontal Impedances for Radially Inhomogeneous Viscoelastic Soil Layers," by A.S. Veletsos and K.W. Dotson, 10/15/87, (PB88-150859, A04, MF-A01).

NCEER-87-0022 "Seismic Damage Assessment of Reinforced Concrete Members," by Y.S. Chung, C. Meyer and M. Shinozuka, 10/9/87, (PB88-150867, A05, MF-A01). This report is available only through NTIS (see address given above).

NCEER-87-0023 "Active Structural Control in Civil Engineering," by T.T. Soong, 11/11/87, (PB88-187778, A03, MF-A01).

NCEER-87-0024 "Vertical and Torsional Impedances for Radially Inhomogeneous Viscoelastic Soil Layers," by K.W. Dotson and A.S. Veletsos, 12/87, (PB88-187786, A03, MF-A01).

NCEER-87-0025 "Proceedings from the Symposium on Seismic Hazards, Ground Motions, Soil-Liquefaction and Engineering Practice in Eastern North America," October 20-22, 1987, edited by K.H. Jacob, 12/87, (PB88-188115, A23, MF-A01). This report is available only through NTIS (see address given above).

NCEER-87-0026 "Report on the Whittier-Narrows, California, Earthquake of October 1, 1987," by J. Pantelic and A. Reinhorn, 11/87, (PB88-187752, A03, MF-A01). This report is available only through NTIS (see address given above).

NCEER-87-0027 "Design of a Modular Program for Transient Nonlinear Analysis of Large 3-D Building Structures," by S. Srivastav and J.F. Abel, 12/30/87, (PB88-187950, A05, MF-A01). This report is only available through NTIS (see address given above).

NCEER-87-0028 "Second-Year Program in Research, Education and Technology Transfer," 3/8/88, (PB88-219480, A04, MF-A01).

NCEER-88-0001 "Workshop on Seismic Computer Analysis and Design of Buildings With Interactive Graphics," by W. McGuire, J.F. Abel and C.H. Conley, 1/18/88, (PB88-187760, A03, MF-A01). This report is only available through NTIS (see address given above).

NCEER-88-0002 "Optimal Control of Nonlinear Flexible Structures," by J.N. Yang, F.X. Long and D. Wong, 1/22/88, (PB88-213772, A06, MF-A01).

NCEER-88-0003 "Substructuring Techniques in the Time Domain for Primary-Secondary Structural Systems," by G.D. Manolis and G. Juhn, 2/10/88, (PB88-213780, A04, MF-A01).

NCEER-88-0004 "Iterative Seismic Analysis of Primary-Secondary Systems," by A. Singhal, L.D. Lutes and P.D. Spanos, 2/23/88, (PB88-213798, A04, MF-A01).

NCEER-88-0005 "Stochastic Finite Element Expansion for Random Media," by P.D. Spanos and R. Ghanem, 3/14/88, (PB88-213806, A03, MF-A01).

NCEER-88-0006 "Combining Structural Optimization and Structural Control," by F.Y. Cheng and C.P. Pantelides, 1/10/88, (PB88-213814, A05, MF-A01).

NCEER-88-0007 "Seismic Performance Assessment of Code-Designed Structures," by H.H-M. Hwang, J-W. Jaw and H-J. Shau, 3/20/88, (PB88-219423, A04, MF-A01). This report is only available through NTIS (see address given above).

NCEER-88-0008 "Reliability Analysis of Code-Designed Structures Under Natural Hazards," by H.H-M. Hwang, H. Ushiba and M. Shinozuka, 2/29/88, (PB88-229471, A07, MF-A01). This report is only available through NTIS (see address given above).

NCEER-88-0009 "Seismic Fragility Analysis of Shear Wall Structures," by J-W Jaw and H.H-M. Hwang, 4/30/88, (PB89-102867, A04, MF-A01).

NCEER-88-0010 "Base Isolation of a Multi-Story Building Under a Harmonic Ground Motion - A Comparison of Performances of Various Systems," by F-G Fan, G. Ahmadi and I.G. Tadjbakhsh, 5/18/88, (PB89-122238, A06, MF-A01). This report is only available through NTIS (see address given above).

NCEER-88-0011 "Seismic Floor Response Spectra for a Combined System by Green's Functions," by F.M. Lavelle, L.A. Bergman and P.D. Spanos, 5/1/88, (PB89-102875, A03, MF-A01).

NCEER-88-0012 "A New Solution Technique for Randomly Excited Hysteretic Structures," by G.Q. Cai and Y.K. Lin, 5/16/88, (PB89-102883, A03, MF-A01).

NCEER-88-0013 "A Study of Radiation Damping and Soil-Structure Interaction Effects in the Centrifuge," by K. Weissman, supervised by J.H. Prevost, 5/24/88, (PB89-144703, A06, MF-A01).

NCEER-88-0014 "Parameter Identification and Implementation of a Kinematic Plasticity Model for Frictional Soils," by J.H. Prevost and D.V. Griffiths, to be published.

NCEER-88-0015 "Two- and Three- Dimensional Dynamic Finite Element Analyses of the Long Valley Dam," by D.V. Griffiths and J.H. Prevost, 6/17/88, (PB89-144711, A04, MF-A01).

NCEER-88-0016 "Damage Assessment of Reinforced Concrete Structures in Eastern United States," by A.M. Reinhorn, M.J. Seidel, S.K. Kunnath and Y.J. Park, 6/15/88, (PB89-122220, A04, MF-A01). This report is only available through NTIS (see address given above).

NCEER-88-0017 "Dynamic Compliance of Vertically Loaded Strip Foundations in Multilayered Viscoelastic Soils," by S. Ahmad and A.S.M. Israil, 6/17/88, (PB89-102891, A04, MF-A01).

NCEER-88-0018 "An Experimental Study of Seismic Structural Response With Added Viscoelastic Dampers," by R.C. Lin, Z. Liang, T.T. Soong and R.H. Zhang, 6/30/88, (PB89-122212, A05, MF-A01). This report is available only through NTIS (see address given above).

NCEER-88-0019 "Experimental Investigation of Primary - Secondary System Interaction," by G.D. Manolis, G. Juhn and A.M. Reinhorn, 5/27/88, (PB89-122204, A04, MF-A01).

NCEER-88-0020 "A Response Spectrum Approach For Analysis of Nonclassically Damped Structures," by J.N. Yang, S. Sarkani and F.X. Long, 4/22/88, (PB89-102909, A04, MF-A01).

NCEER-88-0021 "Seismic Interaction of Structures and Soils: Stochastic Approach," by A.S. Veletsos and A.M. Prasad, 7/21/88, (PB89-122196, A04, MF-A01). This report is only available through NTIS (see address given above).

NCEER-88-0022 "Identification of the Serviceability Limit State and Detection of Seismic Structural Damage," by E. DiPasquale and A.S. Cakmak, 6/15/88, (PB89-122188, A05, MF-A01). This report is available only through NTIS (see address given above).

NCEER-88-0023 "Multi-Hazard Risk Analysis: Case of a Simple Offshore Structure," by B.K. Bhartia and E.H. Vanmarcke, 7/21/88, (PB89-145213, A05, MF-A01).

NCEER-88-0024 "Automated Seismic Design of Reinforced Concrete Buildings," by Y.S. Chung, C. Meyer and M. Shinozuka, 7/5/88, (PB89-122170, A06, MF-A01). This report is available only through NTIS (see address given above).

NCEER-88-0025 "Experimental Study of Active Control of MDOF Structures Under Seismic Excitations," by L.L. Chung, R.C. Lin, T.T. Soong and A.M. Reinhorn, 7/10/88, (PB89-122600, A04, MF-A01).

NCEER-88-0026 "Earthquake Simulation Tests of a Low-Rise Metal Structure," by J.S. Hwang, K.C. Chang, G.C. Lee and R.L. Ketter, 8/1/88, (PB89-102917, A04, MF-A01).

NCEER-88-0027 "Systems Study of Urban Response and Reconstruction Due to Catastrophic Earthquakes," by F. Kozin and H.K. Zhou, 9/22/88, (PB90-162348, A04, MF-A01).

NCEER-88-0028 "Seismic Fragility Analysis of Plane Frame Structures," by H.H-M. Hwang and Y.K. Low, 7/31/88, (PB89-131445, A06, MF-A01).

NCEER-88-0029 "Response Analysis of Stochastic Structures," by A. Kardara, C. Bucher and M. Shinozuka, 9/22/88, (PB89-174429, A04, MF-A01).

NCEER-88-0030 "Nonnormal Accelerations Due to Yielding in a Primary Structure," by D.C.K. Chen and L.D. Lutes, 9/19/88, (PB89-131437, A04, MF-A01).

NCEER-88-0031 "Design Approaches for Soil-Structure Interaction," by A.S. Veletsos, A.M. Prasad and Y. Tang, 12/30/88, (PB89-174437, A03, MF-A01). This report is available only through NTIS (see address given above).

NCEER-88-0032 "A Re-evaluation of Design Spectra for Seismic Damage Control," by C.J. Turkstra and A.G. Tallin, 11/7/88, (PB89-145221, A05, MF-A01).

NCEER-88-0033 "The Behavior and Design of Noncontact Lap Splices Subjected to Repeated Inelastic Tensile Loading," by V.E. Sagan, P. Gergely and R.N. White, 12/8/88, (PB89-163737, A08, MF-A01).

NCEER-88-0034 "Seismic Response of Pile Foundations," by S.M. Mamoon, P.K. Banerjee and S. Ahmad, 11/1/88, (PB89-145239, A04, MF-A01).

NCEER-88-0035 "Modeling of R/C Building Structures With Flexible Floor Diaphragms (IDARC2)," by A.M. Reinhorn, S.K. Kunnath and N. Panahshahi, 9/7/88, (PB89-207153, A07, MF-A01).

NCEER-88-0036 "Solution of the Dam-Reservoir Interaction Problem Using a Combination of FEM, BEM with Particular Integrals, Modal Analysis, and Substructuring," by C-S. Tsai, G.C. Lee and R.L. Ketter, 12/31/88, (PB89-207146, A04, MF-A01).

NCEER-88-0037 "Optimal Placement of Actuators for Structural Control," by F.Y. Cheng and C.P. Pantelides, 8/15/88, (PB89-162846, A05, MF-A01).

NCEER-88-0038 "Teflon Bearings in Aseismic Base Isolation: Experimental Studies and Mathematical Modeling," by A. Mokha, M.C. Constantinou and A.M. Reinhorn, 12/5/88, (PB89-218457, A10, MF-A01). This report is available only through NTIS (see address given above).

NCEER-88-0039 "Seismic Behavior of Flat Slab High-Rise Buildings in the New York City Area," by P. Weidlinger and M. Ettouney, 10/15/88, (PB90-145681, A04, MF-A01).

NCEER-88-0040 "Evaluation of the Earthquake Resistance of Existing Buildings in New York City," by P. Weidlinger and M. Ettouney, 10/15/88, to be published.

NCEER-88-0041 "Small-Scale Modeling Techniques for Reinforced Concrete Structures Subjected to Seismic Loads," by W. Kim, A. El-Attar and R.N. White, 11/22/88, (PB89-189625, A05, MF-A01).

NCEER-88-0042 "Modeling Strong Ground Motion from Multiple Event Earthquakes," by G.W. Ellis and A.S. Cakmak, 10/15/88, (PB89-174445, A03, MF-A01).

NCEER-88-0043 "Nonstationary Models of Seismic Ground Acceleration," by M. Grigoriu, S.E. Ruiz and E. Rosenblueth, 7/15/88, (PB89-189617, A04, MF-A01).

NCEER-88-0044 "SARCF User's Guide: Seismic Analysis of Reinforced Concrete Frames," by Y.S. Chung, C. Meyer and M. Shinozuka, 11/9/88, (PB89-174452, A08, MF-A01).

NCEER-88-0045 "First Expert Panel Meeting on Disaster Research and Planning," edited by J. Pantelic and J. Stoyle, 9/15/88, (PB89-174460, A05, MF-A01).

NCEER-88-0046 "Preliminary Studies of the Effect of Degrading Infill Walls on the Nonlinear Seismic Response of Steel Frames," by C.Z. Chrysostomou, P. Gergely and J.F. Abel, 12/19/88, (PB89-208383, A05, MF-A01).

NCEER-88-0047 "Reinforced Concrete Frame Component Testing Facility - Design, Construction, Instrumentation and Operation," by S.P. Pessiki, C. Conley, T. Bond, P. Gergely and R.N. White, 12/16/88, (PB89-174478, A04, MF-A01).

NCEER-89-0001 "Effects of Protective Cushion and Soil Compliancy on the Response of Equipment Within a Seismically Excited Building," by J.A. HoLung, 2/16/89, (PB89-207179, A04, MF-A01).

NCEER-89-0002 "Statistical Evaluation of Response Modification Factors for Reinforced Concrete Structures," by H.H-M. Hwang and J-W. Jaw, 2/17/89, (PB89-207187, A05, MF-A01).

NCEER-89-0003 "Hysteretic Columns Under Random Excitation," by G-Q. Cai and Y.K. Lin, 1/9/89, (PB89-196513, A03, MF-A01).

NCEER-89-0004 "Experimental Study of `Elephant Foot Bulge' Instability of Thin-Walled Metal Tanks," by Z-H. Jia and R.L. Ketter, 2/22/89, (PB89-207195, A03, MF-A01).

NCEER-89-0005 "Experiment on Performance of Buried Pipelines Across San Andreas Fault," by J. Isenberg, E. Richardson and T.D. O'Rourke, 3/10/89, (PB89-218440, A04, MF-A01). This report is available only through NTIS (see address given above).

NCEER-89-0006 "A Knowledge-Based Approach to Structural Design of Earthquake-Resistant Buildings," by M. Subramani, P. Gergely, C.H. Conley, J.F. Abel and A.H. Zaghw, 1/15/89, (PB89-218465, A06, MF-A01).

NCEER-89-0007 "Liquefaction Hazards and Their Effects on Buried Pipelines," by T.D. O'Rourke and P.A. Lane, 2/1/89, (PB89-218481, A09, MF-A01).

NCEER-89-0008 "Fundamentals of System Identification in Structural Dynamics," by H. Imai, C-B. Yun, O. Maruyama and M. Shinozuka, 1/26/89, (PB89-207211, A04, MF-A01).

NCEER-89-0009 "Effects of the 1985 Michoacan Earthquake on Water Systems and Other Buried Lifelines in Mexico," by A.G. Ayala and M.J. O'Rourke, 3/8/89, (PB89-207229, A06, MF-A01).

NCEER-89-R010 "NCEER Bibliography of Earthquake Education Materials," by K.E.K. Ross, Second Revision, 9/1/89, (PB90-125352, A05, MF-A01). This report is replaced by NCEER-92-0018.

NCEER-89-0011 "Inelastic Three-Dimensional Response Analysis of Reinforced Concrete Building Structures (IDARC-3D), Part I - Modeling," by S.K. Kunnath and A.M. Reinhorn, 4/17/89, (PB90-114612, A07, MF-A01). This report is available only through NTIS (see address given above).

NCEER-89-0012 "Recommended Modifications to ATC-14," by C.D. Poland and J.O. Malley, 4/12/89, (PB90-108648, A15, MF-A01).

NCEER-89-0013 "Repair and Strengthening of Beam-to-Column Connections Subjected to Earthquake Loading," by M. Corazao and A.J. Durrani, 2/28/89, (PB90-109885, A06, MF-A01).

NCEER-89-0014 "Program EXKAL2 for Identification of Structural Dynamic Systems," by O. Maruyama, C-B. Yun, M. Hoshiya and M. Shinozuka, 5/19/89, (PB90-109877, A09, MF-A01).

NCEER-89-0015 "Response of Frames With Bolted Semi-Rigid Connections, Part I - Experimental Study and Analytical Predictions," by P.J. DiCorso, A.M. Reinhorn, J.R. Dickerson, J.B. Radziminski and W.L. Harper, 6/1/89, to be published.

NCEER-89-0016 "ARMA Monte Carlo Simulation in Probabilistic Structural Analysis," by P.D. Spanos and M.P. Mignolet, 7/10/89, (PB90-109893, A03, MF-A01).

NCEER-89-P017 "Preliminary Proceedings from the Conference on Disaster Preparedness - The Place of Earthquake Education in Our Schools," Edited by K.E.K. Ross, 6/23/89, (PB90-108606, A03, MF-A01).

NCEER-89-0017 "Proceedings from the Conference on Disaster Preparedness - The Place of Earthquake Education in Our Schools," Edited by K.E.K. Ross, 12/31/89, (PB90-207895, A012, MF-A02). This report is available only through NTIS (see address given above).

NCEER-89-0018 "Multidimensional Models of Hysteretic Material Behavior for Vibration Analysis of Shape Memory Energy Absorbing Devices, by E.J. Graesser and F.A. Cozzarelli, 6/7/89, (PB90-164146, A04, MF-A01).

NCEER-89-0019 "Nonlinear Dynamic Analysis of Three-Dimensional Base Isolated Structures (3D-BASIS)," by S. Nagarajaiah, A.M. Reinhorn and M.C. Constantinou, 8/3/89, (PB90-161936, A06, MF-A01). This report has been replaced by NCEER-93-0011.

NCEER-89-0020 "Structural Control Considering Time-Rate of Control Forces and Control Rate Constraints," by F.Y. Cheng and C.P. Pantelides, 8/3/89, (PB90-120445, A04, MF-A01).

NCEER-89-0021 "Subsurface Conditions of Memphis and Shelby County," by K.W. Ng, T-S. Chang and H-H.M. Hwang, 7/26/89, (PB90-120437, A03, MF-A01).

NCEER-89-0022 "Seismic Wave Propagation Effects on Straight Jointed Buried Pipelines," by K. Elhmadi and M.J. O'Rourke, 8/24/89, (PB90-162322, A10, MF-A02).

NCEER-89-0023 "Workshop on Serviceability Analysis of Water Delivery Systems," edited by M. Grigoriu, 3/6/89, (PB90-127424, A03, MF-A01).

NCEER-89-0024 "Shaking Table Study of a 1/5 Scale Steel Frame Composed of Tapered Members," by K.C. Chang, J.S. Hwang and G.C. Lee, 9/18/89, (PB90-160169, A04, MF-A01).

NCEER-89-0025 "DYNA1D: A Computer Program for Nonlinear Seismic Site Response Analysis - Technical Documentation," by Jean H. Prevost, 9/14/89, (PB90-161944, A07, MF-A01). This report is available only through NTIS (see address given above).

NCEER-89-0026 "1:4 Scale Model Studies of Active Tendon Systems and Active Mass Dampers for Aseismic Protection," by A.M. Reinhorn, T.T. Soong, R.C. Lin, Y.P. Yang, Y. Fukao, H. Abe and M. Nakai, 9/15/89, (PB90-173246, A10, MF-A02). This report is available only through NTIS (see address given above).

NCEER-89-0027 "Scattering of Waves by Inclusions in a Nonhomogeneous Elastic Half Space Solved by Boundary Element Methods," by P.K. Hadley, A. Askar and A.S. Cakmak, 6/15/89, (PB90-145699, A07, MF-A01).

NCEER-89-0028 "Statistical Evaluation of Deflection Amplification Factors for Reinforced Concrete Structures," by H.H.M. Hwang, J-W. Jaw and A.L. Ch'ng, 8/31/89, (PB90-164633, A05, MF-A01).

NCEER-89-0029 "Bedrock Accelerations in Memphis Area Due to Large New Madrid Earthquakes," by H.H.M. Hwang, C.H.S. Chen and G. Yu, 11/7/89, (PB90-162330, A04, MF-A01).

NCEER-89-0030 "Seismic Behavior and Response Sensitivity of Secondary Structural Systems," by Y.Q. Chen and T.T. Soong, 10/23/89, (PB90-164658, A08, MF-A01).

NCEER-89-0031 "Random Vibration and Reliability Analysis of Primary-Secondary Structural Systems," by Y. Ibrahim, M. Grigoriu and T.T. Soong, 11/10/89, (PB90-161951, A04, MF-A01).

NCEER-89-0032 "Proceedings from the Second U.S. - Japan Workshop on Liquefaction, Large Ground Deformation and Their Effects on Lifelines, September 26-29, 1989," Edited by T.D. O'Rourke and M. Hamada, 12/1/89, (PB90-209388, A22, MF-A03).

NCEER-89-0033 "Deterministic Model for Seismic Damage Evaluation of Reinforced Concrete Structures," by J.M. Bracci, A.M. Reinhorn, J.B. Mander and S.K. Kunnath, 9/27/89, (PB91-108803, A06, MF-A01).

NCEER-89-0034 "On the Relation Between Local and Global Damage Indices," by E. DiPasquale and A.S. Cakmak, 8/15/89, (PB90-173865, A05, MF-A01).

NCEER-89-0035 "Cyclic Undrained Behavior of Nonplastic and Low Plasticity Silts," by A.J. Walker and H.E. Stewart, 7/26/89, (PB90-183518, A10, MF-A01).

NCEER-89-0036 "Liquefaction Potential of Surficial Deposits in the City of Buffalo, New York," by M. Budhu, R. Giese and L. Baumgrass, 1/17/89, (PB90-208455, A04, MF-A01).

NCEER-89-0037 "A Deterministic Assessment of Effects of Ground Motion Incoherence," by A.S. Veletsos and Y. Tang, 7/15/89, (PB90-164294, A03, MF-A01).

NCEER-89-0038 "Workshop on Ground Motion Parameters for Seismic Hazard Mapping," July 17-18, 1989, edited by R.V. Whitman, 12/1/89, (PB90-173923, A04, MF-A01).

NCEER-89-0039 "Seismic Effects on Elevated Transit Lines of the New York City Transit Authority," by C.J. Costantino, C.A. Miller and E. Heymsfield, 12/26/89, (PB90-207887, A06, MF-A01).

NCEER-89-0040 "Centrifugal Modeling of Dynamic Soil-Structure Interaction," by K. Weissman, Supervised by J.H. Prevost, 5/10/89, (PB90-207879, A07, MF-A01).

NCEER-89-0041 "Linearized Identification of Buildings With Cores for Seismic Vulnerability Assessment," by I-K. Ho and A.E. Aktan, 11/1/89, (PB90-251943, A07, MF-A01).

NCEER-90-0001 "Geotechnical and Lifeline Aspects of the October 17, 1989 Loma Prieta Earthquake in San Francisco," by T.D. O'Rourke, H.E. Stewart, F.T. Blackburn and T.S. Dickerman, 1/90, (PB90-208596, A05, MF-A01).

NCEER-90-0002 "Nonnormal Secondary Response Due to Yielding in a Primary Structure," by D.C.K. Chen and L.D. Lutes, 2/28/90, (PB90-251976, A07, MF-A01).

NCEER-90-0003 "Earthquake Education Materials for Grades K-12," by K.E.K. Ross, 4/16/90, (PB91-251984, A05, MF-A05). This report has been replaced by NCEER-92-0018.

NCEER-90-0004 "Catalog of Strong Motion Stations in Eastern North America," by R.W. Busby, 4/3/90, (PB90-251984, A05, MF-A01).

NCEER-90-0005 "NCEER Strong-Motion Data Base: A User Manual for the GeoBase Release (Version 1.0 for the Sun3)," by P. Friberg and K. Jacob, 3/31/90 (PB90-258062, A04, MF-A01).

NCEER-90-0006 "Seismic Hazard Along a Crude Oil Pipeline in the Event of an 1811-1812 Type New Madrid Earthquake," by H.H.M. Hwang and C-H.S. Chen, 4/16/90, (PB90-258054, A04, MF-A01).

NCEER-90-0007 "Site-Specific Response Spectra for Memphis Sheahan Pumping Station," by H.H.M. Hwang and C.S. Lee, 5/15/90, (PB91-108811, A05, MF-A01).

NCEER-90-0008 "Pilot Study on Seismic Vulnerability of Crude Oil Transmission Systems," by T. Ariman, R. Dobry, M. Grigoriu, F. Kozin, M. O'Rourke, T. O'Rourke and M. Shinozuka, 5/25/90, (PB91-108837, A06, MF-A01).

NCEER-90-0009 "A Program to Generate Site Dependent Time Histories: EQGEN," by G.W. Ellis, M. Srinivasan and A.S. Cakmak, 1/30/90, (PB91-108829, A04, MF-A01).

NCEER-90-0010 "Active Isolation for Seismic Protection of Operating Rooms," by M.E. Talbott, Supervised by M. Shinozuka, 6/8/9, (PB91-110205, A05, MF-A01).

NCEER-90-0011 "Program LINEARID for Identification of Linear Structural Dynamic Systems," by C-B. Yun and M. Shinozuka, 6/25/90, (PB91-110312, A08, MF-A01).

NCEER-90-0012 "Two-Dimensional Two-Phase Elasto-Plastic Seismic Response of Earth Dams," by A.N. Yiagos, Supervised by J.H. Prevost, 6/20/90, (PB91-110197, A13, MF-A02).

NCEER-90-0013 "Secondary Systems in Base-Isolated Structures: Experimental Investigation, Stochastic Response and Stochastic Sensitivity," by G.D. Manolis, G. Juhn, M.C. Constantinou and A.M. Reinhorn, 7/1/90, (PB91-110320, A08, MF-A01).

NCEER-90-0014 "Seismic Behavior of Lightly-Reinforced Concrete Column and Beam-Column Joint Details," by S.P. Pessiki, C.H. Conley, P. Gergely and R.N. White, 8/22/90, (PB91-108795, A11, MF-A02).

NCEER-90-0015 "Two Hybrid Control Systems for Building Structures Under Strong Earthquakes," by J.N. Yang and A. Danielians, 6/29/90, (PB91-125393, A04, MF-A01).

NCEER-90-0016 "Instantaneous Optimal Control with Acceleration and Velocity Feedback," by J.N. Yang and Z. Li, 6/29/90, (PB91-125401, A03, MF-A01).

NCEER-90-0017 "Reconnaissance Report on the Northern Iran Earthquake of June 21, 1990," by M. Mehrain, 10/4/90, (PB91-125377, A03, MF-A01).

NCEER-90-0018 "Evaluation of Liquefaction Potential in Memphis and Shelby County," by T.S. Chang, P.S. Tang, C.S. Lee and H. Hwang, 8/10/90, (PB91-125427, A09, MF-A01).

NCEER-90-0019 "Experimental and Analytical Study of a Combined Sliding Disc Bearing and Helical Steel Spring Isolation System," by M.C. Constantinou, A.S. Mokha and A.M. Reinhorn, 10/4/90, (PB91-125385, A06, MF-A01). This report is available only through NTIS (see address given above).

NCEER-90-0020 "Experimental Study and Analytical Prediction of Earthquake Response of a Sliding Isolation System with a Spherical Surface," by A.S. Mokha, M.C. Constantinou and A.M. Reinhorn, 10/11/90, (PB91-125419, A05, MF-A01).

NCEER-90-0021 "Dynamic Interaction Factors for Floating Pile Groups," by G. Gazetas, K. Fan, A. Kaynia and E. Kausel, 9/10/90, (PB91-170381, A05, MF-A01).

NCEER-90-0022 "Evaluation of Seismic Damage Indices for Reinforced Concrete Structures," by S. Rodriguez-Gomez and A.S. Cakmak, 9/30/90, PB91-171322, A06, MF-A01).

NCEER-90-0023 "Study of Site Response at a Selected Memphis Site," by H. Desai, S. Ahmad, E.S. Gazetas and M.R. Oh, 10/11/90, (PB91-196857, A03, MF-A01).

NCEER-90-0024 "A User's Guide to Strongmo: Version 1.0 of NCEER's Strong-Motion Data Access Tool for PCs and Terminals," by P.A. Friberg and C.A.T. Susch, 11/15/90, (PB91-171272, A03, MF-A01).

NCEER-90-0025 "A Three-Dimensional Analytical Study of Spatial Variability of Seismic Ground Motions," by L-L. Hong and A.H.-S. Ang, 10/30/90, (PB91-170399, A09, MF-A01).

NCEER-90-0026 "MUMOID User's Guide - A Program for the Identification of Modal Parameters," by S. Rodriguez-Gomez and E. DiPasquale, 9/30/90, (PB91-171298, A04, MF-A01).

NCEER-90-0027 "SARCF-II User's Guide - Seismic Analysis of Reinforced Concrete Frames," by S. Rodriguez-Gomez, Y.S. Chung and C. Meyer, 9/30/90, (PB91-171280, A05, MF-A01).

NCEER-90-0028 "Viscous Dampers: Testing, Modeling and Application in Vibration and Seismic Isolation," by N. Makris and M.C. Constantinou, 12/20/90 (PB91-190561, A06, MF-A01).

NCEER-90-0029 "Soil Effects on Earthquake Ground Motions in the Memphis Area," by H. Hwang, C.S. Lee, K.W. Ng and T.S. Chang, 8/2/90, (PB91-190751, A05, MF-A01).

NCEER-91-0001 "Proceedings from the Third Japan-U.S. Workshop on Earthquake Resistant Design of Lifeline Facilities and Countermeasures for Soil Liquefaction, December 17-19, 1990," edited by T.D. O'Rourke and M. Hamada, 2/1/91, (PB91-179259, A99, MF-A04).

NCEER-91-0002 "Physical Space Solutions of Non-Proportionally Damped Systems," by M. Tong, Z. Liang and G.C. Lee, 1/15/91, (PB91-179242, A04, MF-A01).

NCEER-91-0003 "Seismic Response of Single Piles and Pile Groups," by K. Fan and G. Gazetas, 1/10/91, (PB92-174994, A04, MF-A01).

NCEER-91-0004 "Damping of Structures: Part 1 - Theory of Complex Damping," by Z. Liang and G. Lee, 10/10/91, (PB92-197235, A12, MF-A03).

NCEER-91-0005 "3D-BASIS - Nonlinear Dynamic Analysis of Three Dimensional Base Isolated Structures: Part II," by S. Nagarajaiah, A.M. Reinhorn and M.C. Constantinou, 2/28/91, (PB91-190553, A07, MF-A01). This report has been replaced by NCEER-93-0011.

NCEER-91-0006 "A Multidimensional Hysteretic Model for Plasticity Deforming Metals in Energy Absorbing Devices," by E.J. Graesser and F.A. Cozzarelli, 4/9/91, (PB92-108364, A04, MF-A01).

NCEER-91-0007 "A Framework for Customizable Knowledge-Based Expert Systems with an Application to a KBES for Evaluating the Seismic Resistance of Existing Buildings," by E.G. Ibarra-Anaya and S.J. Fenves, 4/9/91, (PB91-210930, A08, MF-A01).

NCEER-91-0008 "Nonlinear Analysis of Steel Frames with Semi-Rigid Connections Using the Capacity Spectrum Method," by G.G. Deierlein, S-H. Hsieh, Y-J. Shen and J.F. Abel, 7/2/91, (PB92-113828, A05, MF-A01).

NCEER-91-0009 "Earthquake Education Materials for Grades K-12," by K.E.K. Ross, 4/30/91, (PB91-212142, A06, MF-A01). This report has been replaced by NCEER-92-0018.

NCEER-91-0010 "Phase Wave Velocities and Displacement Phase Differences in a Harmonically Oscillating Pile," by N. Makris and G. Gazetas, 7/8/91, (PB92-108356, A04, MF-A01).

NCEER-91-0011 "Dynamic Characteristics of a Full-Size Five-Story Steel Structure and a 2/5 Scale Model," by K.C. Chang, G.C. Yao, G.C. Lee, D.S. Hao and Y.C. Yeh," 7/2/91, (PB93-116648, A06, MF-A02).

NCEER-91-0012 "Seismic Response of a 2/5 Scale Steel Structure with Added Viscoelastic Dampers," by K.C. Chang, T.T. Soong, S-T. Oh and M.L. Lai, 5/17/91, (PB92-110816, A05, MF-A01).

NCEER-91-0013 "Earthquake Response of Retaining Walls; Full-Scale Testing and Computational Modeling," by S. Alampalli and A-W.M. Elgamal, 6/20/91, to be published.

NCEER-91-0014 "3D-BASIS-M: Nonlinear Dynamic Analysis of Multiple Building Base Isolated Structures," by P.C. Tsopelas, S. Nagarajaiah, M.C. Constantinou and A.M. Reinhorn, 5/28/91, (PB92-113885, A09, MF-A02).

NCEER-91-0015 "Evaluation of SEAOC Design Requirements for Sliding Isolated Structures," by D. Theodossiou and M.C. Constantinou, 6/10/91, (PB92-114602, A11, MF-A03).

NCEER-91-0016 "Closed-Loop Modal Testing of a 27-Story Reinforced Concrete Flat Plate-Core Building," by H.R. Somaprasad, T. Toksoy, H. Yoshiyuki and A.E. Aktan, 7/15/91, (PB92-129980, A07, MF-A02).

NCEER-91-0017 "Shake Table Test of a 1/6 Scale Two-Story Lightly Reinforced Concrete Building," by A.G. El-Attar, R.N. White and P. Gergely, 2/28/91, (PB92-222447, A06, MF-A02).

NCEER-91-0018 "Shake Table Test of a 1/8 Scale Three-Story Lightly Reinforced Concrete Building," by A.G. El-Attar, R.N. White and P. Gergely, 2/28/91, (PB93-116630, A08, MF-A02).

NCEER-91-0019 "Transfer Functions for Rigid Rectangular Foundations," by A.S. Veletsos, A.M. Prasad and W.H. Wu, 7/31/91, to be published.

NCEER-91-0020 "Hybrid Control of Seismic-Excited Nonlinear and Inelastic Structural Systems," by J.N. Yang, Z. Li and A. Danielians, 8/1/91, (PB92-143171, A06, MF-A02).

NCEER-91-0021 "The NCEER-91 Earthquake Catalog: Improved Intensity-Based Magnitudes and Recurrence Relations for U.S. Earthquakes East of New Madrid," by L. Seeber and J.G. Armbruster, 8/28/91, (PB92-176742, A06, MF-A02).

NCEER-91-0022 "Proceedings from the Implementation of Earthquake Planning and Education in Schools: The Need for Change - The Roles of the Changemakers," by K.E.K. Ross and F. Winslow, 7/23/91, (PB92-129998, A12, MF-A03).

NCEER-91-0023 "A Study of Reliability-Based Criteria for Seismic Design of Reinforced Concrete Frame Buildings," by H.H.M. Hwang and H-M. Hsu, 8/10/91, (PB92-140235, A09, MF-A02).

NCEER-91-0024 "Experimental Verification of a Number of Structural System Identification Algorithms," by R.G. Ghanem, H. Gavin and M. Shinozuka, 9/18/91, (PB92-176577, A18, MF-A04).

NCEER-91-0025 "Probabilistic Evaluation of Liquefaction Potential," by H.H.M. Hwang and C.S. Lee," 11/25/91, (PB92-143429, A05, MF-A01).

NCEER-91-0026 "Instantaneous Optimal Control for Linear, Nonlinear and Hysteretic Structures - Stable Controllers," by J.N. Yang and Z. Li, 11/15/91, (PB92-163807, A04, MF-A01).

NCEER-91-0027 "Experimental and Theoretical Study of a Sliding Isolation System for Bridges," by M.C. Constantinou, A. Kartoum, A.M. Reinhorn and P. Bradford, 11/15/91, (PB92-176973, A10, MF-A03).

NCEER-92-0001 "Case Studies of Liquefaction and Lifeline Performance During Past Earthquakes, Volume 1: Japanese Case Studies," Edited by M. Hamada and T. O'Rourke, 2/17/92, (PB92-197243, A18, MF-A04).

NCEER-92-0002 "Case Studies of Liquefaction and Lifeline Performance During Past Earthquakes, Volume 2: United States Case Studies," Edited by T. O'Rourke and M. Hamada, 2/17/92, (PB92-197250, A20, MF-A04).

NCEER-92-0003 "Issues in Earthquake Education," Edited by K. Ross, 2/3/92, (PB92-222389, A07, MF-A02).

NCEER-92-0004 "Proceedings from the First U.S. - Japan Workshop on Earthquake Protective Systems for Bridges," Edited by I.G. Buckle, 2/4/92, (PB94-142239, A99, MF-A06).

NCEER-92-0005 "Seismic Ground Motion from a Haskell-Type Source in a Multiple-Layered Half-Space," A.P. Theoharis, G. Deodatis and M. Shinozuka, 1/2/92, to be published.

NCEER-92-0006 "Proceedings from the Site Effects Workshop," Edited by R. Whitman, 2/29/92, (PB92-197201, A04, MF-A01).

NCEER-92-0007 "Engineering Evaluation of Permanent Ground Deformations Due to Seismically-Induced Liquefaction," by M.H. Baziar, R. Dobry and A-W.M. Elgamal, 3/24/92, (PB92-222421, A13, MF-A03).

NCEER-92-0008 "A Procedure for the Seismic Evaluation of Buildings in the Central and Eastern United States," by C.D. Poland and J.O. Malley, 4/2/92, (PB92-222439, A20, MF-A04).

NCEER-92-0009 "Experimental and Analytical Study of a Hybrid Isolation System Using Friction Controllable Sliding Bearings," by M.Q. Feng, S. Fujii and M. Shinozuka, 5/15/92, (PB93-150282, A06, MF-A02).

NCEER-92-0010 "Seismic Resistance of Slab-Column Connections in Existing Non-Ductile Flat-Plate Buildings," by A.J. Durrani and Y. Du, 5/18/92, (PB93-116812, A06, MF-A02).

NCEER-92-0011 "The Hysteretic and Dynamic Behavior of Brick Masonry Walls Upgraded by Ferrocement Coatings Under Cyclic Loading and Strong Simulated Ground Motion," by H. Lee and S.P. Prawel, 5/11/92, to be published.

NCEER-92-0012 "Study of Wire Rope Systems for Seismic Protection of Equipment in Buildings," by G.F. Demetriades, M.C. Constantinou and A.M. Reinhorn, 5/20/92, (PB93-116655, A08, MF-A02).

NCEER-92-0013 "Shape Memory Structural Dampers: Material Properties, Design and Seismic Testing," by P.R. Witting and F.A. Cozzarelli, 5/26/92, (PB93-116663, A05, MF-A01).

NCEER-92-0014 "Longitudinal Permanent Ground Deformation Effects on Buried Continuous Pipelines," by M.J. O'Rourke, and C. Nordberg, 6/15/92, (PB93-116671, A08, MF-A02).

NCEER-92-0015 "A Simulation Method for Stationary Gaussian Random Functions Based on the Sampling Theorem," by M. Grigoriu and S. Balopoulou, 6/11/92, (PB93-127496, A05, MF-A01).

NCEER-92-0016 "Gravity-Load-Designed Reinforced Concrete Buildings: Seismic Evaluation of Existing Construction and Detailing Strategies for Improved Seismic Resistance," by G.W. Hoffmann, S.K. Kunnath, A.M. Reinhorn and J.B. Mander, 7/15/92, (PB94-142007, A08, MF-A02).

NCEER-92-0017 "Observations on Water System and Pipeline Performance in the Limón Area of Costa Rica Due to the April 22, 1991 Earthquake," by M. O'Rourke and D. Ballantyne, 6/30/92, (PB93-126811, A06, MF-A02).

NCEER-92-0018 "Fourth Edition of Earthquake Education Materials for Grades K-12," Edited by K.E.K. Ross, 8/10/92, (PB93-114023, A07, MF-A02).

NCEER-92-0019 "Proceedings from the Fourth Japan-U.S. Workshop on Earthquake Resistant Design of Lifeline Facilities and Countermeasures for Soil Liquefaction," Edited by M. Hamada and T.D. O'Rourke, 8/12/92, (PB93-163939, A99, MF-E11).

NCEER-92-0020 "Active Bracing System: A Full Scale Implementation of Active Control," by A.M. Reinhorn, T.T. Soong, R.C. Lin, M.A. Riley, Y.P. Wang, S. Aizawa and M. Higashino, 8/14/92, (PB93-127512, A06, MF-A02).

NCEER-92-0021 "Empirical Analysis of Horizontal Ground Displacement Generated by Liquefaction-Induced Lateral Spreads," by S.F. Bartlett and T.L. Youd, 8/17/92, (PB93-188241, A06, MF-A02).

NCEER-92-0022 "IDARC Version 3.0: Inelastic Damage Analysis of Reinforced Concrete Structures," by S.K. Kunnath, A.M. Reinhorn and R.F. Lobo, 8/31/92, (PB93-227502, A07, MF-A02).

NCEER-92-0023 "A Semi-Empirical Analysis of Strong-Motion Peaks in Terms of Seismic Source, Propagation Path and Local Site Conditions, by M. Kamiyama, M.J. O'Rourke and R. Flores-Berrones, 9/9/92, (PB93-150266, A08, MF-A02).

NCEER-92-0024 "Seismic Behavior of Reinforced Concrete Frame Structures with Nonductile Details, Part I: Summary of Experimental Findings of Full Scale Beam-Column Joint Tests," by A. Beres, R.N. White and P. Gergely, 9/30/92, (PB93-227783, A05, MF-A01).

NCEER-92-0025 "Experimental Results of Repaired and Retrofitted Beam-Column Joint Tests in Lightly Reinforced Concrete Frame Buildings," by A. Beres, S. El-Borgi, R.N. White and P. Gergely, 10/29/92, (PB93-227791, A05, MF-A01).

NCEER-92-0026 "A Generalization of Optimal Control Theory: Linear and Nonlinear Structures," by J.N. Yang, Z. Li and S. Vongchavalitkul, 11/2/92, (PB93-188621, A05, MF-A01).

NCEER-92-0027 "Seismic Resistance of Reinforced Concrete Frame Structures Designed Only for Gravity Loads: Part I - Design and Properties of a One-Third Scale Model Structure," by J.M. Bracci, A.M. Reinhorn and J.B. Mander, 12/1/92, (PB94-104502, A08, MF-A02).

NCEER-92-0028 "Seismic Resistance of Reinforced Concrete Frame Structures Designed Only for Gravity Loads: Part II - Experimental Performance of Subassemblages," by L.E. Aycardi, J.B. Mander and A.M. Reinhorn, 12/1/92, (PB94-104510, A08, MF-A02).

NCEER-92-0029 "Seismic Resistance of Reinforced Concrete Frame Structures Designed Only for Gravity Loads: Part III - Experimental Performance and Analytical Study of a Structural Model," by J.M. Bracci, A.M. Reinhorn and J.B. Mander, 12/1/92, (PB93-227528, A09, MF-A01).

NCEER-92-0030 "Evaluation of Seismic Retrofit of Reinforced Concrete Frame Structures: Part I - Experimental Performance of Retrofitted Subassemblages," by D. Choudhuri, J.B. Mander and A.M. Reinhorn, 12/8/92, (PB93-198307, A07, MF-A02).

NCEER-92-0031 "Evaluation of Seismic Retrofit of Reinforced Concrete Frame Structures: Part II - Experimental Performance and Analytical Study of a Retrofitted Structural Model," by J.M. Bracci, A.M. Reinhorn and J.B. Mander, 12/8/92, (PB93-198315, A09, MF-A03).

NCEER-92-0032 "Experimental and Analytical Investigation of Seismic Response of Structures with Supplemental Fluid Viscous Dampers," by M.C. Constantinou and M.D. Symans, 12/21/92, (PB93-191435, A10, MF-A03). This report is available only through NTIS (see address given above).

NCEER-92-0033 "Reconnaissance Report on the Cairo, Egypt Earthquake of October 12, 1992," by M. Khater, 12/23/92, (PB93-188621, A03, MF-A01).

NCEER-92-0034 "Low-Level Dynamic Characteristics of Four Tall Flat-Plate Buildings in New York City," by H. Gavin, S. Yuan, J. Grossman, E. Pekelis and K. Jacob, 12/28/92, (PB93-188217, A07, MF-A02).

NCEER-93-0001 "An Experimental Study on the Seismic Performance of Brick-Infilled Steel Frames With and Without Retrofit," by J.B. Mander, B. Nair, K. Wojtkowski and J. Ma, 1/29/93, (PB93-227510, A07, MF-A02).

NCEER-93-0002 "Social Accounting for Disaster Preparedness and Recovery Planning," by S. Cole, E. Pantoja and V. Razak, 2/22/93, (PB94-142114, A12, MF-A03).

NCEER-93-0003 "Assessment of 1991 NEHRP Provisions for Nonstructural Components and Recommended Revisions," by T.T. Soong, G. Chen, Z. Wu, R-H. Zhang and M. Grigoriu, 3/1/93, (PB93-188639, A06, MF-A02).

NCEER-93-0004 "Evaluation of Static and Response Spectrum Analysis Procedures of SEAOC/UBC for Seismic Isolated Structures," by C.W. Winters and M.C. Constantinou, 3/23/93, (PB93-198299, A10, MF-A03).

NCEER-93-0005 "Earthquakes in the Northeast - Are We Ignoring the Hazard? A Workshop on Earthquake Science and Safety for Educators," edited by K.E.K. Ross, 4/2/93, (PB94-103066, A09, MF-A02).

NCEER-93-0006 "Inelastic Response of Reinforced Concrete Structures with Viscoelastic Braces," by R.F. Lobo, J.M. Bracci, K.L. Shen, A.M. Reinhorn and T.T. Soong, 4/5/93, (PB93-227486, A05, MF-A02).

NCEER-93-0007 "Seismic Testing of Installation Methods for Computers and Data Processing Equipment," by K. Kosar, T.T. Soong, K.L. Shen, J.A. HoLung and Y.K. Lin, 4/12/93, (PB93-198299, A07, MF-A02).

NCEER-93-0008 "Retrofit of Reinforced Concrete Frames Using Added Dampers," by A. Reinhorn, M. Constantinou and C. Li, to be published.

NCEER-93-0009 "Seismic Behavior and Design Guidelines for Steel Frame Structures with Added Viscoelastic Dampers," by K.C. Chang, M.L. Lai, T.T. Soong, D.S. Hao and Y.C. Yeh, 5/1/93, (PB94-141959, A07, MF-A02).

NCEER-93-0010 "Seismic Performance of Shear-Critical Reinforced Concrete Bridge Piers," by J.B. Mander, S.M. Waheed, M.T.A. Chaudhary and S.S. Chen, 5/12/93, (PB93-227494, A08, MF-A02).

NCEER-93-0011 "3D-BASIS-TABS: Computer Program for Nonlinear Dynamic Analysis of Three Dimensional Base Isolated Structures," by S. Nagarajaiah, C. Li, A.M. Reinhorn and M.C. Constantinou, 8/2/93, (PB94-141819, A09, MF-A02).

NCEER-93-0012 "Effects of Hydrocarbon Spills from an Oil Pipeline Break on Ground Water," by O.J. Helweg and H.H.M. Hwang, 8/3/93, (PB94-141942, A06, MF-A02).

NCEER-93-0013 "Simplified Procedures for Seismic Design of Nonstructural Components and Assessment of Current Code Provisions," by M.P. Singh, L.E. Suarez, E.E. Matheu and G.O. Maldonado, 8/4/93, (PB94-141827, A09, MF-A02).

NCEER-93-0014 "An Energy Approach to Seismic Analysis and Design of Secondary Systems," by G. Chen and T.T. Soong, 8/6/93, (PB94-142767, A11, MF-A03).

NCEER-93-0015 "Proceedings from School Sites: Becoming Prepared for Earthquakes - Commemorating the Third Anniversary of the Loma Prieta Earthquake," Edited by F.E. Winslow and K.E.K. Ross, 8/16/93, (PB94-154275, A16, MF-A02).

NCEER-93-0016 "Reconnaissance Report of Damage to Historic Monuments in Cairo, Egypt Following the October 12, 1992 Dahshur Earthquake," by D. Sykora, D. Look, G. Croci, E. Karaesmen and E. Karaesmen, 8/19/93, (PB94-142221, A08, MF-A02).

NCEER-93-0017 "The Island of Guam Earthquake of August 8, 1993," by S.W. Swan and S.K. Harris, 9/30/93, (PB94-141843, A04, MF-A01).

NCEER-93-0018 "Engineering Aspects of the October 12, 1992 Egyptian Earthquake," by A.W. Elgamal, M. Amer, K. Adalier and A. Abul-Fadl, 10/7/93, (PB94-141983, A05, MF-A01).

NCEER-93-0019 "Development of an Earthquake Motion Simulator and its Application in Dynamic Centrifuge Testing," by I. Krstelj, Supervised by J.H. Prevost, 10/23/93, (PB94-181773, A-10, MF-A03).

NCEER-93-0020 "NCEER-Taisei Corporation Research Program on Sliding Seismic Isolation Systems for Bridges: Experimental and Analytical Study of a Friction Pendulum System (FPS)," by M.C. Constantinou, P. Tsopelas, Y-S. Kim and S. Okamoto, 11/1/93, (PB94-142775, A08, MF-A02).

NCEER-93-0021 "Finite Element Modeling of Elastomeric Seismic Isolation Bearings," by L.J. Billings, Supervised by R. Shepherd, 11/8/93, to be published.

NCEER-93-0022 "Seismic Vulnerability of Equipment in Critical Facilities: Life-Safety and Operational Consequences," by K. Porter, G.S. Johnson, M.M. Zadeh, C. Scawthorn and S. Eder, 11/24/93, (PB94-181765, A16, MF-A03).

NCEER-93-0023 "Hokkaido Nansei-oki, Japan Earthquake of July 12, 1993, by P.I. Yanev and C.R. Scawthorn, 12/23/93, (PB94-181500, A07, MF-A01).

NCEER-94-0001 "An Evaluation of Seismic Serviceability of Water Supply Networks with Application to the San Francisco Auxiliary Water Supply System," by I. Markov, Supervised by M. Grigoriu and T. O'Rourke, 1/21/94, (PB94-204013, A07, MF-A02).

NCEER-94-0002 "NCEER-Taisei Corporation Research Program on Sliding Seismic Isolation Systems for Bridges: Experimental and Analytical Study of Systems Consisting of Sliding Bearings, Rubber Restoring Force Devices and Fluid Dampers," Volumes I and II, by P. Tsopelas, S. Okamoto, M.C. Constantinou, D. Ozaki and S. Fujii, 2/4/94, (PB94-181740, A09, MF-A02 and PB94-181757, A12, MF-A03).

NCEER-94-0003 "A Markov Model for Local and Global Damage Indices in Seismic Analysis," by S. Rahman and M. Grigoriu, 2/18/94, (PB94-206000, A12, MF-A03).

NCEER-94-0004 "Proceedings from the NCEER Workshop on Seismic Response of Masonry Infills," edited by D.P. Abrams, 3/1/94, (PB94-180783, A07, MF-A02).

NCEER-94-0005 "The Northridge, California Earthquake of January 17, 1994: General Reconnaissance Report," edited by J.D. Goltz, 3/11/94, (PB94-193943, A10, MF-A03).

NCEER-94-0006 "Seismic Energy Based Fatigue Damage Analysis of Bridge Columns: Part I - Evaluation of Seismic Capacity," by G.A. Chang and J.B. Mander, 3/14/94, (PB94-219185, A11, MF-A03).

NCEER-94-0007 "Seismic Isolation of Multi-Story Frame Structures Using Spherical Sliding Isolation Systems," by T.M. Al-Hussaini, V.A. Zayas and M.C. Constantinou, 3/17/94, (PB94-193745, A09, MF-A02).

NCEER-94-0008 "The Northridge, California Earthquake of January 17, 1994: Performance of Highway Bridges," edited by I.G. Buckle, 3/24/94, (PB94-193851, A06, MF-A02).

NCEER-94-0009 "Proceedings of the Third U.S.-Japan Workshop on Earthquake Protective Systems for Bridges," edited by I.G. Buckle and I. Friedland, 3/31/94, (PB94-195815, A99, MF-A06).

NCEER-94-0010 "3D-BASIS-ME: Computer Program for Nonlinear Dynamic Analysis of Seismically Isolated Single and Multiple Structures and Liquid Storage Tanks," by P.C. Tsopelas, M.C. Constantinou and A.M. Reinhorn, 4/12/94, (PB94-204922, A09, MF-A02).

NCEER-94-0011 "The Northridge, California Earthquake of January 17, 1994: Performance of Gas Transmission Pipelines," by T.D. O'Rourke and M.C. Palmer, 5/16/94, (PB94-204989, A05, MF-A01).

NCEER-94-0012 "Feasibility Study of Replacement Procedures and Earthquake Performance Related to Gas Transmission Pipelines," by T.D. O'Rourke and M.C. Palmer, 5/25/94, (PB94-206638, A09, MF-A02).

NCEER-94-0013 "Seismic Energy Based Fatigue Damage Analysis of Bridge Columns: Part II - Evaluation of Seismic Demand," by G.A. Chang and J.B. Mander, 6/1/94, (PB95-18106, A08, MF-A02).

NCEER-94-0014 "NCEER-Taisei Corporation Research Program on Sliding Seismic Isolation Systems for Bridges: Experimental and Analytical Study of a System Consisting of Sliding Bearings and Fluid Restoring Force/Damping Devices," by P. Tsopelas and M.C. Constantinou, 6/13/94, (PB94-219144, A10, MF-A03).

NCEER-94-0015 "Generation of Hazard-Consistent Fragility Curves for Seismic Loss Estimation Studies," by H. Hwang and J-R. Huo, 6/14/94, (PB95-181996, A09, MF-A02).

NCEER-94-0016 "Seismic Study of Building Frames with Added Energy-Absorbing Devices," by W.S. Pong, C.S. Tsai and G.C. Lee, 6/20/94, (PB94-219136, A10, A03).

NCEER-94-0017 "Sliding Mode Control for Seismic-Excited Linear and Nonlinear Civil Engineering Structures," by J. Yang, J. Wu, A. Agrawal and Z. Li, 6/21/94, (PB95-138483, A06, MF-A02).

NCEER-94-0018 "3D-BASIS-TABS Version 2.0: Computer Program for Nonlinear Dynamic Analysis of Three Dimensional Base Isolated Structures," by A.M. Reinhorn, S. Nagarajaiah, M.C. Constantinou, P. Tsopelas and R. Li, 6/22/94, (PB95-182176, A08, MF-A02).

NCEER-94-0019 "Proceedings of the International Workshop on Civil Infrastructure Systems: Application of Intelligent Systems and Advanced Materials on Bridge Systems," Edited by G.C. Lee and K.C. Chang, 7/18/94, (PB95-252474, A20, MF-A04).

NCEER-94-0020 "Study of Seismic Isolation Systems for Computer Floors," by V. Lambrou and M.C. Constantinou, 7/19/94, (PB95-138533, A10, MF-A03).

NCEER-94-0021 "Proceedings of the U.S.-Italian Workshop on Guidelines for Seismic Evaluation and Rehabilitation of Unreinforced Masonry Buildings," Edited by D.P. Abrams and G.M. Calvi, 7/20/94, (PB95-138749, A13, MF-A03).

NCEER-94-0022 "NCEER-Taisei Corporation Research Program on Sliding Seismic Isolation Systems for Bridges: Experimental and Analytical Study of a System Consisting of Lubricated PTFE Sliding Bearings and Mild Steel Dampers," by P. Tsopelas and M.C. Constantinou, 7/22/94, (PB95-182184, A08, MF-A02).

NCEER-94-0023 “Development of Reliability-Based Design Criteria for Buildings Under Seismic Load,” by Y.K. Wen, H. Hwang and M. Shinozuka, 8/1/94, (PB95-211934, A08, MF-A02).

NCEER-94-0024 “Experimental Verification of Acceleration Feedback Control Strategies for an Active Tendon System,” by S.J. Dyke, B.F. Spencer, Jr., P. Quast, M.K. Sain, D.C. Kaspari, Jr. and T.T. Soong, 8/29/94, (PB95-212320, A05, MF-A01).

NCEER-94-0025 “Seismic Retrofitting Manual for Highway Bridges,” Edited by I.G. Buckle and I.F. Friedland, published by the Federal Highway Administration (PB95-212676, A15, MF-A03).

NCEER-94-0026 “Proceedings from the Fifth U.S.-Japan Workshop on Earthquake Resistant Design of Lifeline Facilities and Countermeasures Against Soil Liquefaction,” Edited by T.D. O’Rourke and M. Hamada, 11/7/94, (PB95-220802, A99, MF-E08).

NCEER-95-0001 "Experimental and Analytical Investigation of Seismic Retrofit of Structures with Supplemental Damping: Part 1 - Fluid Viscous Damping Devices," by A.M. Reinhorn, C. Li and M.C. Constantinou, 1/3/95, (PB95-266599, A09, MF-A02).

NCEER-95-0002 "Experimental and Analytical Study of Low-Cycle Fatigue Behavior of Semi-Rigid Top-And-Seat Angle Connections," by G. Pekcan, J.B. Mander and S.S. Chen, 1/5/95, (PB95-220042, A07, MF-A02).

NCEER-95-0003 "NCEER-ATC Joint Study on Fragility of Buildings," by T. Anagnos, C. Rojahn and A.S. Kiremidjian, 1/20/95, (PB95-220026, A06, MF-A02).

NCEER-95-0004 "Nonlinear Control Algorithms for Peak Response Reduction," by Z. Wu, T.T. Soong, V. Gattulli and R.C. Lin, 2/16/95, (PB95-220349, A05, MF-A01).

NCEER-95-0005 "Pipeline Replacement Feasibility Study: A Methodology for Minimizing Seismic and Corrosion Risks to Underground Natural Gas Pipelines," by R.T. Eguchi, H.A. Seligson and D.G. Honegger, 3/2/95, (PB95-252326, A06, MF-A02).

NCEER-95-0006 "Evaluation of Seismic Performance of an 11-Story Frame Building During the 1994 Northridge Earthquake," by F. Naeim, R. DiSulio, K. Benuska, A. Reinhorn and C. Li, to be published.

NCEER-95-0007 "Prioritization of Bridges for Seismic Retrofitting," by N. Basöz and A.S. Kiremidjian, 4/24/95, (PB95-252300, A08, MF-A02).

NCEER-95-0008 "Method for Developing Motion Damage Relationships for Reinforced Concrete Frames," by A. Singhal and A.S. Kiremidjian, 5/11/95, (PB95-266607, A06, MF-A02).

NCEER-95-0009 "Experimental and Analytical Investigation of Seismic Retrofit of Structures with Supplemental Damping: Part II - Friction Devices," by C. Li and A.M. Reinhorn, 7/6/95, (PB96-128087, A11, MF-A03).

NCEER-95-0010 "Experimental Performance and Analytical Study of a Non-Ductile Reinforced Concrete Frame Structure Retrofitted with Elastomeric Spring Dampers," by G. Pekcan, J.B. Mander and S.S. Chen, 7/14/95, (PB96-137161, A08, MF-A02).

NCEER-95-0011 "Development and Experimental Study of Semi-Active Fluid Damping Devices for Seismic Protection of Structures," by M.D. Symans and M.C. Constantinou, 8/3/95, (PB96-136940, A23, MF-A04).

NCEER-95-0012 "Real-Time Structural Parameter Modification (RSPM): Development of Innervated Structures," by Z. Liang, M. Tong and G.C. Lee, 4/11/95, (PB96-137153, A06, MF-A01).

NCEER-95-0013 "Experimental and Analytical Investigation of Seismic Retrofit of Structures with Supplemental Damping: Part III - Viscous Damping Walls," by A.M. Reinhorn and C. Li, 10/1/95, (PB96-176409, A11, MF-A03).

NCEER-95-0014 "Seismic Fragility Analysis of Equipment and Structures in a Memphis Electric Substation," by J-R. Huo and H.H.M. Hwang, 8/10/95, (PB96-128087, A09, MF-A02).

NCEER-95-0015 "The Hanshin-Awaji Earthquake of January 17, 1995: Performance of Lifelines," Edited by M. Shinozuka, 11/3/95, (PB96-176383, A15, MF-A03).

NCEER-95-0016 "Highway Culvert Performance During Earthquakes," by T.L. Youd and C.J. Beckman, available as NCEER-96-0015.

NCEER-95-0017 "The Hanshin-Awaji Earthquake of January 17, 1995: Performance of Highway Bridges," Edited by I.G. Buckle, 12/1/95, to be published.

NCEER-95-0018 "Modeling of Masonry Infill Panels for Structural Analysis," by A.M. Reinhorn, A. Madan, R.E. Valles, Y. Reichmann and J.B. Mander, 12/8/95, (PB97-110886, MF-A01, A06).

NCEER-95-0019 "Optimal Polynomial Control for Linear and Nonlinear Structures," by A.K. Agrawal and J.N. Yang, 12/11/95, (PB96-168737, A07, MF-A02).

NCEER-95-0020 "Retrofit of Non-Ductile Reinforced Concrete Frames Using Friction Dampers," by R.S. Rao, P. Gergely and R.N. White, 12/22/95, (PB97-133508, A10, MF-A02).

NCEER-95-0021 "Parametric Results for Seismic Response of Pile-Supported Bridge Bents," by G. Mylonakis, A. Nikolaou and G. Gazetas, 12/22/95, (PB97-100242, A12, MF-A03).

NCEER-95-0022 "Kinematic Bending Moments in Seismically Stressed Piles," by A. Nikolaou, G. Mylonakis and G. Gazetas, 12/23/95, (PB97-113914, MF-A03, A13).

NCEER-96-0001 "Dynamic Response of Unreinforced Masonry Buildings with Flexible Diaphragms," by A.C. Costley and D.P. Abrams," 10/10/96, (PB97-133573, MF-A03, A15).

NCEER-96-0002 "State of the Art Review: Foundations and Retaining Structures," by I. Po Lam, to be published.

NCEER-96-0003 "Ductility of Rectangular Reinforced Concrete Bridge Columns with Moderate Confinement," by N. Wehbe, M. Saiidi, D. Sanders and B. Douglas, 11/7/96, (PB97-133557, A06, MF-A02).

NCEER-96-0004 "Proceedings of the Long-Span Bridge Seismic Research Workshop," edited by I.G. Buckle and I.M. Friedland, to be published.

NCEER-96-0005 "Establish Representative Pier Types for Comprehensive Study: Eastern United States," by J. Kulicki and Z. Prucz, 5/28/96, (PB98-119217, A07, MF-A02).

NCEER-96-0006 "Establish Representative Pier Types for Comprehensive Study: Western United States," by R. Imbsen, R.A. Schamber and T.A. Osterkamp, 5/28/96, (PB98-118607, A07, MF-A02).

NCEER-96-0007 "Nonlinear Control Techniques for Dynamical Systems with Uncertain Parameters," by R.G. Ghanem and M.I. Bujakov, 5/27/96, (PB97-100259, A17, MF-A03).

NCEER-96-0008 "Seismic Evaluation of a 30-Year Old Non-Ductile Highway Bridge Pier and Its Retrofit," by J.B. Mander, B. Mahmoodzadegan, S. Bhadra and S.S. Chen, 5/31/96, (PB97-110902, MF-A03, A10).

NCEER-96-0009 "Seismic Performance of a Model Reinforced Concrete Bridge Pier Before and After Retrofit," by J.B. Mander, J.H. Kim and C.A. Ligozio, 5/31/96, (PB97-110910, MF-A02, A10).

NCEER-96-0010 "IDARC2D Version 4.0: A Computer Program for the Inelastic Damage Analysis of Buildings," by R.E. Valles, A.M. Reinhorn, S.K. Kunnath, C. Li and A. Madan, 6/3/96, (PB97-100234, A17, MF-A03).

NCEER-96-0011 "Estimation of the Economic Impact of Multiple Lifeline Disruption: Memphis Light, Gas and Water Division Case Study," by S.E. Chang, H.A. Seligson and R.T. Eguchi, 8/16/96, (PB97-133490, A11, MF-A03).

NCEER-96-0012 "Proceedings from the Sixth Japan-U.S. Workshop on Earthquake Resistant Design of Lifeline Facilities and Countermeasures Against Soil Liquefaction, Edited by M. Hamada and T. O'Rourke, 9/11/96, (PB97-133581, A99, MF-A06).

NCEER-96-0013 "Chemical Hazards, Mitigation and Preparedness in Areas of High Seismic Risk: A Methodology for Estimating the Risk of Post-Earthquake Hazardous Materials Release," by H.A. Seligson, R.T. Eguchi, K.J. Tierney and K. Richmond, 11/7/96, (PB97-133565, MF-A02, A08).

NCEER-96-0014 "Response of Steel Bridge Bearings to Reversed Cyclic Loading," by J.B. Mander, D-K. Kim, S.S. Chen and G.J. Premus, 11/13/96, (PB97-140735, A12, MF-A03).

NCEER-96-0015 "Highway Culvert Performance During Past Earthquakes," by T.L. Youd and C.J. Beckman, 11/25/96, (PB97-133532, A06, MF-A01).

NCEER-97-0001 "Evaluation, Prevention and Mitigation of Pounding Effects in Building Structures," by R.E. Valles and A.M. Reinhorn, 2/20/97, (PB97-159552, A14, MF-A03).

NCEER-97-0002 "Seismic Design Criteria for Bridges and Other Highway Structures," by C. Rojahn, R. Mayes, D.G. Anderson, J. Clark, J.H. Hom, R.V. Nutt and M.J. O'Rourke, 4/30/97, (PB97-194658, A06, MF-A03).

NCEER-97-0003 “Proceedings of the U.S.-Italian Workshop on Seismic Evaluation and Retrofit,” Edited by D.P. Abrams and G.M. Calvi, 3/19/97, (PB97-194666, A13, MF-A03).

NCEER-97-0004 "Investigation of Seismic Response of Buildings with Linear and Nonlinear Fluid Viscous Dampers," by A.A. Seleemah and M.C. Constantinou, 5/21/97, (PB98-109002, A15, MF-A03).

NCEER-97-0005 "Proceedings of the Workshop on Earthquake Engineering Frontiers in Transportation Facilities," edited by G.C. Lee and I.M. Friedland, 8/29/97, (PB98-128911, A25, MR-A04).

NCEER-97-0006 "Cumulative Seismic Damage of Reinforced Concrete Bridge Piers," by S.K. Kunnath, A. El-Bahy, A. Taylor and W. Stone, 9/2/97, (PB98-108814, A11, MF-A03).

NCEER-97-0007 "Structural Details to Accommodate Seismic Movements of Highway Bridges and Retaining Walls," by R.A. Imbsen, R.A. Schamber, E. Thorkildsen, A. Kartoum, B.T. Martin, T.N. Rosser and J.M. Kulicki, 9/3/97, (PB98-108996, A09, MF-A02).

NCEER-97-0008 "A Method for Earthquake Motion-Damage Relationships with Application to Reinforced Concrete Frames," by A. Singhal and A.S. Kiremidjian, 9/10/97, (PB98-108988, A13, MF-A03).

NCEER-97-0009 "Seismic Analysis and Design of Bridge Abutments Considering Sliding and Rotation," by K. Fishman and R. Richards, Jr., 9/15/97, (PB98-108897, A06, MF-A02).

NCEER-97-0010 "Proceedings of the FHWA/NCEER Workshop on the National Representation of Seismic Ground Motion for New and Existing Highway Facilities," edited by I.M. Friedland, M.S. Power and R.L. Mayes, 9/22/97, (PB98-128903, A21, MF-A04).

NCEER-97-0011 "Seismic Analysis for Design or Retrofit of Gravity Bridge Abutments," by K.L. Fishman, R. Richards, Jr. and R.C. Divito, 10/2/97, (PB98-128937, A08, MF-A02).

NCEER-97-0012 "Evaluation of Simplified Methods of Analysis for Yielding Structures," by P. Tsopelas, M.C. Constantinou, C.A. Kircher and A.S. Whittaker, 10/31/97, (PB98-128929, A10, MF-A03).

NCEER-97-0013 "Seismic Design of Bridge Columns Based on Control and Repairability of Damage," by C-T. Cheng and J.B. Mander, 12/8/97, (PB98-144249, A11, MF-A03).

NCEER-97-0014 "Seismic Resistance of Bridge Piers Based on Damage Avoidance Design," by J.B. Mander and C-T. Cheng, 12/10/97, (PB98-144223, A09, MF-A02).

NCEER-97-0015 “Seismic Response of Nominally Symmetric Systems with Strength Uncertainty,” by S. Balopoulou and M. Grigoriu, 12/23/97, (PB98-153422, A11, MF-A03).

NCEER-97-0016 “Evaluation of Seismic Retrofit Methods for Reinforced Concrete Bridge Columns,” by T.J. Wipf, F.W. Klaiber and F.M. Russo, 12/28/97, (PB98-144215, A12, MF-A03).

NCEER-97-0017 “Seismic Fragility of Existing Conventional Reinforced Concrete Highway Bridges,” by C.L. Mullen and A.S. Cakmak, 12/30/97, (PB98-153406, A08, MF-A02).

NCEER-97-0018 “Loss Asssessment of Memphis Buildings,” edited by D.P. Abrams and M. Shinozuka, 12/31/97, (PB98-144231, A13, MF-A03).

NCEER-97-0019 “Seismic Evaluation of Frames with Infill Walls Using Quasi-static Experiments,” by K.M. Mosalam, R.N. White and P. Gergely, 12/31/97, (PB98-153455, A07, MF-A02).

NCEER-97-0020 “Seismic Evaluation of Frames with Infill Walls Using Pseudo-dynamic Experiments,” by K.M. Mosalam, R.N. White and P. Gergely, 12/31/97, (PB98-153430, A07, MF-A02).

NCEER-97-0021 “Computational Strategies for Frames with Infill Walls: Discrete and Smeared Crack Analyses and Seismic Fragility,” by K.M. Mosalam, R.N. White and P. Gergely, 12/31/97, (PB98-153414, A10, MF-A02).

NCEER-97-0022 "Proceedings of the NCEER Workshop on Evaluation of Liquefaction Resistance of Soils," edited by T.L. Youd and I.M. Idriss, 12/31/97, (PB98-155617, A15, MF-A03).

MCEER-98-0001 "Extraction of Nonlinear Hysteretic Properties of Seismically Isolated Bridges from Quick-Release Field Tests," by Q. Chen, B.M. Douglas, E.M. Maragakis and I.G. Buckle, 5/26/98, (PB99-118838, A06, MF-A01).

MCEER-98-0002 "Methodologies for Evaluating the Importance of Highway Bridges," by A. Thomas, S. Eshenaur and J. Kulicki, 5/29/98, (PB99-118846, A10, MF-A02).

MCEER-98-0003 "Capacity Design of Bridge Piers and the Analysis of Overstrength," by J.B. Mander, A. Dutta and P. Goel, 6/1/98, (PB99-118853, A09, MF-A02).

MCEER-98-0004 "Evaluation of Bridge Damage Data from the Loma Prieta and Northridge, California Earthquakes," by N. Basoz and A. Kiremidjian, 6/2/98, (PB99-118861, A15, MF-A03).

MCEER-98-0005 "Screening Guide for Rapid Assessment of Liquefaction Hazard at Highway Bridge Sites," by T. L. Youd, 6/16/98, (PB99-118879, A06, not available on microfiche).

MCEER-98-0006 "Structural Steel and Steel/Concrete Interface Details for Bridges," by P. Ritchie, N. Kauhl and J. Kulicki, 7/13/98, (PB99-118945, A06, MF-A01).

MCEER-98-0007 "Capacity Design and Fatigue Analysis of Confined Concrete Columns," by A. Dutta and J.B. Mander, 7/14/98, (PB99-118960, A14, MF-A03).

MCEER-98-0008 "Proceedings of the Workshop on Performance Criteria for Telecommunication Services Under Earthquake Conditions," edited by A.J. Schiff, 7/15/98, (PB99-118952, A08, MF-A02).

MCEER-98-0009 "Fatigue Analysis of Unconfined Concrete Columns," by J.B. Mander, A. Dutta and J.H. Kim, 9/12/98, (PB99-123655, A10, MF-A02).

MCEER-98-0010 "Centrifuge Modeling of Cyclic Lateral Response of Pile-Cap Systems and Seat-Type Abutments in Dry Sands," by A.D. Gadre and R. Dobry, 10/2/98, (PB99-123606, A13, MF-A03).

MCEER-98-0011 "IDARC-BRIDGE: A Computational Platform for Seismic Damage Assessment of Bridge Structures," by A.M. Reinhorn, V. Simeonov, G. Mylonakis and Y. Reichman, 10/2/98, (PB99-162919, A15, MF-A03).

MCEER-98-0012 "Experimental Investigation of the Dynamic Response of Two Bridges Before and After Retrofitting with Elastomeric Bearings," by D.A. Wendichansky, S.S. Chen and J.B. Mander, 10/2/98, (PB99-162927, A15, MF-A03).

MCEER-98-0013 "Design Procedures for Hinge Restrainers and Hinge Sear Width for Multiple-Frame Bridges," by R. Des Roches and G.L. Fenves, 11/3/98, (PB99-140477, A13, MF-A03).

MCEER-98-0014 "Response Modification Factors for Seismically Isolated Bridges," by M.C. Constantinou and J.K. Quarshie, 11/3/98, (PB99-140485, A14, MF-A03).

MCEER-98-0015 "Proceedings of the U.S.-Italy Workshop on Seismic Protective Systems for Bridges," edited by I.M. Friedland and M.C. Constantinou, 11/3/98, (PB2000-101711, A22, MF-A04).

MCEER-98-0016 "Appropriate Seismic Reliability for Critical Equipment Systems: Recommendations Based on Regional Analysis of Financial and Life Loss," by K. Porter, C. Scawthorn, C. Taylor and N. Blais, 11/10/98, (PB99-157265, A08, MF-A02).

MCEER-98-0017 "Proceedings of the U.S. Japan Joint Seminar on Civil Infrastructure Systems Research," edited by M. Shinozuka and A. Rose, 11/12/98, (PB99-156713, A16, MF-A03).

MCEER-98-0018 "Modeling of Pile Footings and Drilled Shafts for Seismic Design," by I. PoLam, M. Kapuskar and D. Chaudhuri, 12/21/98, (PB99-157257, A09, MF-A02).

MCEER-99-0001 "Seismic Evaluation of a Masonry Infilled Reinforced Concrete Frame by Pseudodynamic Testing," by S.G. Buonopane and R.N. White, 2/16/99, (PB99-162851, A09, MF-A02).

MCEER-99-0002 "Response History Analysis of Structures with Seismic Isolation and Energy Dissipation Systems: Verification Examples for Program SAP2000," by J. Scheller and M.C. Constantinou, 2/22/99, (PB99-162869, A08, MF-A02).

MCEER-99-0003 "Experimental Study on the Seismic Design and Retrofit of Bridge Columns Including Axial Load Effects," by A. Dutta, T. Kokorina and J.B. Mander, 2/22/99, (PB99-162877, A09, MF-A02).

MCEER-99-0004 "Experimental Study of Bridge Elastomeric and Other Isolation and Energy Dissipation Systems with Emphasis on Uplift Prevention and High Velocity Near-source Seismic Excitation," by A. Kasalanati and M. C. Constantinou, 2/26/99, (PB99-162885, A12, MF-A03).

MCEER-99-0005 "Truss Modeling of Reinforced Concrete Shear-flexure Behavior," by J.H. Kim and J.B. Mander, 3/8/99, (PB99-163693, A12, MF-A03).

MCEER-99-0006 "Experimental Investigation and Computational Modeling of Seismic Response of a 1:4 Scale Model Steel Structure with a Load Balancing Supplemental Damping System," by G. Pekcan, J.B. Mander and S.S. Chen, 4/2/99, (PB99-162893, A11, MF-A03).

MCEER-99-0007 "Effect of Vertical Ground Motions on the Structural Response of Highway Bridges," by M.R. Button, C.J. Cronin and R.L. Mayes, 4/10/99, (PB2000-101411, A10, MF-A03).

MCEER-99-0008 "Seismic Reliability Assessment of Critical Facilities: A Handbook, Supporting Documentation, and Model Code Provisions," by G.S. Johnson, R.E. Sheppard, M.D. Quilici, S.J. Eder and C.R. Scawthorn, 4/12/99, (PB2000-101701, A18, MF-A04).

MCEER-99-0009 "Impact Assessment of Selected MCEER Highway Project Research on the Seismic Design of Highway Structures," by C. Rojahn, R. Mayes, D.G. Anderson, J.H. Clark, D'Appolonia Engineering, S. Gloyd and R.V. Nutt, 4/14/99, (PB99-162901, A10, MF-A02).

MCEER-99-0010 "Site Factors and Site Categories in Seismic Codes," by R. Dobry, R. Ramos and M.S. Power, 7/19/99, (PB2000-101705, A08, MF-A02).

MCEER-99-0011 "Restrainer Design Procedures for Multi-Span Simply-Supported Bridges," by M.J. Randall, M. Saiidi, E. Maragakis and T. Isakovic, 7/20/99, (PB2000-101702, A10, MF-A02).

MCEER-99-0012 "Property Modification Factors for Seismic Isolation Bearings," by M.C. Constantinou, P. Tsopelas, A. Kasalanati and E. Wolff, 7/20/99, (PB2000-103387, A11, MF-A03).

MCEER-99-0013 "Critical Seismic Issues for Existing Steel Bridges," by P. Ritchie, N. Kauhl and J. Kulicki, 7/20/99, (PB2000-101697, A09, MF-A02).

MCEER-99-0014 "Nonstructural Damage Database," by A. Kao, T.T. Soong and A. Vender, 7/24/99, (PB2000-101407, A06, MF-A01).

MCEER-99-0015 "Guide to Remedial Measures for Liquefaction Mitigation at Existing Highway Bridge Sites," by H.G. Cooke and J. K. Mitchell, 7/26/99, (PB2000-101703, A11, MF-A03).

MCEER-99-0016 "Proceedings of the MCEER Workshop on Ground Motion Methodologies for the Eastern United States," edited by N. Abrahamson and A. Becker, 8/11/99, (PB2000-103385, A07, MF-A02).

MCEER-99-0017 "Quindío, Colombia Earthquake of January 25, 1999: Reconnaissance Report," by A.P. Asfura and P.J. Flores, 10/4/99, (PB2000-106893, A06, MF-A01).

MCEER-99-0018 "Hysteretic Models for Cyclic Behavior of Deteriorating Inelastic Structures," by M.V. Sivaselvan and A.M. Reinhorn, 11/5/99, (PB2000-103386, A08, MF-A02).

MCEER-99-0019 "Proceedings of the 7th U.S.- Japan Workshop on Earthquake Resistant Design of Lifeline Facilities and Countermeasures Against Soil Liquefaction," edited by T.D. O'Rourke, J.P. Bardet and M. Hamada, 11/19/99, (PB2000-103354, A99, MF-A06).

MCEER-99-0020 "Development of Measurement Capability for Micro-Vibration Evaluations with Application to Chip Fabrication Facilities," by G.C. Lee, Z. Liang, J.W. Song, J.D. Shen and W.C. Liu, 12/1/99, (PB2000-105993, A08, MF-A02).

MCEER-99-0021 "Design and Retrofit Methodology for Building Structures with Supplemental Energy Dissipating Systems," by G. Pekcan, J.B. Mander and S.S. Chen, 12/31/99, (PB2000-105994, A11, MF-A03).

MCEER-00-0001 "The Marmara, Turkey Earthquake of August 17, 1999: Reconnaissance Report," edited by C. Scawthorn; with major contributions by M. Bruneau, R. Eguchi, T. Holzer, G. Johnson, J. Mander, J. Mitchell, W. Mitchell, A. Papageorgiou, C. Scaethorn, and G. Webb, 3/23/00, (PB2000-106200, A11, MF-A03).

MCEER-00-0002 "Proceedings of the MCEER Workshop for Seismic Hazard Mitigation of Health Care Facilities," edited by G.C. Lee, M. Ettouney, M. Grigoriu, J. Hauer and J. Nigg, 3/29/00, (PB2000-106892, A08, MF-A02).

MCEER-00-0003 "The Chi-Chi, Taiwan Earthquake of September 21, 1999: Reconnaissance Report," edited by G.C. Lee and C.H. Loh, with major contributions by G.C. Lee, M. Bruneau, I.G. Buckle, S.E. Chang, P.J. Flores, T.D. O'Rourke, M. Shinozuka, T.T. Soong, C-H. Loh, K-C. Chang, Z-J. Chen, J-S. Hwang, M-L. Lin, G-Y. Liu, K-C. Tsai, G.C. Yao and C-L. Yen, 4/30/00, (PB2001-100980, A10, MF-A02).

MCEER-00-0004 "Seismic Retrofit of End-Sway Frames of Steel Deck-Truss Bridges with a Supplemental Tendon System: Experimental and Analytical Investigation," by G. Pekcan, J.B. Mander and S.S. Chen, 7/1/00, (PB2001-100982, A10, MF-A02).

MCEER-00-0005 "Sliding Fragility of Unrestrained Equipment in Critical Facilities," by W.H. Chong and T.T. Soong, 7/5/00, (PB2001-100983, A08, MF-A02).

MCEER-00-0006 "Seismic Response of Reinforced Concrete Bridge Pier Walls in the Weak Direction," by N. Abo-Shadi, M. Saiidi and D. Sanders, 7/17/00, (PB2001-100981, A17, MF-A03).

MCEER-00-0007 "Low-Cycle Fatigue Behavior of Longitudinal Reinforcement in Reinforced Concrete Bridge Columns," by J. Brown and S.K. Kunnath, 7/23/00, (PB2001-104392, A08, MF-A02).

MCEER-00-0008 "Soil Structure Interaction of Bridges for Seismic Analysis," I. PoLam and H. Law, 9/25/00, (PB2001-105397, A08, MF-A02).

MCEER-00-0009 "Proceedings of the First MCEER Workshop on Mitigation of Earthquake Disaster by Advanced Technologies (MEDAT-1), edited by M. Shinozuka, D.J. Inman and T.D. O'Rourke, 11/10/00, (PB2001-105399, A14, MF-A03).

MCEER-00-0010 "Development and Evaluation of Simplified Procedures for Analysis and Design of Buildings with Passive Energy Dissipation Systems, Revision 01," by O.M. Ramirez, M.C. Constantinou, C.A. Kircher, A.S. Whittaker, M.W. Johnson, J.D. Gomez and C. Chrysostomou, 11/16/01, (PB2001-105523, A23, MF-A04).

MCEER-00-0011 "Dynamic Soil-Foundation-Structure Interaction Analyses of Large Caissons," by C-Y. Chang, C-M. Mok, Z-L. Wang, R. Settgast, F. Waggoner, M.A. Ketchum, H.M. Gonnermann and C-C. Chin, 12/30/00, (PB2001-104373, A07, MF-A02).

MCEER-00-0012 "Experimental Evaluation of Seismic Performance of Bridge Restrainers," by A.G. Vlassis, E.M. Maragakis and M. Saiid Saiidi, 12/30/00, (PB2001-104354, A09, MF-A02).

MCEER-00-0013 "Effect of Spatial Variation of Ground Motion on Highway Structures," by M. Shinozuka, V. Saxena and G. Deodatis, 12/31/00, (PB2001-108755, A13, MF-A03).

MCEER-00-0014 "A Risk-Based Methodology for Assessing the Seismic Performance of Highway Systems," by S.D. Werner, C.E. Taylor, J.E. Moore, II, J.S. Walton and S. Cho, 12/31/00, (PB2001-108756, A14, MF-A03).

MCEER-01-0001 "Experimental Investigation of P-Delta Effects to Collapse During Earthquakes," by D. Vian and M. Bruneau, 6/25/01, (PB2002-100534, A17, MF-A03).

MCEER-01-0002 "Proceedings of the Second MCEER Workshop on Mitigation of Earthquake Disaster by Advanced Technologies (MEDAT-2)," edited by M. Bruneau and D.J. Inman, 7/23/01, (PB2002-100434, A16, MF-A03).

MCEER-01-0003 "Sensitivity Analysis of Dynamic Systems Subjected to Seismic Loads," by C. Roth and M. Grigoriu, 9/18/01, (PB2003-100884, A12, MF-A03).

MCEER-01-0004 "Overcoming Obstacles to Implementing Earthquake Hazard Mitigation Policies: Stage 1 Report," by D.J. Alesch and W.J. Petak, 12/17/01, (PB2002-107949, A07, MF-A02).

MCEER-01-0005 "Updating Real-Time Earthquake Loss Estimates: Methods, Problems and Insights," by C.E. Taylor, S.E. Chang and R.T. Eguchi, 12/17/01, (PB2002-107948, A05, MF-A01).

MCEER-01-0006 "Experimental Investigation and Retrofit of Steel Pile Foundations and Pile Bents Under Cyclic Lateral Loadings," by A. Shama, J. Mander, B. Blabac and S. Chen, 12/31/01, (PB2002-107950, A13, MF-A03).

MCEER-02-0001 "Assessment of Performance of Bolu Viaduct in the 1999 Duzce Earthquake in Turkey" by P.C. Roussis, M.C. Constantinou, M. Erdik, E. Durukal and M. Dicleli, 5/8/02, (PB2003-100883, A08, MF-A02).

MCEER-02-0002 "Seismic Behavior of Rail Counterweight Systems of Elevators in Buildings," by M.P. Singh, Rildova and L.E. Suarez, 5/27/02. (PB2003-100882, A11, MF-A03).

MCEER-02-0003 "Development of Analysis and Design Procedures for Spread Footings," by G. Mylonakis, G. Gazetas, S. Nikolaou and A. Chauncey, 10/02/02, (PB2004-101636, A13, MF-A03, CD-A13).

MCEER-02-0004 "Bare-Earth Algorithms for Use with SAR and LIDAR Digital Elevation Models," by C.K. Huyck, R.T. Eguchi and B. Houshmand, 10/16/02, (PB2004-101637, A07, CD-A07).

MCEER-02-0005 "Review of Energy Dissipation of Compression Members in Concentrically Braced Frames," by K.Lee and M. Bruneau, 10/18/02, (PB2004-101638, A10, CD-A10).

MCEER-03-0001 "Experimental Investigation of Light-Gauge Steel Plate Shear Walls for the Seismic Retrofit of Buildings" by J. Berman and M. Bruneau, 5/2/03, (PB2004-101622, A10, MF-A03, CD-A10).

MCEER-03-0002 "Statistical Analysis of Fragility Curves," by M. Shinozuka, M.Q. Feng, H. Kim, T. Uzawa and T. Ueda, 6/16/03, (PB2004-101849, A09, CD-A09).

MCEER-03-0003 "Proceedings of the Eighth U.S.-Japan Workshop on Earthquake Resistant Design f Lifeline Facilities and Countermeasures Against Liquefaction," edited by M. Hamada, J.P. Bardet and T.D. O'Rourke, 6/30/03, (PB2004-104386, A99, CD-A99).

MCEER-03-0004 "Proceedings of the PRC-US Workshop on Seismic Analysis and Design of Special Bridges," edited by L.C. Fan and G.C. Lee, 7/15/03, (PB2004-104387, A14, CD-A14).

MCEER-03-0005 "Urban Disaster Recovery: A Framework and Simulation Model," by S.B. Miles and S.E. Chang, 7/25/03, (PB2004-104388, A07, CD-A07).

MCEER-03-0006 "Behavior of Underground Piping Joints Due to Static and Dynamic Loading," by R.D. Meis, M. Maragakis and R. Siddharthan, 11/17/03, (PB2005-102194, A13, MF-A03, CD-A00).

MCEER-04-0001 "Experimental Study of Seismic Isolation Systems with Emphasis on Secondary System Response and Verification of Accuracy of Dynamic Response History Analysis Methods," by E. Wolff and M. Constantinou, 1/16/04 (PB2005-102195, A99, MF-E08, CD-A00).

MCEER-04-0002 "Tension, Compression and Cyclic Testing of Engineered Cementitious Composite Materials," by K. Kesner and S.L. Billington, 3/1/04, (PB2005-102196, A08, CD-A08).

MCEER-04-0003 "Cyclic Testing of Braces Laterally Restrained by Steel Studs to Enhance Performance During Earthquakes," by O.C. Celik, J.W. Berman and M. Bruneau, 3/16/04, (PB2005-102197, A13, MF-A03, CD-A00).

MCEER-04-0004 "Methodologies for Post Earthquake Building Damage Detection Using SAR and Optical Remote Sensing: Application to the August 17, 1999 Marmara, Turkey Earthquake," by C.K. Huyck, B.J. Adams, S. Cho, R.T. Eguchi, B. Mansouri and B. Houshmand, 6/15/04, (PB2005-104888, A10, CD-A00).

MCEER-04-0005 "Nonlinear Structural Analysis Towards Collapse Simulation: A Dynamical Systems Approach," by M.V. Sivaselvan and A.M. Reinhorn, 6/16/04, (PB2005-104889, A11, MF-A03, CD-A00).

MCEER-04-0006 "Proceedings of the Second PRC-US Workshop on Seismic Analysis and Design of Special Bridges," edited by G.C. Lee and L.C. Fan, 6/25/04, (PB2005-104890, A16, CD-A00).

MCEER-04-0007 "Seismic Vulnerability Evaluation of Axially Loaded Steel Built-up Laced Members," by K. Lee and M. Bruneau, 6/30/04, (PB2005-104891, A16, CD-A00).

MCEER-04-0008 "Evaluation of Accuracy of Simplified Methods of Analysis and Design of Buildings with Damping Systems for Near-Fault and for Soft-Soil Seismic Motions," by E.A. Pavlou and M.C. Constantinou, 8/16/04, (PB2005-104892, A08, MF-A02, CD-A00).

MCEER-04-0009 "Assessment of Geotechnical Issues in Acute Care Facilities in California," by M. Lew, T.D. O'Rourke, R. Dobry and M. Koch, 9/15/04, (PB2005-104893, A08, CD-A00).

MCEER-04-0010 "Scissor-Jack-Damper Energy Dissipation System," by A.N. Sigaher-Boyle and M.C. Constantinou, 12/1/04 (PB2005-108221).

MCEER-04-0011 "Seismic Retrofit of Bridge Steel Truss Piers Using a Controlled Rocking Approach," by M. Pollino and M. Bruneau, 12/20/04 (PB2006-105795).

MCEER-05-0001 "Experimental and Analytical Studies of Structures Seismically Isolated with an Uplift-Restraint Isolation System," by P.C. Roussis and M.C. Constantinou, 1/10/05 (PB2005-108222).

MCEER-05-0002 "A Versatile Experimentation Model for Study of Structures Near Collapse Applied to Seismic Evaluation of Irregular Structures," by D. Kusumastuti, A.M. Reinhorn and A. Rutenberg, 3/31/05 (PB2006-101523).

MCEER-05-0003 "Proceedings of the Third PRC-US Workshop on Seismic Analysis and Design of Special Bridges," edited by L.C. Fan and G.C. Lee, 4/20/05, (PB2006-105796).

MCEER-05-0004 "Approaches for the Seismic Retrofit of Braced Steel Bridge Piers and Proof-of-Concept Testing of an Eccentrically Braced Frame with Tubular Link," by J.W. Berman and M. Bruneau, 4/21/05 (PB2006-101524).

MCEER-05-0005 "Simulation of Strong Ground Motions for Seismic Fragility Evaluation of Nonstructural Components in Hospitals," by A. Wanitkorkul and A. Filiatrault, 5/26/05 (PB2006-500027).

MCEER-05-0006 "Seismic Safety in California Hospitals: Assessing an Attempt to Accelerate the Replacement or Seismic Retrofit of Older Hospital Facilities," by D.J. Alesch, L.A. Arendt and W.J. Petak, 6/6/05 (PB2006-105794).

MCEER-05-0007 "Development of Seismic Strengthening and Retrofit Strategies for Critical Facilities Using Engineered Cementitious Composite Materials," by K. Kesner and S.L. Billington, 8/29/05 (PB2006-111701).

MCEER-05-0008 "Experimental and Analytical Studies of Base Isolation Systems for Seismic Protection of Power Transformers," by N. Murota, M.Q. Feng and G-Y. Liu, 9/30/05 (PB2006-111702).

MCEER-05-0009 "3D-BASIS-ME-MB: Computer Program for Nonlinear Dynamic Analysis of Seismically Isolated Structures," by P.C. Tsopelas, P.C. Roussis, M.C. Constantinou, R. Buchanan and A.M. Reinhorn, 10/3/05 (PB2006-111703).

MCEER-05-0010 "Steel Plate Shear Walls for Seismic Design and Retrofit of Building Structures," by D. Vian and M. Bruneau, 12/15/05 (PB2006-111704).

MCEER-05-0011 "The Performance-Based Design Paradigm," by M.J. Astrella and A. Whittaker, 12/15/05 (PB2006-111705).

MCEER-06-0001 "Seismic Fragility of Suspended Ceiling Systems," H. Badillo-Almaraz, A.S. Whittaker, A.M. Reinhorn and G.P. Cimellaro, 2/4/06 (PB2006-111706).

MCEER-06-0002 "Multi-Dimensional Fragility of Structures," by G.P. Cimellaro, A.M. Reinhorn and M. Bruneau, 3/1/06 (PB2007-106974, A09, MF-A02, CD A00).

MCEER-06-0003 "Built-Up Shear Links as Energy Dissipators for Seismic Protection of Bridges," by P. Dusicka, A.M. Itani and I.G. Buckle, 3/15/06 (PB2006-111708).

MCEER-06-0004 "Analytical Investigation of the Structural Fuse Concept," by R.E. Vargas and M. Bruneau, 3/16/06 (PB2006-111709).

MCEER-06-0005 "Experimental Investigation of the Structural Fuse Concept," by R.E. Vargas and M. Bruneau, 3/17/06 (PB2006-111710).

MCEER-06-0006 "Further Development of Tubular Eccentrically Braced Frame Links for the Seismic Retrofit of Braced Steel Truss Bridge Piers," by J.W. Berman and M. Bruneau, 3/27/06 (PB2007-105147).

MCEER-06-0007 "REDARS Validation Report," by S. Cho, C.K. Huyck, S. Ghosh and R.T. Eguchi, 8/8/06 (PB2007-106983).

MCEER-06-0008 "Review of Current NDE Technologies for Post-Earthquake Assessment of Retrofitted Bridge Columns," by J.W. Song, Z. Liang and G.C. Lee, 8/21/06 (PB2007-106984).

MCEER-06-0009 "Liquefaction Remediation in Silty Soils Using Dynamic Compaction and Stone Columns," by S. Thevanayagam, G.R. Martin, R. Nashed, T. Shenthan, T. Kanagalingam and N. Ecemis, 8/28/06 (PB2007-106985).

MCEER-06-0010 "Conceptual Design and Experimental Investigation of Polymer Matrix Composite Infill Panels for Seismic Retrofitting," by W. Jung, M. Chiewanichakorn and A.J. Aref, 9/21/06 (PB2007-106986).

MCEER-06-0011 "A Study of the Coupled Horizontal-Vertical Behavior of Elastomeric and Lead-Rubber Seismic Isolation Bearings," by G.P. Warn and A.S. Whittaker, 9/22/06 (PB2007-108679).

MCEER-06-0012 "Proceedings of the Fourth PRC-US Workshop on Seismic Analysis and Design of Special Bridges: Advancing Bridge Technologies in Research, Design, Construction and Preservation," Edited by L.C. Fan, G.C. Lee and L. Ziang, 10/12/06 (PB2007-109042).

MCEER-06-0013 "Cyclic Response and Low Cycle Fatigue Characteristics of Plate Steels," by P. Dusicka, A.M. Itani and I.G. Buckle, 11/1/06 06 (PB2007-106987).

MCEER-06-0014 "Proceedings of the Second US-Taiwan Bridge Engineering Workshop," edited by W.P. Yen, J. Shen, J-Y. Chen and M. Wang, 11/15/06 (PB2008-500041).

MCEER-06-0015 "User Manual and Technical Documentation for the REDARS^{TM} Import Wizard," by S. Cho, S. Ghosh, C.K. Huyck and S.D. Werner, 11/30/06 (PB2007-114766).

MCEER-06-0016 "Hazard Mitigation Strategy and Monitoring Technologies for Urban and Infrastructure Public Buildings: Proceedings of the China-US Workshops," edited by X.Y. Zhou, A.L. Zhang, G.C. Lee and M. Tong, 12/12/06 (PB2008-500018).

MCEER-07-0001 "Static and Kinetic Coefficients of Friction for Rigid Blocks," by C. Kafali, S. Fathali, M. Grigoriu and A.S. Whittaker, 3/20/07 (PB2007-114767).

MCEER-07-0002 "Hazard Mitigation Investment Decision Making: Organizational Response to Legislative Mandate," by L.A. Arendt, D.J. Alesch and W.J. Petak, 4/9/07 (PB2007-114768).

MCEER-07-0003 "Seismic Behavior of Bidirectional-Resistant Ductile End Diaphragms with Unbonded Braces in Straight or Skewed Steel Bridges," by O. Celik and M. Bruneau, 4/11/07 (PB2008-105141).

MCEER-07-0004 "Modeling Pile Behavior in Large Pile Groups Under Lateral Loading," by A.M. Dodds and G.R. Martin, 4/16/07(PB2008-105142).

MCEER-07-0005 "Experimental Investigation of Blast Performance of Seismically Resistant Concrete-Filled Steel Tube Bridge Piers," by S. Fujikura, M. Bruneau and D. Lopez-Garcia, 4/20/07 (PB2008-105143).

MCEER-07-0006 "Seismic Analysis of Conventional and Isolated Liquefied Natural Gas Tanks Using Mechanical Analogs," by I.P. Christovasilis and A.S. Whittaker, 5/1/07.

MCEER-07-0007 "Experimental Seismic Performance Evaluation of Isolation/Restraint Systems for Mechanical Equipment – Part 1: Heavy Equipment Study," by S. Fathali and A. Filiatrault, 6/6/07 (PB2008-105144).

MCEER-07-0008 "Seismic Vulnerability of Timber Bridges and Timber Substructures," by A.A. Sharma, J.B. Mander, I.M. Friedland and D.R. Allicock, 6/7/07 (PB2008-105145).

MCEER-07-0009 "Experimental and Analytical Study of the XY-Friction Pendulum (XY-FP) Bearing for Bridge Applications," by C.C. Marin-Artieda, A.S. Whittaker and M.C. Constantinou, 6/7/07 (PB2008-105191).

MCEER-07-0010 "Proceedings of the PRC-US Earthquake Engineering Forum for Young Researchers," Edited by G.C. Lee and X.Z. Qi, 6/8/07 (PB2008-500058).

MCEER-07-0011 "Design Recommendations for Perforated Steel Plate Shear Walls," by R. Purba and M. Bruneau, 6/18/07, (PB2008-105192).

MCEER-07-0012 "Performance of Seismic Isolation Hardware Under Service and Seismic Loading," by M.C. Constantinou, A.S. Whittaker, Y. Kalpakidis, D.M. Fenz and G.P. Warn, 8/27/07, (PB2008-105193).

MCEER-07-0013 "Experimental Evaluation of the Seismic Performance of Hospital Piping Subassemblies," by E.R. Goodwin, E. Maragakis and A.M. Itani, 9/4/07, (PB2008-105194).

MCEER-07-0014 "A Simulation Model of Urban Disaster Recovery and Resilience: Implementation for the 1994 Northridge Earthquake," by S. Miles and S.E. Chang, 9/7/07, (PB2008-106426).

MCEER-07-0015 "Statistical and Mechanistic Fragility Analysis of Concrete Bridges," by M. Shinozuka, S. Banerjee and S-H. Kim, 9/10/07, (PB2008-106427).

MCEER-07-0016 "Three-Dimensional Modeling of Inelastic Buckling in Frame Structures," by M. Schachter and AM. Reinhorn, 9/13/07, (PB2008-108125).

MCEER-07-0017 "Modeling of Seismic Wave Scattering on Pile Groups and Caissons," by I. Po Lam, H. Law and C.T. Yang, 9/17/07 (PB2008-108150).

MCEER-07-0018 "Bridge Foundations: Modeling Large Pile Groups and Caissons for Seismic Design," by I. Po Lam, H. Law and G.R. Martin (Coordinating Author), 12/1/07 (PB2008-111190).

MCEER-07-0019 "Principles and Performance of Roller Seismic Isolation Bearings for Highway Bridges," by G.C. Lee, Y.C. Ou, Z. Liang, T.C. Niu and J. Song, 12/10/07 (PB2009-110466).

MCEER-07-0020 "Centrifuge Modeling of Permeability and Pinning Reinforcement Effects on Pile Response to Lateral Spreading," by L.L Gonzalez-Lagos, T. Abdoun and R. Dobry, 12/10/07 (PB2008-111191).

MCEER-07-0021 "Damage to the Highway System from the Pisco, Perú Earthquake of August 15, 2007," by J.S. O'Connor, L. Mesa and M. Nykamp, 12/10/07, (PB2008-108126).

MCEER-07-0022 "Experimental Seismic Performance Evaluation of Isolation/Restraint Systems for Mechanical Equipment – Part 2: Light Equipment Study," by S. Fathali and A. Filiatrault, 12/13/07 (PB2008-111192).

MCEER-07-0023 "Fragility Considerations in Highway Bridge Design," by M. Shinozuka, S. Banerjee and S.H. Kim, 12/14/07 (PB2008-111193).

MCEER-07-0024 "Performance Estimates for Seismically Isolated Bridges," by G.P. Warn and A.S. Whittaker, 12/30/07 (PB2008-112230).

MCEER-08-0001 "Seismic Performance of Steel Girder Bridge Superstructures with Conventional Cross Frames," by L.P. Carden, A.M. Itani and I.G. Buckle, 1/7/08, (PB2008-112231).

MCEER-08-0002 "Seismic Performance of Steel Girder Bridge Superstructures with Ductile End Cross Frames with Seismic Isolators," by L.P. Carden, A.M. Itani and I.G. Buckle, 1/7/08 (PB2008-112232).

MCEER-08-0003 "Analytical and Experimental Investigation of a Controlled Rocking Approach for Seismic Protection of Bridge Steel Truss Piers," by M. Pollino and M. Bruneau, 1/21/08 (PB2008-112233).

MCEER-08-0004 "Linking Lifeline Infrastructure Performance and Community Disaster Resilience: Models and Multi-Stakeholder Processes," by S.E. Chang, C. Pasion, K. Tatebe and R. Ahmad, 3/3/08 (PB2008-112234).

MCEER-08-0005 "Modal Analysis of Generally Damped Linear Structures Subjected to Seismic Excitations," by J. Song, Y-L. Chu, Z. Liang and G.C. Lee, 3/4/08 (PB2009-102311).

MCEER-08-0006 "System Performance Under Multi-Hazard Environments," by C. Kafali and M. Grigoriu, 3/4/08 (PB2008-112235).

MCEER-08-0007 "Mechanical Behavior of Multi-Spherical Sliding Bearings," by D.M. Fenz and M.C. Constantinou, 3/6/08 (PB2008-112236).

MCEER-08-0008 "Post-Earthquake Restoration of the Los Angeles Water Supply System," by T.H.P. Tabucchi and R.A. Davidson, 3/7/08 (PB2008-112237).

MCEER-08-0009 "Fragility Analysis of Water Supply Systems," by A. Jacobson and M. Grigoriu, 3/10/08 (PB2009-105545).

MCEER-08-0010 "Experimental Investigation of Full-Scale Two-Story Steel Plate Shear Walls with Reduced Beam Section Connections," by B. Qu, M. Bruneau, C-H. Lin and K-C. Tsai, 3/17/08 (PB2009-106368).

MCEER-08-0011 "Seismic Evaluation and Rehabilitation of Critical Components of Electrical Power Systems," S. Ersoy, B. Feizi, A. Ashrafi and M. Ala Saadeghvaziri, 3/17/08 (PB2009-105546).

MCEER-08-0012 "Seismic Behavior and Design of Boundary Frame Members of Steel Plate Shear Walls," by B. Qu and M. Bruneau, 4/26/08 . (PB2009-106744).

MCEER-08-0013 "Development and Appraisal of a Numerical Cyclic Loading Protocol for Quantifying Building System Performance," by A. Filiatrault, A. Wanitkorkul and M. Constantinou, 4/27/08 (PB2009-107906).

MCEER-08-0014 "Structural and Nonstructural Earthquake Design: The Challenge of Integrating Specialty Areas in Designing Complex, Critical Facilities," by W.J. Petak and D.J. Alesch, 4/30/08 (PB2009-107907).

MCEER-08-0015 "Seismic Performance Evaluation of Water Systems," by Y. Wang and T.D. O'Rourke, 5/5/08 (PB2009-107908).

MCEER-08-0016 "Seismic Response Modeling of Water Supply Systems," by P. Shi and T.D. O'Rourke, 5/5/08 (PB2009-107910).

MCEER-08-0017 "Numerical and Experimental Studies of Self-Centering Post-Tensioned Steel Frames," by D. Wang and A. Filiatrault, 5/12/08 (PB2009-110479).

MCEER-08-0018 "Development, Implementation and Verification of Dynamic Analysis Models for Multi-Spherical Sliding Bearings," by D.M. Fenz and M.C. Constantinou, 8/15/08 (PB2009-107911).

MCEER-08-0019 "Performance Assessment of Conventional and Base Isolated Nuclear Power Plants for Earthquake Blast Loadings," by Y.N. Huang, A.S. Whittaker and N. Luco, 10/28/08 (PB2009-107912).

MCEER-08-0020 "Remote Sensing for Resilient Multi-Hazard Disaster Response – Volume I: Introduction to Damage Assessment Methodologies," by B.J. Adams and R.T. Eguchi, 11/17/08.

MCEER-08-0021 "Remote Sensing for Resilient Multi-Hazard Disaster Response – Volume II: Counting the Number of Collapsed Buildings Using an Object-Oriented Analysis: Case Study of the 2003 Bam Earthquake," by L. Gusella, C.K. Huyck and B.J. Adams, 11/17/08.

MCEER-08-0022 "Remote Sensing for Resilient Multi-Hazard Disaster Response – Volume III: Multi-Sensor Image Fusion Techniques for Robust Neighborhood-Scale Urban Damage Assessment," by B.J. Adams and A. McMillan, 11/17/08.

MCEER-08-0023 "Remote Sensing for Resilient Multi-Hazard Disaster Response – Volume IV: A Study of Multi-Temporal and Multi-Resolution SAR Imagery for Post-Katrina Flood Monitoring in New Orleans," by A. McMillan, J.G. Morley, B.J. Adams and S. Chesworth, 11/17/08.

MCEER-08-0024 "Remote Sensing for Resilient Multi-Hazard Disaster Response – Volume V: Integration of Remote Sensing Imagery and VIEWS^{TM} Field Data for Post-Hurricane Charley Building Damage Assessment," by J.A. Womble, K. Mehta and B.J. Adams, 11/17/08.

MCEER-08-0025 "Building Inventory Compilation for Disaster Management: Application of Remote Sensing and Statistical Modeling," by P. Sarabandi, A.S. Kiremidjian, R.T. Eguchi and B. J. Adams, 11/20/08 (PB2009-110484).

MCEER-08-0026 "New Experimental Capabilities and Loading Protocols for Seismic Qualification and Fragility Assessment of Nonstructural Systems," by R. Retamales, G. Mosqueda, A. Filiatrault and A. Reinhorn, 11/24/08 (PB2009-110485).

MCEER-08-0027 "Effects of Heating and Load History on the Behavior of Lead-Rubber Bearings," by I.V. Kalpakidis and M.C. Constantinou, 12/1/08.

MCEER-08-0028 "Experimental and Analytical Investigation of Blast Performance of Seismically Resistant Bridge Piers," by S.Fujikura and M. Bruneau, 12/8/08.

MCEER-08-0029 "Evolutionary Methodology for Aseismic Decision Support," by Y. Hu and G. Dargush, 12/15/08.

MCEER-08-0030 "Development of a Steel Plate Shear Wall Bridge Pier System Conceived from a Multi-Hazard Perspective," by D. Keller and M. Bruneau, 12/19/08.

MCEER-09-0001 "Modal Analysis of Arbitrarily Damped Three-Dimensional Linear Structures Subjected to Seismic Excitations," by Y.L. Chu, J. Song and G.C. Lee, 1/31/09.

MCEER-09-0002 "Air-Blast Effects on Structural Shapes," by G. Ballantyne and A.S. Whittaker, 2/12/09.

MCEER-09-0003 "Water Supply Performance During Earthquakes and Extreme Events," by A.L. Bonneau and T.D. O'Rourke, 2/16/09.

MCEER-09-0004 "Generalized Linear (Mixed) Models of Post-Earthquake Ignitions," by R.A. Davidson, 7/20/09.

MCEER-09-0005 "Seismic Testing of a Full-Scale Two-Story Light-Frame Wood Building: NEESWood Benchmark Test," by I.P. Christovasilis, A. Filiatrault and A. Wanitkorkul, 7/22/09.

MCEER-09-0006 "IDARC2D Version 7.0: A Program for the Inelastic Damage Analysis of Structures," by A.M. Reinhorn, H. Roh, M. Sivaselvan, S.K. Kunnath, R.E. Valles, A. Madan, C. Li, R. Lobo and Y.J. Park, 7/28/09.

MCEER-09-0007 "Enhancements to Hospital Resiliency: Improving Emergency Planning for and Response to Hurricanes," by D.B. Hess and L.A. Arendt, 7/30/09.

MCEER-09-0008 "Assessment of Base-Isolated Nuclear Structures for Design and Beyond-Design Basis Earthquake Shaking," by Y.N. Huang, A.S. Whittaker, R.P. Kennedy and R.L. Mayes, 8/20/09.

MCEER
EARTHQUAKE ENGINEERING TO EXTREME EVENTS
University at Buffalo, The State University of New York
Red Jacket Quadrangle ▪ Buffalo, New York 14261
Phone: (716) 645-3391 ▪ Fax: (716) 645-3399
E-mail: *mceer@buffalo.edu* ▪ WWW Site *http://mceer.buffalo.edu*
University at Buffalo *The State University of New York*

ISSN 1520-295X